2012

Beta-diketone and beta-ketoenamine based molecular squares

Jackson Kiplagat Cherutoi
Louisiana State University and Agricultural and Mechanical College, jcheru1@lsu.edu

Follow this and additional works at: https://digitalcommons.lsu.edu/gradschool_dissertations

Part of the Chemistry Commons

BETA-DIKETONE AND BETA-KETOENAMINE BASED MOLECULAR SQUARES

A Dissertation

Submitted to the Graduate Faculty of the
Louisiana State University and
Agricultural and Mechanical College
in partial fulfillment of the
requirements for the degree of
Doctor of Philosophy

in

The Department of Chemistry

by
Jackson Kiplagat Cherutoi
B.Ed (Sc), Moi University, 1996
M.Sc., Moi University, 2002
August 2012

Table of Contents

List of Tables

List of Figures

Abstract

This dissertation focuses on synthesis of β-diketone and β-ketoenamine ligands for molecular polygons. Previous work with the bis(β-diketone) m-pbaH$_2$ showed that it can be converted to a copper molecular square, Cu$_4$(m-pba)$_4$, but its use in host-guest reactions was limited by its low solubility in most organic solvents. Accordingly, in the present work, the m-pbhxH$_2$ ligand, with pentyl chains replacing the methyl groups in the β-diketone moieties of m-pbaH$_2$, was successfully prepared beginning with 6-dodecyne. This ligand reacts with Cu^{2+} to make the molecular square Cu$_4$(m-pbhx)$_4$, which is soluble in a wider range of solvents. Host-guest reactions of Cu$_4$(m-pbhx)$_4$ with a variety of guest molecules were studied. The structures of the "empty" square, [Cu$_4$(m-pbhx)$_4$(CH$_3$OH)$_2$], and its adducts with several guest molecules, were determined by single crystal X-ray analysis. In these host-guest adducts, the Cu---Cu distances range from 13.7-15.1 Å.

As part of a study of the effects of substituents on the properties of the resulting molecular squares, the 2-MeO-m-pbaH$_2$ ligand had been prepared previously. This dissertation reports an improved synthesis of 2-MeO-m-pbaH$_2$, and its larger homolog 2-MeO-m-pbprH$_2$ was synthesized as well. Treatment of 2-MeO-m-pbprH$_2$ with Cu^{2+} afforded a molecular square that is soluble in chloroform and dichloromethane. Treatment of the square with guest molecules did not yield adducts, most likely because of steric interference from the internal methoxy groups.

The two ligands m-pbaH$_2$ and m-pbprH$_2$ were converted to their ketoenamine analogs m-pbiH$_2$ and m-pbpriH$_2$ through microwave-assisted synthesis. The molecular squares Cu$_4$(m-pbi)$_4$,

$Cu_4(m\text{-pbpri})_4$, and $Ni_4(m\text{-pbpri})_4$ were prepared from these ligands and characterized by single crystal X-ray analysis, UV-Vis spectroscopy, and cyclic voltammetry.

Two new bis(β-diketone) ligands based on triphenylamine were prepared for the first time. The new ligands were designed to make Cu(II) molecular squares that are larger (Cu---Cu ca. 21 Å) than $Cu_4(m\text{-pba})_4$ and its derivatives.

Chapter 1: Introduction - Porous Metal-Organic Materials

Porous materials have continued to attract attention from researchers because of their potential applications in areas such as gas storage,[1-3] catalysis,[4-7] and separations.[8-10] Different types of porous materials are known, including carbon nanotubes, zeolites, activated carbon, and metal-organic materials. This chapter will concentrate on supramolecular metal-organic molecules; molecules prepared by combining multidentate organic linkers with metal ions. There are three common kinds of metal-organic molecules: metal-organic frameworks (MOFs) (Figure 1.1), metal-organic polygons (metallacycles) (see Figure 1.4), and metal-organic polyhedra (MOPs) (see Figure 1.5).
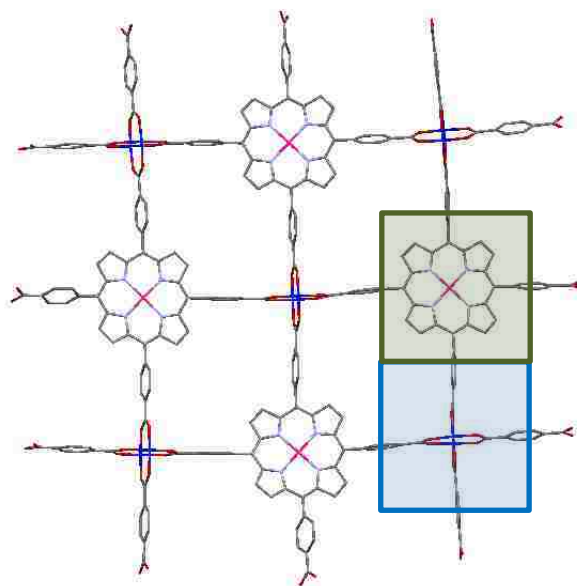
Figure 1.1 Structure of a portion of a metal-organic framework (MOF).[11] This material is composed of metalloporphyrin units (one highlighted in green box) linked by dicobalt carboxylate bridging groups (one highlighted in blue box) in a 2-dimensional square grid.

MOFs are sometimes referred to as porous coordination polymers (PCPs) or 2- or 3-dimensional infinite structures. A portion of a 2-D MOF structure is shown in Figure 1.1. This structure contains dimetal carboxylate bridging groups commonly known as paddle-wheel units, $M_2(COO)_4$ (M = Zn, Co) (see Figure 1.2) linked to metalloporphyrin units M(TCPP) (see Figure 1.3) resulting in a 2-D square grid network.[11]
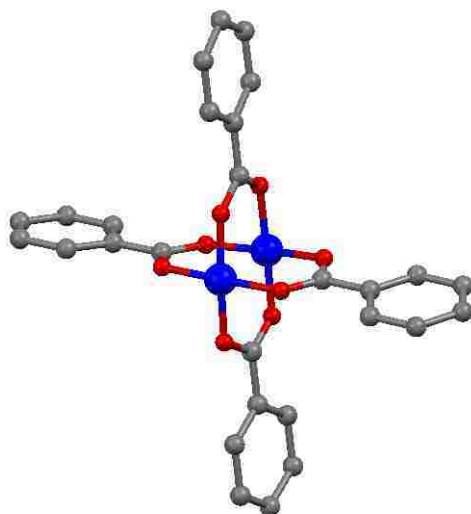
Figure 1.2 A $Cu_2(O_2CPh)_4$ paddle wheel-unit. Hydrogen atoms omitted for clarity.

A variety of multidentate organic linkers have been utilized in the preparation of MOFs; the most common are polycarboxylic acids such as 1,4-benzenedicarboxylic acid (BDC), 1,3,5-benzenetricarboxylic acid (BTC), and M(TCPP) (see Figure 1.3). Many 3-D MOF compounds from polycarboxylic acids[12-14] and other organic linkers[15-17] are known. One unique property of MOF compounds is that they have large surface areas, some exceeding 4000 m^2 g^{-1},[18,19]; in comparison the highest value reported for activated carbon is 2030 m^2 g^{-1},[20] and for zeolites is 904 m^2 g^{-1}.[21] As a result, metal-organic frameworks are being investigated for applications in gas storage,[2] among other potential applications.
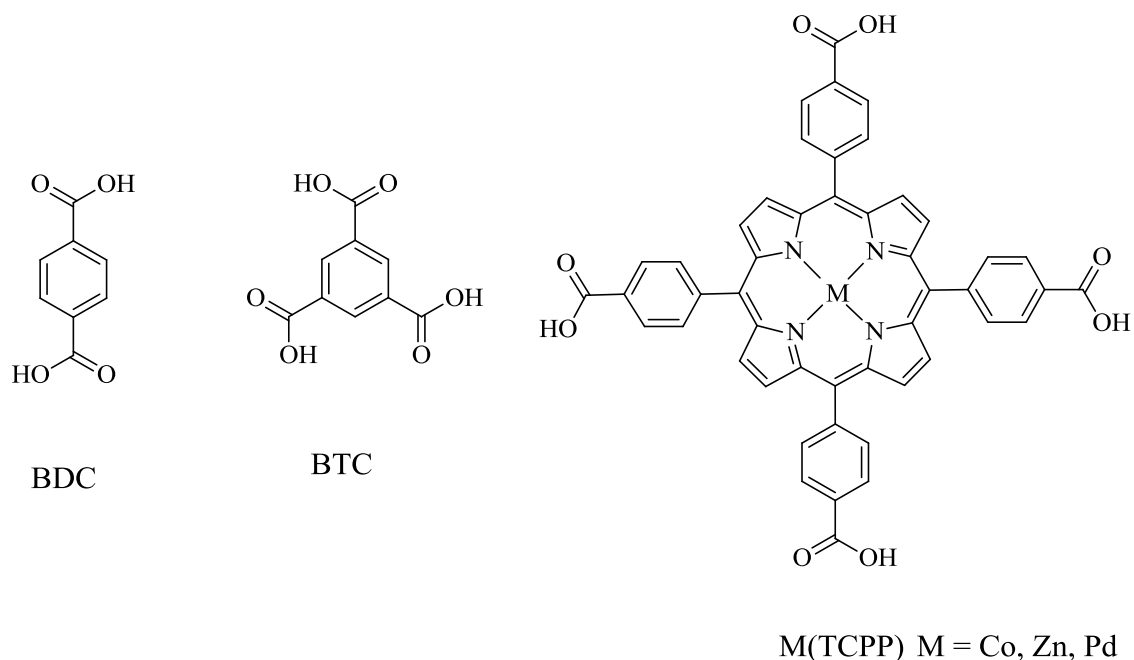
Figure 1.3 Polycarboxylic acid linkers for making MOFs.

Metal-organic polygons (metallacycles) constitute the second class of metal-organic molecules. These are discrete 2-dimensional assemblies and are represented by the molecular square in Figure 1.4. This molecular square[22] was reported in 1990 by the Fujita group. The square was made by reaction between 4,4'-bipyridine and (en)Pd(NO$_3$)$_2$ (en = ethylenediamine) (Figure 1.4). The palladium centers were capped by ethylenediamine and the resulting (en)(Pd)$^{2+}$ units after removal of nitrate groups provide the 90° "corners" of the square. Thus the corners of the square are the metal ions and the linkers are the edges. The square has an overall charge of +8 since 4,4'-bpy and ethylenediamine are neutral; this charge is balanced by the nitrate ions from the starting material. Because of the large positive charge, the square is soluble in polar solvents such as water. This square encapsulates small organic molecules such as 1,3,5-trimethoxybenzene.
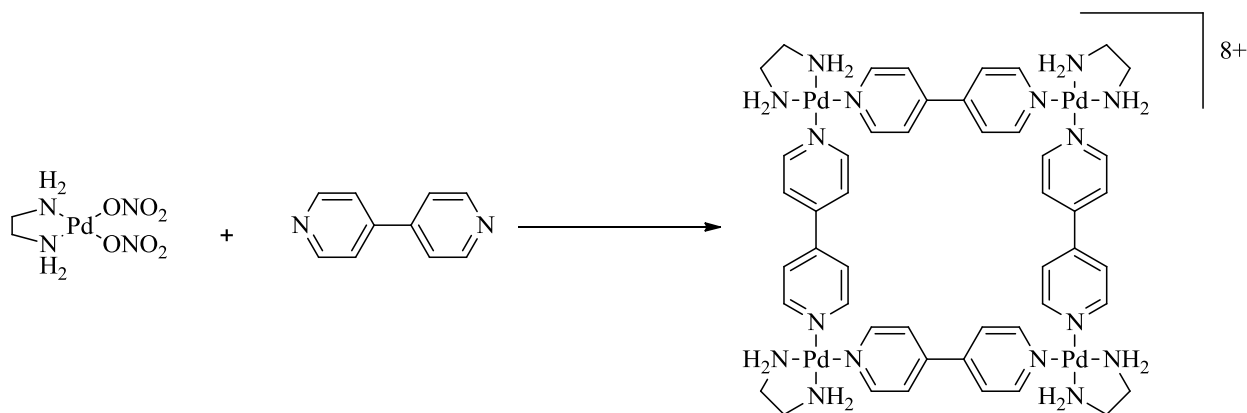
Figure 1.4 Synthesis of the molecular square[22] from (en)Pd(NO$_3$)$_2$ and bpy.

Metal-organic polygons have been prepared from both linear and bent organic linkers. Stang and Olenyuk have developed a general molecular architecture library which can be used to predict the polygon that can be formed based on the geometry of the linker and the chosen metal ion.[23] Sometimes, the product obtained is not what is predicted on the basis of the geometry of the metal ions and linkers.

Metal-organic polyhedra (MOPs) are the third class of metal-organic molecules and they are discrete 3-D structures and the molecular octahedron in Figure 1.5 is a representative of this class of molecules. This structure was reported by the Fujita group in 1995 and was synthesized by treating the tripyridyltriazine organic linker (Figure 1.6a) with (en)Pd(NO$_3$)$_2$.[24] The six vertices of the octahedron are occupied by palladium atoms that are capped by ethylenediamine. Reactions between carefully designed linkers with chosen metal ions have led to the realization of MOPs such as cubes,[25,26] tetrahedra,[27-29] octahedra, [30,31] and others.[32-35] Most of the organic linkers are pyridine-based although other linkers such as carboxylates and catecholates have been used as well (Figure 1.6). MOP molecules have potential applications in catalysis.[36,37]
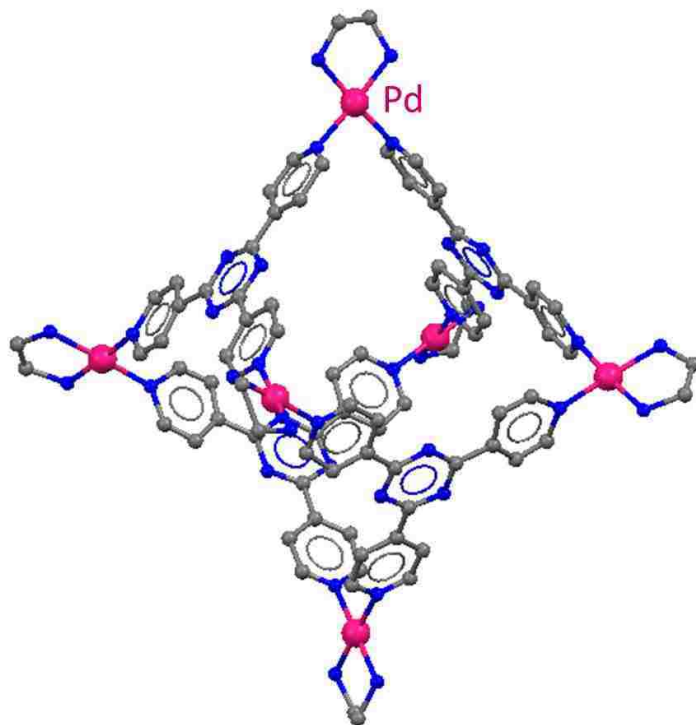
Figure 1.5 The molecular octahedron prepared by the Fujita group.[24] Hydrogen atoms omitted.

a

b

c
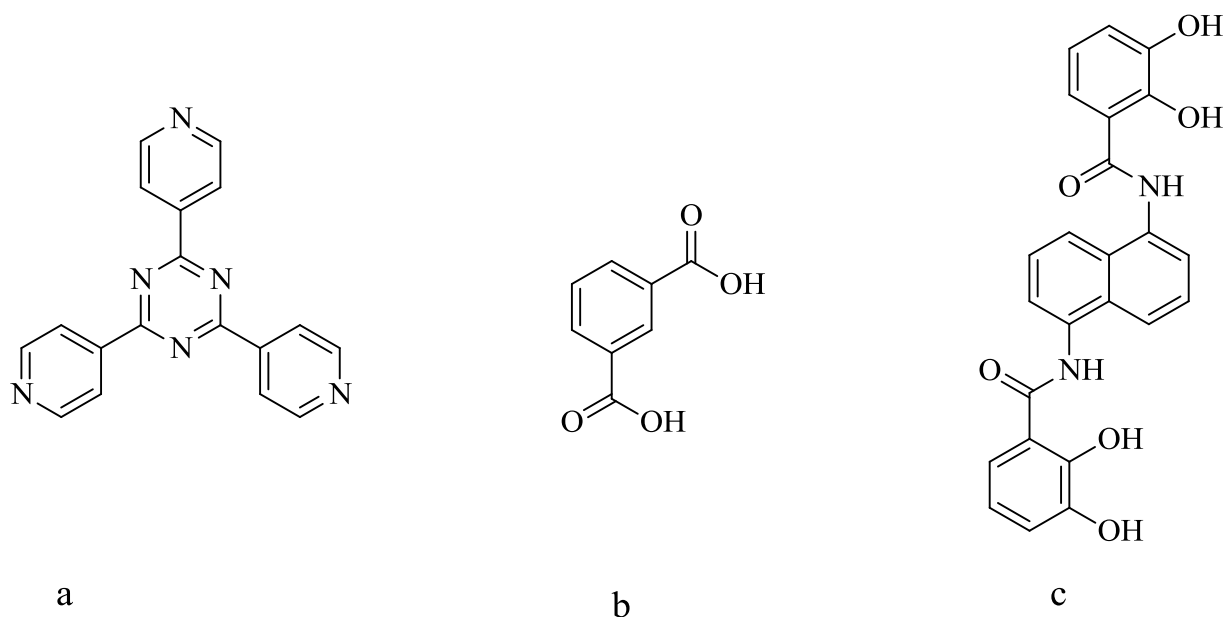
Figure 1.6 Organic linkers that have been used to prepare MOP molecules.

It is important to note that of all the molecular polygons known, molecular squares are the most common and have been studied most extensively. Similar to other molecular polygons, molecular squares are prepared from both linear and bent bidentate linkers; linear linkers as usual require corner capping strategy at the metal center. Also most of the squares are prepared from pyridine-based or nitrogen containing donors. Sometimes molecular squares exist in equilibrium with molecular triangles such as the square in Figure 1.7 and the molecular triangle in Figure 1.8.[38]

Although most of the molecular squares are based on square planar metal centers to provide the 90° corners, octahedral metal centers have also been employed. In 1996, Hupp and co-workers reported molecular squares synthesized from pyridine derivatives such as pyrazine, 4,4'-bipyridine and 1,2-bis(4-pyridyl)ethylene and octahedral rhenium centers. Figure 1.9 shows the formation of one of the squares.[39] The rhenium corner was generated from $Re(CO)_5Cl$ when two of its carbonyl ligands are displaced by the linker during its coordination to the metal.
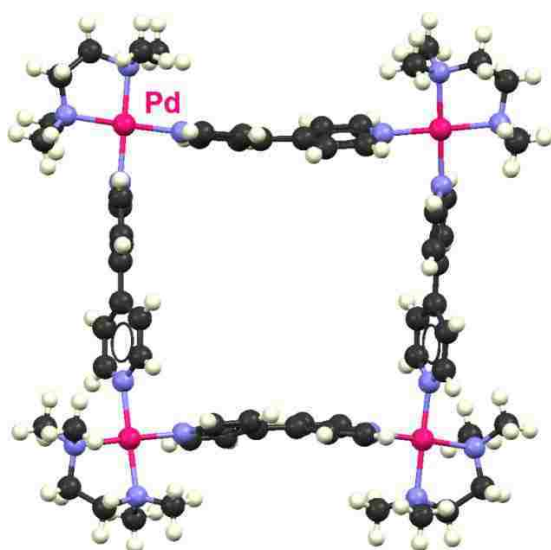
Figure 1.7 Molecular square prepared by the Mizuno group.[38]
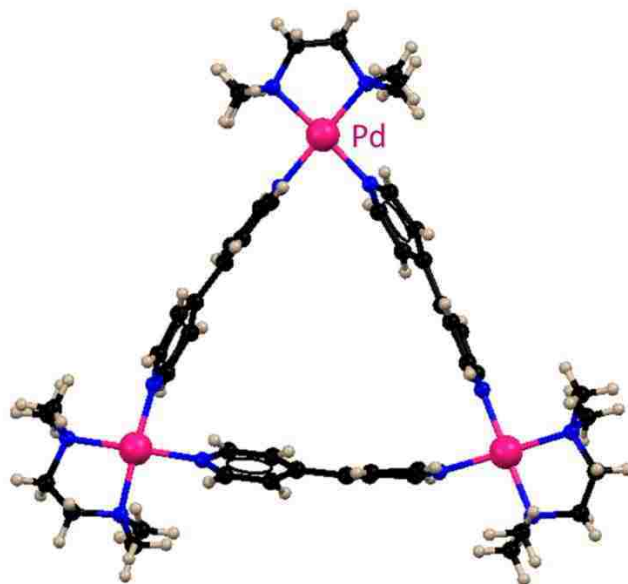
Figure 1.8 Molecular triangle prepared by the Mizuno group.[38]
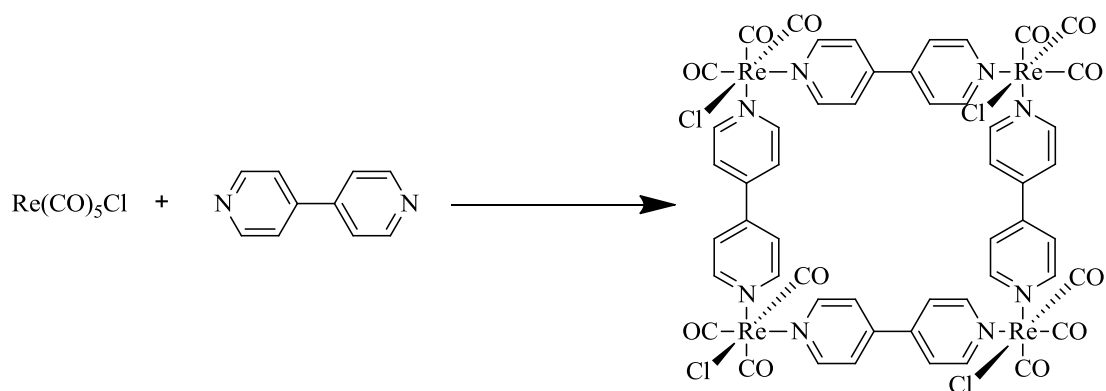
Figure 1.9 Reaction of Re(CO)$_5$Cl and bpy yielded a neutral molecular square.[39]

The coordination chemistry of β-diketone and β-ketoenamine ligands (Figure 1.10) has been studied extensively. They are chelating ligands and readily form stable mononuclear complexes. To generate molecular polygons from these ligands, multidentate β-diketones and β-ketoenamines are required.

7

a   b

Figure 1.10 Structures of: (a) β-diketone and (b) β-ketoenamine ligands.

Because of the chelating nature of these ligands, molecular polygons derived from them may be robust. Fewer molecular polygons have been reported from β-diketone and β-ketoenamine linkers than from pyridine-based linkers. Early reports on metal-organic polygons constructed from bis(β-diketones) and bis(β-ketoenamines) were dimers, $M_2(m\text{-XBA})_2$ and $M_2(BBI)_2$ (Figures 1.11 and 1.12).[40,41]
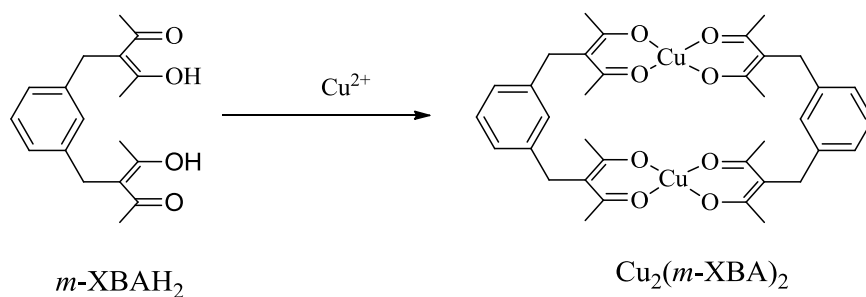
m-XBAH$_2$ Cu$_2$(*m*-XBA)$_2$

Figure 1.11 Reaction of *m*-XBAH$_2$ with Cu^{2+} afforded a molecular dimer, Cu$_2$(*m*-XBA)$_2$.[40]

M = Cu, Ni, Pd
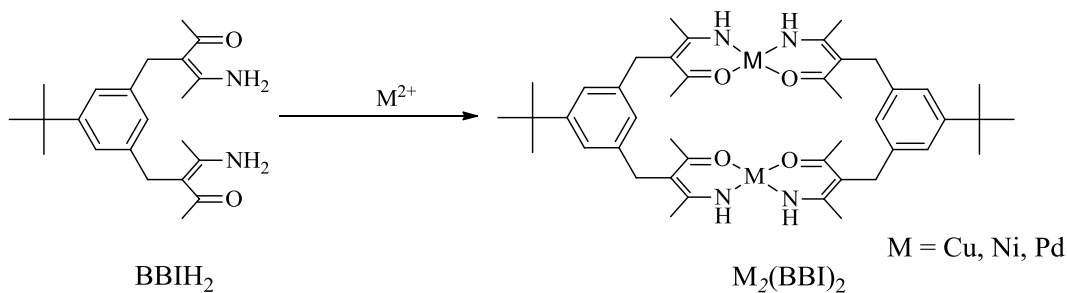
BBIH$_2$ M$_2$(BBI)$_2$

Figure 1.12 Reaction of BBIH$_2$ with Cu^{2+}, Ni^{2+}, or Pd^{2+} yielded molecular dimers, M$_2$(BBI)$_2$.[41]

An attempt to prepare a MOP using a different bis(β-diketone) ligand, *o*-phenylenebis(acetylacetone) (*o*-pbaH$_2$) (Figure 1.13), by reaction with Cu^{2+}, afforded a

molecular dimer instead of the expected molecular triangle. This dimer exhibits a wide range of colors in the solid state.[42]
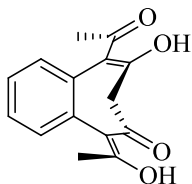
Figure 1.13 *o*-Phenylenebis(acetylacetone), *o*-pbaH$_2$.

A molecular triangle in Figure 1.14 synthesized from the 1,1′-(1,4-phenylene)bis(butane-1,3-dione) ligand (Figure 1.15a) and Cu^{2+} was reported by Clegg et al.[29] The first molecular square to incorporate β-diketone building block was reported by Zhang et al in 1998 (Figure 1.16),[43] and it was prepared by using tetraacetylethane (taeH$_2$) (Figure 1.15b) and an octahedral Co(II) corner that was capped with di-2-pyridylamine (Figure 1.15c).
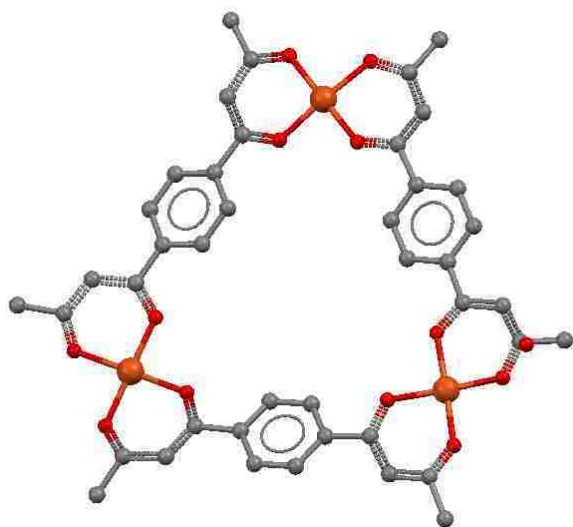
Figure 1.14 The β-diketonate molecular triangle prepared by Clegg et al.[29]
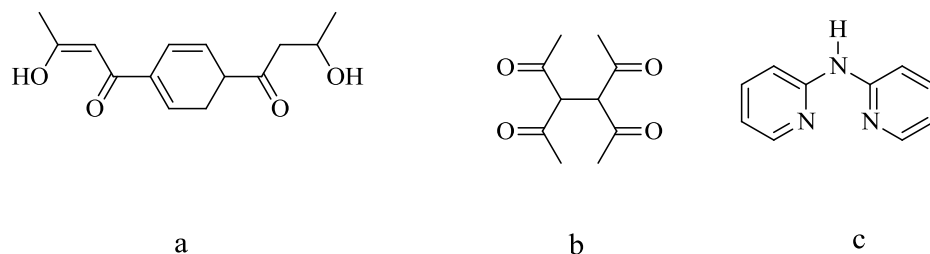
Figure 1.15 Structures of: (a) 1,1′-(1,4′-phenylene)bis(butane-1,3-dione), (b) tetraacetylethane (taeH$_2$) and (c) di-2-pyridylamine (dpa).
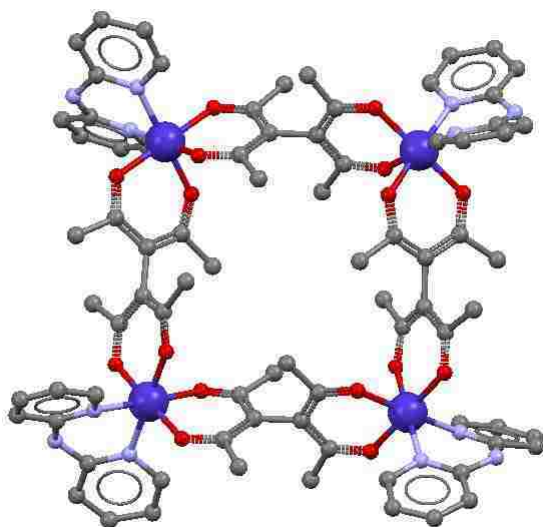
Figure 1.16 Molecular square prepared from Co^{2+}, tae^{2-}, and dpa by Zhang et al.[43]

To date, there are no reports on molecular polygons larger than molecular squares that are derived from β-diketones. We have been interested in porous discrete metal-organic polygons based on multidentate β-diketones.

Here for the first time we report molecular squares based on β-ketoenamine ligands. There are advantages of using β-diketone and β-ketoenamine ligands as building blocks for these molecules. The first one is that their reaction with some metal ions affords complexes with coordinatively unsaturated metal sites. This unsaturation provides room for guest molecules to

10

bind directly to the metal centers. The adducts formed by the reaction of the copper dimer $Cu_2(NBA)_2$ with molecules such as pyrazine and Dabco were early demonstrations of this phenomenon (see Figure 1.17).[44] The ability of the metal centers to bind guest molecules opens pathways for the applications of these molecules in catalysis,[45,46] separations,[47] host-guest chemistry,[44] and gas storage.[2,48]
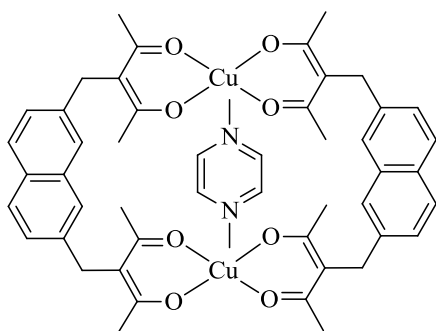
Figure 1.17 Molecular dimer- pyrazine adduct, $[Cu_2(NBA)_2(\mu\text{-}Pz)]$.[44]

The second advantage is that nickel(II) and palladium(II) complexes of β-ketoenamine ligands are diamagnetic which enables them to be studied by NMR.[41,49]

Recently our group reported molecular squares prepared from Cu^{2+} and the bis(β-diketone) ligands **1** (*m*-phenylenebis(acetylacetone)), *m*-pbaH$_2$, and **2** (*m*-phenylenebis(dipropionyl-methane)), *m*-pbprH$_2$ (Figure 1.18).[50] This square is different from the previous squares in two ways: (1) the ligands occupy the corners and the metals form the edges; and (2) the Cu metal centers are not protected and are coordinatively unsaturated, which means they can interact with guest molecules. The new squares bind 4,4'-bipyridine and C_{60};[50] 4,4'-bipyridine is coordinated through its N atoms, while C_{60} is held through π-π interactions. Unfortunately, the squares are soluble only in a limited number of solvents. This limitation

prevents their use in various applications. In addition, a binding constant for the Cu square and C_{60} could not be determined because they are not soluble in the same solvents.
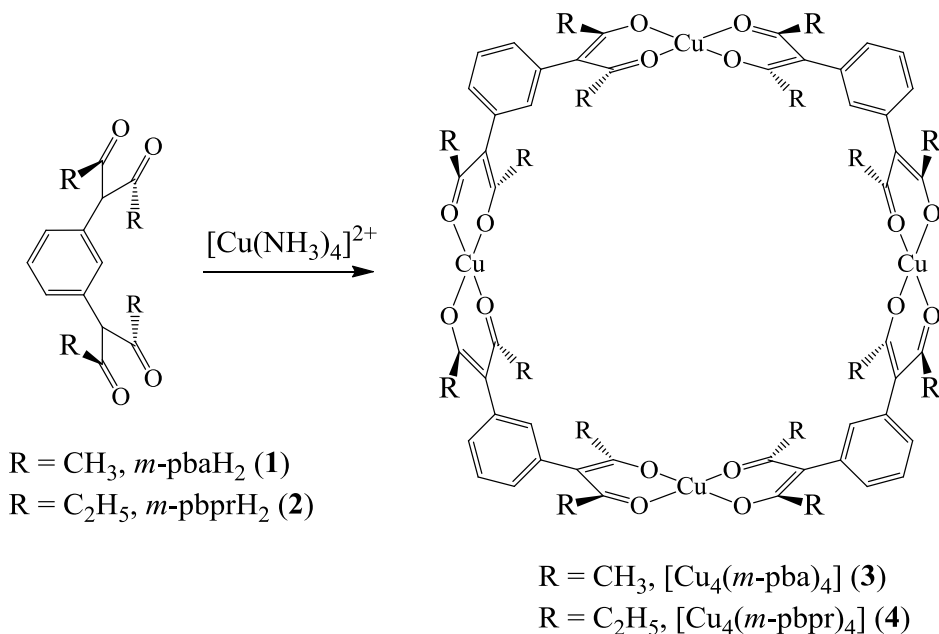
Figure 1.18 Reactions of bis(β-diketone) ligands **1** and **2** with Cu^{2+} afforded molecular squares.[50]

This dissertation reports on the following topics: Syntheses of new derivatives of m-pbaH$_2$ (**1**): In chapter 2, the synthesis of the m-pbhxH$_2$ ligand, with pentyl chains replacing the methyl groups in the β-diketone moieties of m-pbaH$_2$, and the preparation of its molecular square, are described. In chapter 3 syntheses of two new ligands, 2-MeO-m-pbaH$_2$ and 2-MeO-m-pbprH$_2$ (in which a methoxy group is placed in the 2-position of the aromatic ring of m-pbaH$_2$), and their molecular squares are described. Chapter 4 describes the conversion of bis(β-diketones) **1** and **2** to bis(β-ketoenamines). The bis(β-ketoenamines) were treated with Cu^{2+} and Ni^{2+} which afforded molecular squares. The molecular squares have been studied by UV-VIS and by electrochemistry, and the nickel square has been studied by NMR. In an attempt to

prepare molecular squares with larger pore sizes, triphenylamine-based new bis(β-diketones) (Figure 1.19) were prepared and treated with Cu^{2+}. Chapter 5 discusses syntheses of these new bis(β-diketones) and their Cu^{2+} complexes.

R = CH$_3$, tpbaH$_2$
R = C$_2$H$_5$, tpbprH$_2$
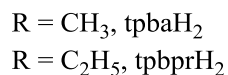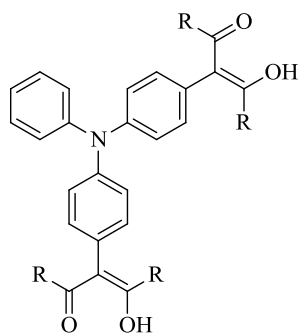
Figure 1.19 Triphenylamine-based bis(β-diketones).

1.1 References

(1)   Thornton, A. W.; Nairn, K. M.; Hill, J. M.; Hill, A. J.; Hill, M. R. *J. Am. Chem. Soc.,* **2009**, *131*, 10662.

(2)   Millward, A. R.; Yaghi, O. M. *J. Am. Chem. Soc.***2005**, *127*, 17998.

(3)   Gordon, P. A.; Saeger, P. B. *Ind. Eng. Chem. Res.,* **1999**, *38*, 4647.

(4)   Martens, J. A.; Verrelst, W. H.; Mathys, G. M.; Brown, S. H.; Jacobs, P. A. *Angew. Chem. Int. Ed.,* **2005**, *44*, 5687.

(5)   Tonigold, M.; Lu, Y.; Bredenkotter, B.; Rieger, B.; Bahnmuller, S.; Hitzbleck, J.; Langstein, G.; Volkmer, D. *Angew. Chem. Int. Ed.,* **2009**, *48*, 7546.

(6)   Dang, D. B.; Wu, P. Y.; He, C.; Xie, Z.; Duan, C. Y. *J. Am. Chem. Soc.,* **2010**, *132*, 14321.

(7)   Shultz, A. M.; Farha, O. K.; Hupp, J. T.; Nguyen, S. T. *J. Am. Chem. Soc.,* **2009**, *131*, 4204.

(8)   Maes, M.; Vermoortele, F.; Alaerts, L.; Couck, S.; Kirschhock, C. E. A.; Denayer, J. F. M.; De Vos, D. E. *J. Am. Chem. Soc.,* **2010**, *132*, 15277.

(9) Lee, C. Y.; Bae, Y. S.; Jeong, N. C.; Farha, O. K.; Sarjeant, A. A.; Stern, C. L.; Nickias, P.; Snurr, R. Q.; Hupp, J. T.; Nguyen, S. T. *J. Am. Chem. Soc.,* **2011**, *133*, 5228.

(10) He, Y.; Xiang, S.; Chen, B. *J. Am. Chem. Soc.,* **2011**, *37*, 14570.

(11) Choi, E. Y.; Barron, P. M.; Novotny, R. W.; Son, H. T.; Hu, C. H.; Choe, W. *Inorg. Chem.,* **2009**, *48*, 426.

(12) Chui, S. S. Y.; Lo, S. M. F.; Charmant, J. P. H.; Orpen, A. G.; Williams, I. D. *Science* **1999**, *283*, 1148.

(13) Eddaoudi, M.; Kim, J.; Rosi, N.; Vodak, D.; Wachter, J.; O'Keeffe, M.; Yaghi, O. M. *Science* **2002**, *295*, 469.

(14) Lin, X.; Telepeni, I.; Blake, A. J.; Dailly, A.; Brown, C. M.; Simmons, J. M.; Zoppi, M.; Walker, G. S.; Thomas, K. M.; Mays, T. J.; Hubberstey, P.; Champness, N. R.; Schroder, M. *J. Am. Chem. Soc.,* **2009**, *131*, 2159.

(15) Sumida, K.; Horike, S.; Kaye, S. S.; Herm, Z. R.; Queen, W. L.; Brown, C. M.; Grandjean, F.; Long, G. J.; Dailly, A.; Long, J. R. *Chem. Sci.,* **2010**, *1*, 184.

(16) Demessence, A.; Long, J. R. *Chem. Eur. J.* **2010**, *16*, 5902.

(17) An, J. Y.; Geib, S. J.; Rosi, N. L. *J. Am. Chem. Soc.,* **2009**, *131*, 8376.

(18) Chae, H. K.; Siberio-Perez, D. Y.; Kim, J.; Go, Y.; Eddaoudi, M.; Matzger, A. J.; O'Keeffe, M.; Yaghi, O. M. *Nature* **2004**, *427*, 523.

(19) Ferey, G.; Mellot-Draznieks, C.; Serre, C.; Millange, F.; Dutour, J.; Surble, S.; Margiolaki, I. *Science* **2005**, *309*, 2040.

(20) Nijkamp, M. G.; Raaymakers, J.; van Dillen, A. J.; de Jong, K. P. *Appl. Phys. Mater. Sci. Proc.* **2001**, *72*, 619.

(21) Chester, A. W.; Clement, P.; Han, S. *US Patent 6136291A.*

(22) Fujita, M.; Yazaki, J.; Ogura, K. *J. Am. Chem. Soc.,* **1990**, *112*, 5645.

(23) Stang, P. J.; Olenyuk, B. *Acc. Chem. Res.,* **1997**, *30*, 502.

(24) Fujita, M.; Oguro, D.; Miyazawa, M.; Oka, H.; Yamaguchi, K.; Ogura, K. *Nature* **1995**, *378*, 469.

(25) Roche, S.; Haslam, C.; Adams, H.; Heath, S. L.; Thomas, J. A. *Chem. Comm.,* **1998**, 1681.

(26) Klausmeyer, K. K.; Wilson, S. R.; Rauchfuss, T. B. *J. Am. Chem. Soc.,* **1999**, *121*, 2705.

(27) Caulder, D. L.; Powers, R. E.; Parac, T. N.; Raymond, K. N. *Angew. Chem. Int. Ed.,* **1998**, *37*, 1840.

(28) Paul, R. L.; Bell, Z. R.; Jeffery, J. C.; McCleverty, J. A.; Ward, M. D. *Proc. Nat. Acad. Sci. USA.,* **2002**, *99*, 4883.

(29) Clegg, J. K.; Lindoy, L. F.; Moubaraki, B.; Murray, K. S.; McMurtrie, J. C. *Dalton Trans.,* **2004**, 2417.

(30) Prakash, M. J.; Zou, Y.; Hong, S.; Park, M.; Bui, M.-P. N.; Seong, G. H.; Lah, M. S. *Inorg. Chem.,* **2009**, *48*, 1281.

(31) Kusukawa, T.; Fujita, M. *J. Am. Chem. Soc.,* **2002**, *124*, 13576.

(32) Eddaoudi, M.; Kim, J.; Wachter, J. B.; Chae, H. K.; O'Keeffe, M.; Yaghi, O. M. *J. Am. Chem. Soc.,* **2001**, *123*, 4368.

(33) Olenyuk, B.; Levin, M. D.; Whiteford, J. A.; Shield, J. E.; Stang, P. J. *J. Am. Chem. Soc.,* **1999**, *121*, 10434.

(34) Schweiger, M.; Seidel, S. R.; Schmitz, M.; Stang, P. J. *Org. Lett.,* **2000**, *2*, 1255.

(35) Bray, D. J.; Antonioli, B.; Clegg, J. K.; Gloe, K.; Gloe, K.; Jolliffe, K. A.; Lindoy, L. F.; Wei, G.; Wenzel, M. *Dalton Trans.,* **2008**, 1683.

(36) Fiedler, D.; Bergman, R. G.; Raymond, K. N. *Angew. Chem. Int. Ed.,* **2004**, *43*, 6748.

(37) Ito, H.; Kusukawa, T.; Fujita, M. *Chem. Lett.,* **2000**, 598.

(38) Uehara, K.; Kasai, K.; Mizuno, N. *Inorg. Chem.,* **2007**, *46*, 2563.

(39) Slone, R. V.; Hupp, J. T.; Stern, C. L.; Albrecht-Schmitt, T. E. *Inorg. Chem.,* **1996**, *35*, 4096.

(40) Maverick, A. W.; Klavetter, F. L. *Inorg. Chem.,* **1984**, *23*, 4129.

(41) Bradbury, J. R.; Hampton, J. L.; Martone, D. P.; Maverick, A. W. *Inorg. Chem.,* **1989**, *28*, 2392.

(42) Pariya, C.; Fronczek, F. R.; Maverick, A. W. *Inorg. Chem.,* **2011**, *50*, 2748.

(43) Zhang, Y. S.; Wang, S. N.; Enright, G. D.; Breeze, S. R. *J. Am. Chem. Soc.,* **1998**, *120*, 9398.

(44)   Maverick, A. W.; Buckingham, S. C.; Yao, Q.; Bradbury, J. R.; Stanley, G. G. *J. Am. Chem. Soc.,* **1986**, *108*, 7430.

(45)   Merlau, M. L.; Mejia, M. D. P.; Nguyen, S. T.; Hupp, J. T. *Angew. Chem. Int. Ed.,* **2001**, *40*, 4239.

(46)   Horike, S.; Dinca, M.; Tamaki, K.; Long, J. R. *J. Am. Chem. Soc.,* **2008**, *130*, 5854.

(47)   Maes, M.; Vermoortele, F.; Alaerts, L.; Denayer, J. F. M.; De Vos, D. E. *J. Phys. Chem., C* **2011**, *115*, 1051.

(48)   Panella, B.; Hirscher, M.; Putter, H.; Muller, U. *Adv. Funct. Mater.,* **2006**, *16*, 520.

(49)   Bennett, A. M. A.; Foulds, G. A.; Thornton, D. A. *Polyhedron* **1989**, *8*, 2305.

(50)   Pariya, C.; Sparrow, C. R.; Back, C.-K.; Sandi, G.; Fronczek, F. R.; Maverick, A. W. *Angew. Chem. Int. Ed.,* **2007**, *46*, 6305.

Chapter 2: Synthesis of a Long-Chain Bis(β-Diketone) for a More Soluble Molecular Square

2.1 Introduction

The ligands *m*-phenylenebis(acetylacetone), *m*-pbaH$_2$ (**1**) and *m*-phenylenebis(dipropionyl-methane), *m*-pbprH$_2$ (**2**) yield molecular squares with formula Cu$_4$L$_4$ (LH$_2$ = *m*-pbaH$_2$ or *m*-pbprH$_2$) when treated with Cu^{2+} ions (Figure 2.1). The squares were shown to form adducts with guest molecules such as 4,4'-bipyridine and C$_{60}$.[1] Solubility of the two squares is limited to a small number of solvents: Cu$_4$(*m*-pba)$_4$ (**3**) is only soluble in chloroform and dichloromethane, and solubility of Cu$_4$(*m*-pbpr)$_4$ (**4**) is only slightly better.

R = CH$_3$, *m*-pbaH$_2$ (**1**)
R = C$_2$H$_5$, *m*-pbprH$_2$ (**2**)

R = CH$_3$, [Cu$_4$(*m*-pba)$_4$] (**3**)
R = C$_2$H$_5$, [Cu$_4$(*m*-pbpr)$_4$] (**4**)
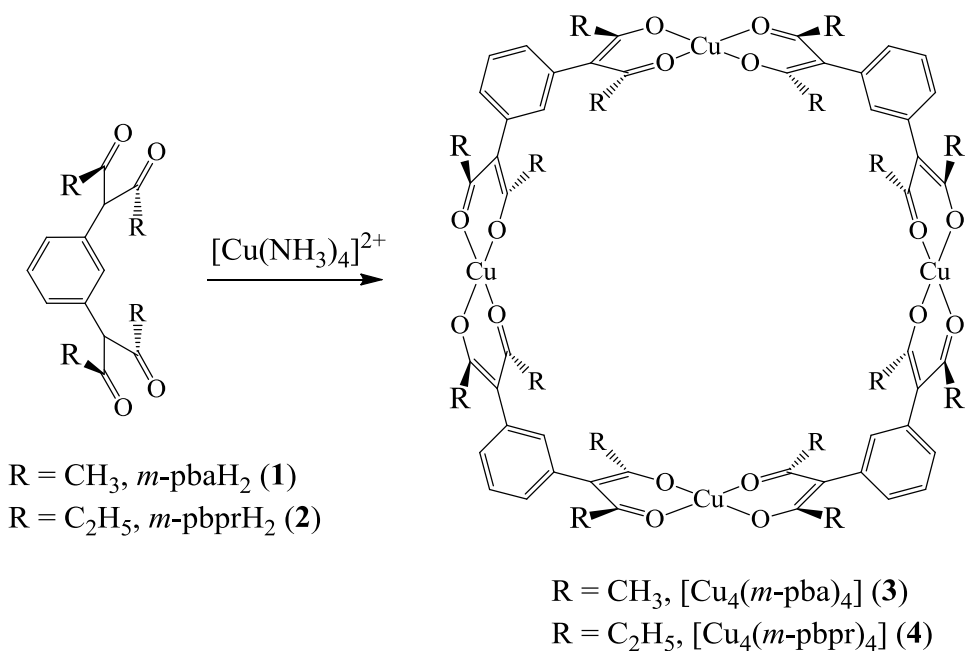
Figure 2.1 Bis(β-diketones), *m*-pbaH$_2$ (**1**) and *m*-pbprH$_2$ (**2**) react with Cu^{2+} to yield molecular squares.

This chapter reports the preparation of a bis(β-diketone) with longer alkyl groups, *m*-pbhxH$_2$ (*m*-phenylenebis(dihexanoylmethane), **5**), as shown in Figure 2.2. I expected its copper

square, $Cu_4(m\text{-pbhx})_4$, to be soluble in a wider range of solvents. The more soluble molecular square will enable us to study its reactions with a variety of guest molecules.
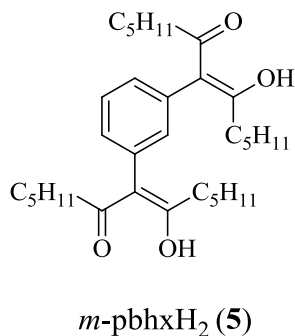
m-pbhxH$_2$ (**5**)

Figure 2.2 m-phenylenebis(dihexanoylmethane), m-pbhxH$_2$ ligand **5**.

The procedure for making **1** and **2** is well established and is achieved in two steps. First, a commercially available α-diketone (butane-2,3-dione (**6**) or hexane-3,4-dione (**7**)) is treated with trimethyl phosphite, which affords 2,2,2-trimethoxy-4,5-dimethyl-1,3,2-dioxaphospholene[2,3] (**8**) or 2,2,2-trimethoxy-4,5-diethyl-1,3,2-dioxaphospholene (**9**)[1] respectively; both are commonly referred to as phospholenes. Then treatment of isophthalaldehyde (**10**) with the phospholene yields m-pbaH$_2$ (**1**) or m-pbprH$_2$ (**2**) (scheme 2.1).

To make the new ligand m-pbhxH$_2$ (**5**) by this method, the α-diketone dodecane-6,7-dione (**12**) was required as the starting material (see scheme 2.2). Then the two steps shown in scheme 2.1 above were followed: treating dodecane-6,7-dione with trimethyl phosphite to generate the phospholene 2,2,2-trimethoxy-4,5-dipentyl-1,3,2-dioxaphospholene (**13**), followed by treatment with isophthalaldehyde to yield the desired product. Since the starting material (dodecane-6,7-dione) is not commercially available, I had to prepare it by oxidation of 6-dodecyne (**11**).

1.

R = CH$_3$, Butane-2,3-dione (**6**)

R = C$_2$H$_5$, Hexane-3,4-dione (**7**)

R = CH$_3$, 2,2,2-trimethoxy-4,5-dimethyl-1,3,2-dioxaphospholene (**8**)

R = C$_2$H$_5$, 2,2,2-trimethoxy-4,5-diethyl-1,3,2-dioxaphospholene (**9**)

2.

Isophthalaldehyde (**10**)

1.

2. MeOH, heat

R = CH$_3$, *m*-pbaH$_2$ (**1**)

R = C$_2$H$_5$, *m*-pbprH$_2$ (**2**)
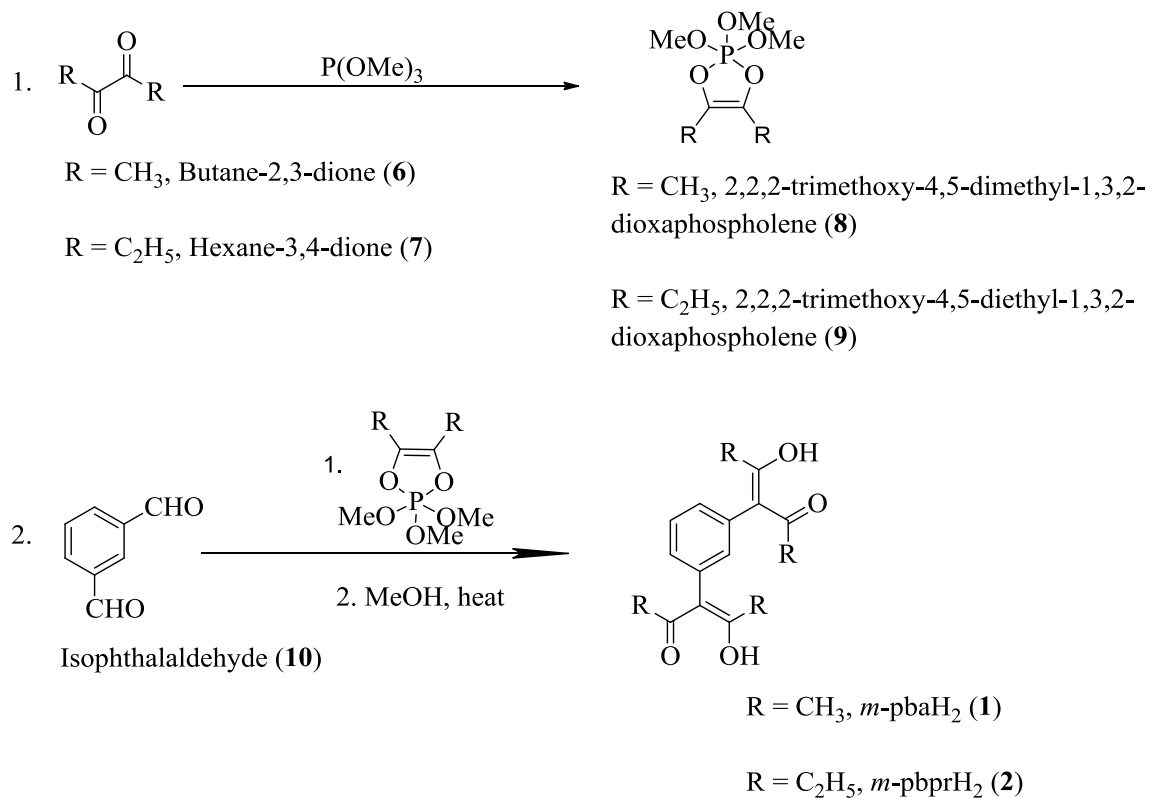
Scheme 2.1 Synthesis of bis(β-diketones) **1** and **2** beginning with α-diketones.

2.2 Results and Discussion

β-Diketones are normally viewed as good ligands, binding readily to many metal ions. However, β-diketones with bulky substituents in the 1, 3, and 5 positions do not always form complexes easily. For example, referring to the illustration in Figure 2.3, ligands such as *m*-xbaH$_2$ with CH$_3$,ArCH$_2$,CH$_3$ substituents in the 1, 3, and 5 positions, and ligands such as *m*-pbaH$_2$ and *m*-pbprH$_2$ with CH$_3$,Ar,CH$_3$ or Et,Ar,Et substituents (see Figure 2.1), form complexes easily. In addition, β-diketones with bulky substituents in the 1 and 5 positions and no substituents in the 3-positions also react with metal ions. Those ligands include dipivaloylmethane (dpmH, t-Bu,H,t-Bu) and dibenzoylmethane (dbmH, Ph,H,Ph). However, β-

diketones with bulky substituents in the 1 and 5 positions and a substituent in the 3-positions are much less likely to form metal complexes, due to steric interference between the substituents. This was observed in ligands such as *m*-xbpH$_2$ (t-Bu,ArCH$_2$,t-Bu) and *m*-xbdH$_2$ (Ph,ArCH$_2$,Ph).

m-XbaH$_2$

a

dipivaloylmethane (dpmH)

b

dibenzoylmethane (dbmH)

c

R = t-Bu, *m*-XbpH$_2$
R = Ph, *m*-XbdH$_2$

d
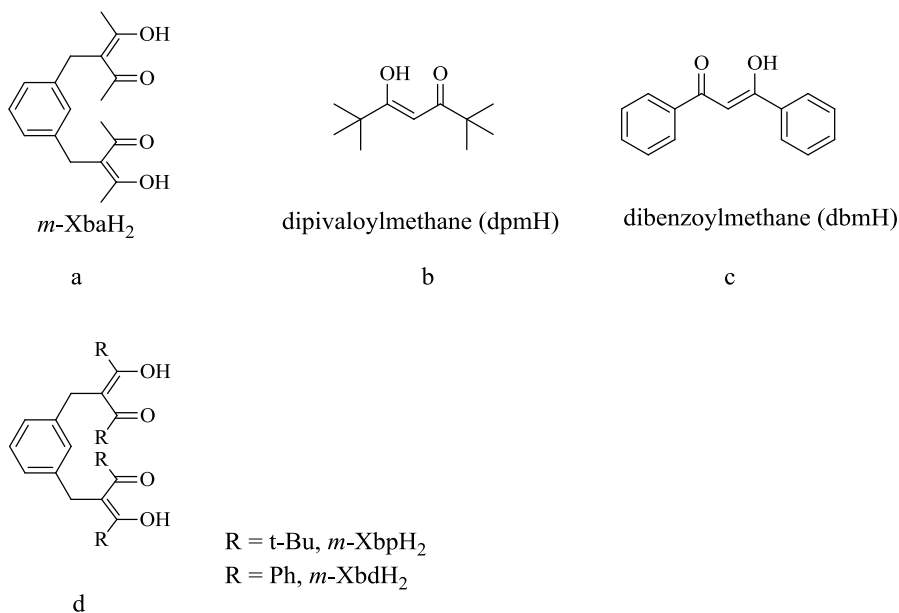
Figure 2.3 β-diketones: (a-c) generate metal complexes, (d) do not generate metal complexes.

Therefore, if we wished to increase the solubility of our molecular squares by modifying the 1 and 5 substituents in our *m*-pbaH$_2$ ligand, we could not use bulky groups like i-Pr, t-Bu, or Ph. This is because such substituent patterns (e.g. t-Bu,Ar,t-Bu) would have been highly hindered and unlikely to make metal complexes. Hence, we focused on linear alkyl groups in the 1 and 5 positions.

To choose a specific linear alkyl group, we noted that the solubility of Cu$_4$(*m*-pba)$_4$ (R = CH$_3$) and Cu$_4$(*m*-pbpr)$_4$ (R = CH$_2$CH$_3$) is similar. Thus, if we wished to change the solubility substantially, a significantly longer R group would probably be necessary. For this reason, we chose R = pentyl (CH$_2$CH$_2$CH$_2$CH$_2$CH$_3$) for our experiments.

Dodecane-6,7-dione (**12**) has been reported, and is prepared via the Grignard route;[4] I tried to repeat this but found the method to be problematic. Instead, I found the $NaIO_4$ method[5] and used it successfully. Briefly, treatment of 6-dodecyne (**11**) with $NaIO_4$ and a catalytic amount of $RuO_2 \cdot H_2O$ in $CCl_4/CH_3CN/H_2O$ solvent mixture in 1:1:1.5 ratios yielded dodecane-6,7-dione (**12**) as a yellow solid (60%). ^1H NMR and GC/MS of the product match those reported for the authentic compound.[4] The yield (60%) is slightly higher than that reported in the literature.[4] Treatment of dodecane-6,7-dione with trimethyl phosphite afforded the desired phospholene, 2,2,2-trimethoxy-4,5-dipentyl-1,3,2-dioxaphospholene (**13**), which reacted with isophthalaldehyde to yield *m*-pbhxH$_2$ (**5**), as a colorless oil after column chromatography. Synthesis of **5** starting with the oxidation of 6-dodecyne is summarized in scheme 2.2.
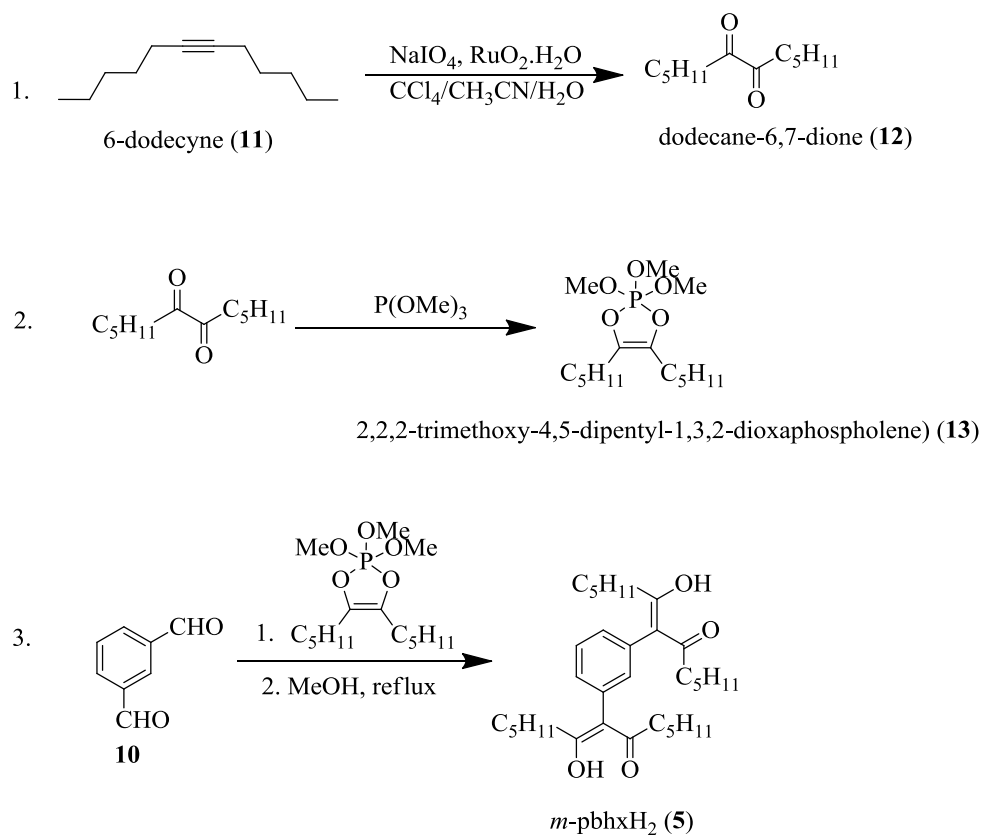
Scheme 2.2 Synthesis of **5** starting with oxidation of 6-dodecyne.

21

When **5** was treated with Cu^{2+}, molecular square **14** (Figure 2.4) was isolated as a dark green solid (97%).

R = C_5H_{11}, [Cu_4(*m*-pbhx)$_4$ (**14**)
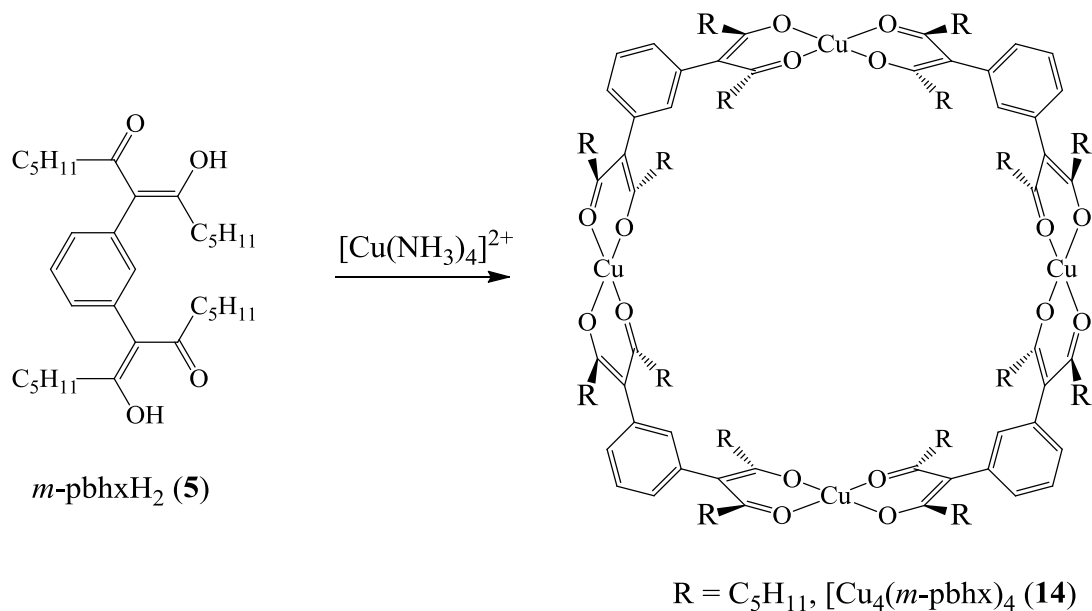
Figure 2.4 Reaction of *m*-pbhxH$_2$ ligand (**5**) with Cu^{2+} affords molecular square **14**.

After obtaining square **14**, the next step was to test its solubility in various solvents, in comparison with the solubility of molecular squares **3** and **4**, and the results are summarized in table 2.1. The new square **14** is soluble in nine organic solvents. The increase in solubility of square **14** is attributed to the presence of the pentyl chains attached to the β-diketone moieties of **5**. All three squares are insoluble in polar solvents such as methanol, acetonitrile and DMF. Other groups have used functional substituents such as alkoxy (OR, R = alkyl),[6,7], and polyethyleneglycol (PEG),[8] in the ligands to enhance solubility of the resulting macrocycles. Macrocycles containing these substituents are often soluble in polar solvents such as water.

Crystals of the new square Cu_4(*m*-pbhx)$_4$ suitable for X-ray diffraction were grown by layering its chloroform solution with methanol. Single crystal X-ray analysis revealed the square,

where two methanol are coordinated to two copper atoms and the remaining two copper atoms are uncoordinated, with the molecular formula $[Cu_4(m\text{-pbhx})_4(CH_3OH)_2]\cdot12CHCl_3$ (see Figure 2.5). For comparison, the crystal structure of square **4** is shown in Figure 2.6.

Table 2.1 Solubility of molecular squares **3**, **4** and **14** in various solvents.

Solvent			
	Square **3** $[Cu_4(m\text{-pba})_4]$	Square **4** $[Cu_4(m\text{-pbpr})_4]$	square **14** $[Cu_4(m\text{-pbhx})_4]$
Chloroform	Soluble	Soluble	Soluble
Dichloromethane	Soluble	Soluble	Soluble
Toluene	Insoluble	Insoluble	Soluble
o-dichlorobenzene	Insoluble	Insoluble	Soluble
Tetrahydrofuran	Insoluble	Insoluble	Soluble
Benzene	Insoluble	Insoluble	Soluble
Bromobenzene	Insoluble	Insoluble	Soluble
Chlorobenzene	Insoluble	Insoluble	Soluble
Carbon disulfide	Insoluble	Insoluble	Soluble
Methanol	Insoluble	Insoluble	Insoluble
Acetonitrile	Insoluble	Insoluble	Insoluble
DMF	Insoluble	Insoluble	Insoluble

Figure 2.5 Crystal structure of the molecular square [Cu$_4$(*m*-pbhx)$_4$(CH$_3$OH)$_2$] (**14**). Hydrogen atoms and solvent molecules have been removed for clarity.
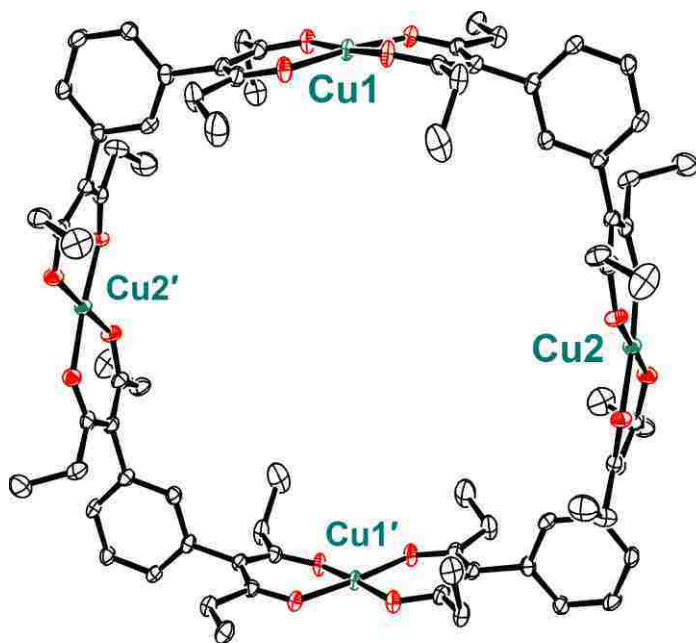
Figure 2.6 Crystal structure of [Cu$_4$(*m*-pbpr)$_4$] (**4**).[1]

Cu---Cu distances in squares **4** and **14** are shown in table 2.2.

Table 2.2 Cu---Cu distances in squares **4** and **14**.

Molecular square	Cu1---Cu1' (Å)	Cu2---Cu2'(Å)
4	14.012	14.661
14	14.047	14.904

The crystal structure of **14** shows that the pentyl groups of the β-diketones coordinated to Cu1 and Cu1' are bent inwards towards the cavity of the square, while those from groups coordinated to Cu2 and Cu2' are bent away from the cavity. This probably is due to steric interaction between these groups. The Cu2---Cu2' distance is slightly longer (14.90 Å) than in Cu1---Cu1' (14.05 Å) due to the slight distortion at Cu2 and Cu2' centers resulting from coordination of methanol leading to square pyramidal geometry at these centers.

2.3 Host-Guest Reactions of Square 14

Square **14** was treated with a large variety of guest molecules (see table 2.3) and the observations made can be classified into three categories: 1) In the first case, green precipitates formed which were suspected to be the unreacted square **14**. These were not analyzed but were collected and used for other experiments. (2) In other cases the solutions changed color, but no product precipitated. (3) In the third case crystals formed that were analyzed by single crystal X-ray. The guests chosen were in two categories: Those that were expected to bind directly to the Cu atoms include 1,2-bis(4-pyridyl)ethylene (bpe) and polyoxometalate, $W_6O_{19}^{2-}$. The $W_6O_{19}^{2-}$ was expected to bind to the coordinatively unsaturated Cu(II) centers via the four equatorial oxygen atoms.[9] Other guest molecules such as anthracene might bind in a π fashion.

Table 2.3 Host-guest experiments with square **14**

#	Complex solvent	Other solvent	Guest	Observation
1	$CHCl_3$	CH_3CN	bpe	Blue crystals formed after 10 days
2	$CHCl_3$	CH_3CH_2CN	bpe	Blue crystals formed
3	$CHCl_3$	CH_3CN	4,4'-bpy	Green crystals formed
4	CS_2	cyclohexane	anthracene	blue-green crystals formed
5	CH_2Cl_2	Hexanes	Anthracene	Green precipitate
6	Toluene	Ethyl acetate	Anthracene	Green precipitate
7	C_6H_5Cl	cyclohexane	Anthracene	Green precipitate
8	C_6H_5Br	Ethyl acetate	Anthracene	Green precipitate
9	$CHCl_3$	CH_3CN	2,7-dihydroxynaphthalene	Dark-blue solution which turned brown and deposited brown powder
10	$CHCl_3$	CH_3COCH_3	2,7-dihydroxynaphthalene	Same observation as 8
11	Toluene	CH_3CN	2,7-dihydroxynaphthalene	Same observation as 8
12	THF	CH_3CN	2,7-dihydroxynaphthalene	Same observation as 8
13	Toluene	MeOH	2-naphthol	Same observation as 9

Table 2.3 (continued)

14	CHCl$_3$	MeOH	2-naphthol	Same observation as 9
15	C$_6$H$_5$Cl	MeOH	Adamantanol	Green precipitate
16	*o*- C$_6$H$_4$Cl$_2$	CH$_3$CN	C$_{70}$	Dark brown crystals
17	*o*-C$_6$H$_4$Cl$_2$	CH$_3$CN	C$_{60}$	Dark brown crystals
18	Toluene	Ethyl acetate	1,4-dinitrobenzene	Green precipitate
19	CHCl$_3$	MeOH	1,4-dicyanobenzene	Green precipitate
20	Toluene	Ethyl acetate	1,3-dicyanobenzene	Green precipitate
21	CH$_2$Cl$_2$	CH$_3$COCH$_3$	Cyclohexane-1,4-dicarbonitrile	Green precipitate
22	C$_6$H$_5$Cl	CH$_3$CN	Adamantanemethanol	Green precipitate
23	Toluene	Methyl-cyclohexane	9,10-dibromoanthracene	Green precipitate
24	CHCl$_3$	Ether	9,10-diphenylanthracene	Green precipitate
25	THF	CH$_3$CN	W$_6$O$_{19}$$^{2-}$	Blue precipitate
26	CHCl$_3$	DMSO	W$_6$O$_{19}$$^{2-}$	Green precipitate
27	Toluene	CH$_3$CN	W$_6$O$_{19}$$^{2-}$	Green precipitate
28	CHCl$_3$	DMF	W$_6$O$_{19}$$^{2-}$	Blue crystals formed
29	CHCl$_3$	MeOH	bpa	Blue crystals formed
30	CHCl$_3$	MeOH	Cyclohexane-1,4-dicarbonitrile	Blue crystals formed

When **14** was treated with guests such as anthracene/anthracene derivatives, adamantanol or dicyanobenzenes, green precipitates formed. When solutions of **14** in different solvents were layered with 2-naphthol or 2,7-dihydroxynaphthalene in acetonitrile or methanol (colorless solutions), the solutions (all initially dark green, except for the solution in THF, which was blue) changed to dark blue within a day, then to brown and eventually brown powder precipitated after a few days. The change in color of the solutions from dark green or blue to dark blue could indicate a strong interaction between the Cu^{2+} centers of the square and the OH groups of the two guests which eventually led to the decomposition of the square as indicated by deposition of brown powder. The square is blue in THF probably because THF through its oxygen atom coordinates to the Cu^{2+} centers of the square changing their coordination geometry from square planar to square pyramidal or octahedral.

Green crystals that formed between the square and 4,4'-bipyridine (Number 3) were not of good quality for X-ray study. Blue-green crystals formed between **14** in carbon disulfide and anthracene in methyl cyclohexane (number 4) but did not diffract well when analyzed by single crystal X-ray. The crystals that formed in number 28 turned out to be a copper cluster, where 12 Cu-carboxylate dimer subunits (paddle-wheel units) combined to generate a Cu_{24} cluster. The carboxylates in this compound are 1,3-benzenedicarboxylate, which was likely formed by oxidative cleavage of the *m*-pbhx ligands in **14**. This Cu_{24} cluster has been studied previously by Zaworotko and co-workers,[10] and it was not studied further here. This may suggest that DMF may not be a good solvent for layering these experiments. Analysis of the crystals in number 30 revealed the host without the guest (see Figure 2.5).

Crystals for single crystal X-ray diffraction were obtained in the following experiments: A solution of the square **14** in chloroform (dark-green) layered with 1,2-bis(4-pyridyl)ethylene

(bpe) or 1,2-bis(4-pyridyl)ethane (bpa) in methanol afforded blue block-shaped crystals. The change in color from dark-green to blue is the usual observation for Cu(β-diketonate)$_2$N formation.[11] Single crystal X-ray analysis of the crystals confirms formation of adducts, **14**-bpe and **14**-bpa, (**15** and **16** respectively) where one bpe or bpa ligand bridges two copper atoms in the square. The two remaining copper atoms of the square have methanol co-ordinated to them from outside (Figures 2.7 and 2.8). This is different from the previously reported adduct of square **3** with 4,4'-bipyridine (**17**)[1] (see Figure 2.9), in which bpy molecules were also coordinated externally. Indeed, under slightly different experimental conditions, crystals of Cu$_4$(*m*-pbhx)$_4$(μ-bpe) were obtained with both internally and externally coordinated bpe ligands. However, these crystals were of lower quality than those of **15**, and those results are not included here.
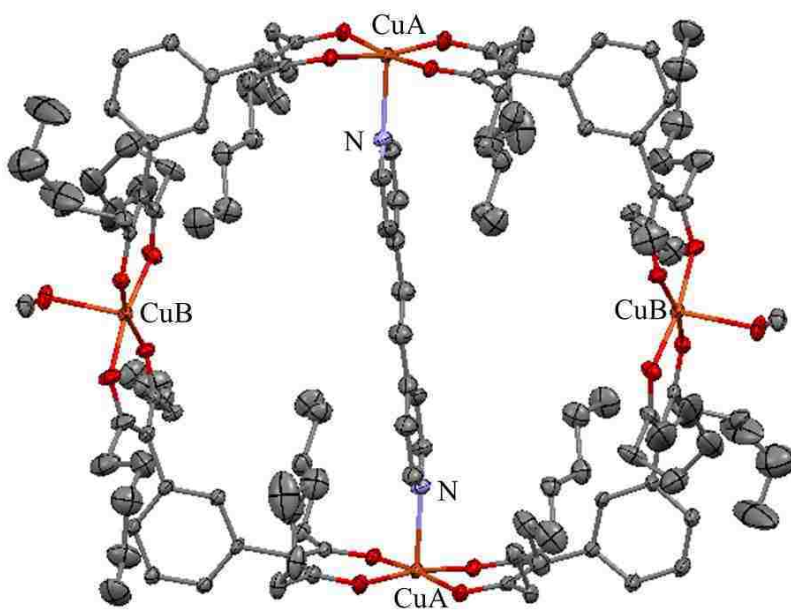
Figure 2.7 Crystal structure of [Cu$_4$(*m*-pbhx)$_4$(μ-bpe)(CH$_3$OH)$_2$] (**15**). H atoms and solvent molecules omitted for clarity.
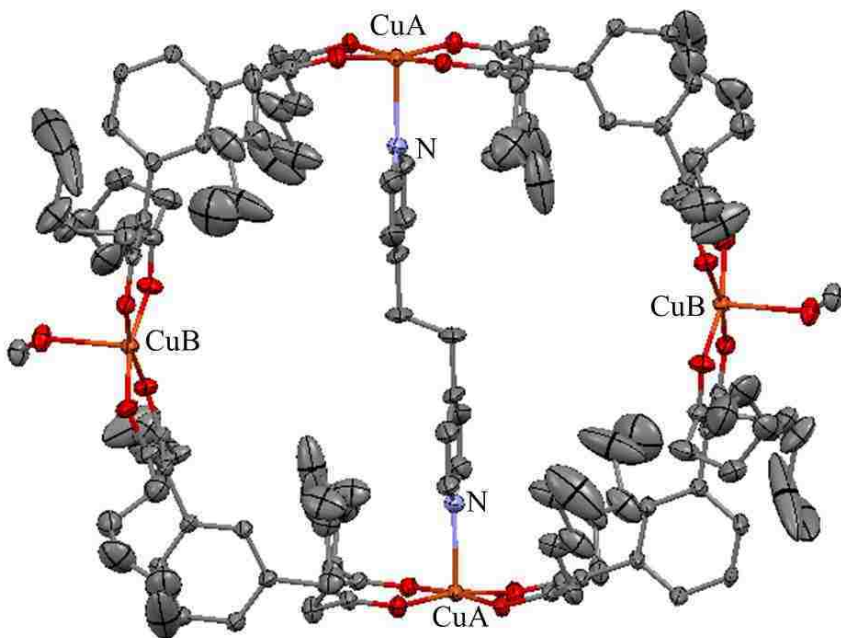
Figure 2.8 Crystal structure of [Cu$_4$(*m*-pbhx)$_4$(μ-bpa)(CH$_3$OH)$_2$] (**16**). H atoms and solvent molecules omitted for clarity.
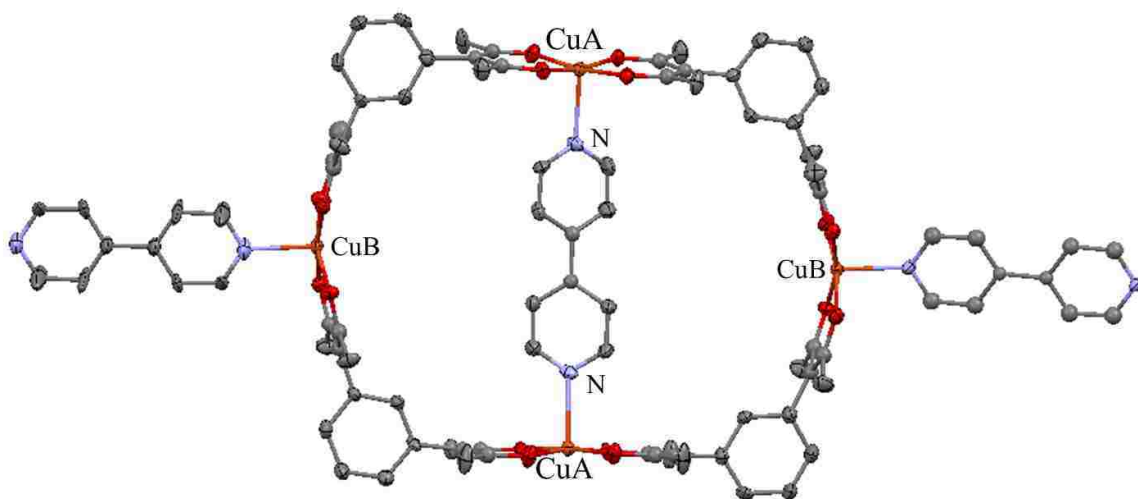
Figure 2.9 Crystal structure of [Cu$_4$(*m*-pba)$_4$(4,4'-bpy)$_2$]$_n$ (**17**).[1] Hydrogen and solvent molecules have been omitted.

Table 2.4 X-ray crystallographic and structure refinement data for **14**.solvate and **16**.solvate

compound	**14**.solvate	**16**.solvate
empirical formula	$C_{128}H_{192}Cu_4O_{16}$ $\cdot 2CH_3OH \cdot 12CHCl_3$	$C_{128}H_{192}Cu_4O_{16}$ $\cdot 2CH_4O.C_{12}H_{12}N_2 \cdot 10CHCl_3$
formula weight	3737.68	3682.98
crystal system	Triclinic	Triclinic
space group	$P\bar{1}$	$P\bar{1}$
a, Å	18.9177(6)	15.0928(7)
b, Å	19.2984(6)	18.3346(8)
c, Å	28.0714(9)	19.5430(8)
α, deg	70.560(2)	63.868(2)
β, deg	76.612(2)	87.850(2)
γ, deg	68.315(2)	68.842(2)
V, Å^3	8911.0(5)	4480.0(3)
Z	2	1
T, K	90	90
D_{calcd}, g cm^{-3}	1.392	1.365
cryst dimen, mm	0.32x0.22x0.14	0.46x0.35x0.18
θ limits, deg	3.6<θ<68.0	3.38<θ<67.80
Rflns, meas/unique/obs	83006/30984/25182	32739/15469/13313
Data/param	30984/1803	15469/983
μ, mm^{-1}	5.945	5.105
R ($I > 2\sigma(I)$)	0.0770	0.0834
R_w (all data)	0.2280	0.2328
GOF	1.445	1.053

Table 2.5 Measured Cu---Cu and Cu-N distances (Å) in adducts **15**, **16** and **17**.

Compound	CuA---CuA	CuB---CuB	Cu-N
15 [Cu$_4$(*m*-pbhx)$_4$(μ-bpe)(CH$_3$OH)$_2$]	13.989	14.666	2.300
16 [Cu$_4$(*m*-pbhx)$_4$(μ-bpa)(CH$_3$OH)$_2$]	13.793	15.077	2.278
17 [Cu$_4$(*m*-pba)$_4$(4,4'-bpy)$_2$]$_n$	11.807	16.226	2.360, 2.363

The CuA---CuA distance in adduct **17** is shorter (11.81 Å) than in adducts **15** and **16** (13.99 and 13.79 Å) because 4,4'-bipyridine is shorter than bpe or bpa, so CuA and CuA atoms are distorted more in **17** than in **15** or **16** in order to coordinate to the nitrogen atoms of 4,4'-bpy leading to a shorter distance.

On the other hand, the CuB---CuB distances behave in the opposite way: adduct **17** has a longer distance (16.23 Å) than in adducts **15** and **16** (14.67 and 15.08 Å respectively) because of coordination of 4,4'-bpy to CuB atoms from outside of the square. The Cu-N distances in **15** (2.30 Å) and in **16** (2.278 Å) are shorter than the corresponding distances in **17** (2.360 and 2.363 Å) on account of the size of bpe and bpa guests which are longer, hence their nitrogen atoms are closer to the copper atoms.

Crystals formed when the square was treated with C$_{60}$ or C$_{70}$ were also analyzed by single crystal X-ray diffraction. The crystals of the square with C$_{70}$ did not diffract well, while a preliminary structure of the square with C$_{60}$ is shown in Figures 2.10 and 2.11 below.
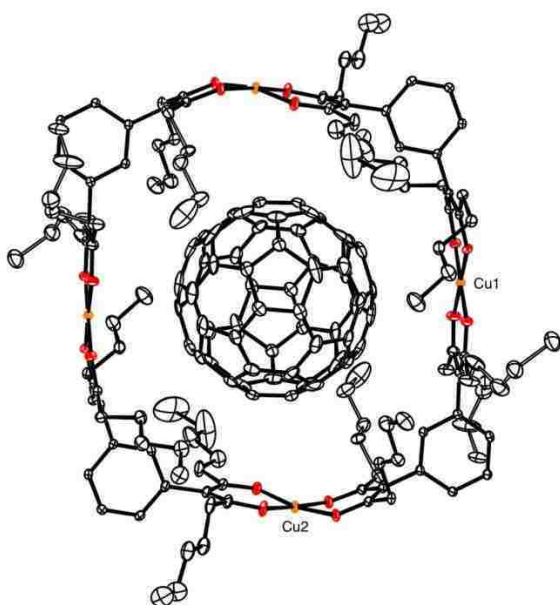
Figure 2.10 Crystal structure of $Cu_4(m\text{-pbhx})_4 \cdot C_{60}$.
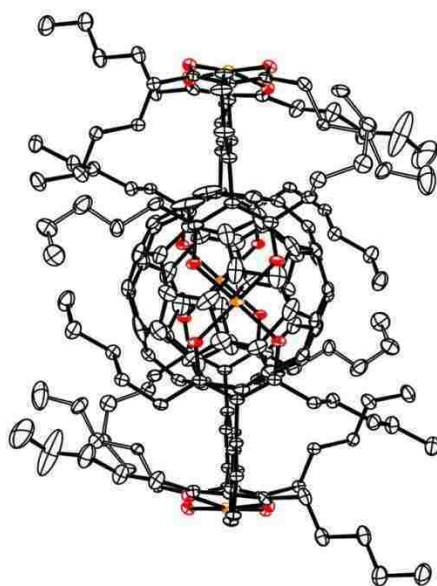
Figure 2.11 Crystal structure of $Cu_4(m\text{-pbhx})_4 \cdot C_{60}$. View perpendicular to that in Figure 2.10.

2.3 Experimental

2.3.1 General Considerations

Sodium metaperiodate (NaIO$_4$) was purchased from Sigma-Aldrich, ruthenium(IV) oxide hydrate was purchased from Acros Organics, and 6-dodecyne was acquired from GFS Chemicals. Elemental analysis was performed by M-H-W Labs, Phoenix, Arizona. NMR spectra were recorded on Bruker (250 or 400 MHz) spectrometers with CDCl$_3$ as the solvent.

2.3.2 Synthesis of Dodecane-6,7-dione (12)

This molecule was made following the reported procedure for making other α-diketones.[5] 6-Dodecyne (5.0 g, 30.0 mmol) was added to CCl$_4$/CH$_3$CN/H$_2$O (40 mL: 40 mL: 60 mL) and the mixture stirred for 10 minutes at room temperature. Into this mixture was added solid NaIO$_4$ (25.72 g, 120.0 mmol) and stirring continued vigorously at room temperature until the solid dissolved, giving two colorless phases. Then RuO$_2$.H$_2$O (0.088 g, 0.66 mmol) was added; immediately, the mixture turned black. Ten minutes later, the color of the mixture changed to dark green and a white solid precipitated out. As stirring continued, the mixture gradually changed to lighter green and finally to yellow. After 12 h, CH$_2$Cl$_2$ (50 mL) was added and the mixture was separated into two phases, and the organic phase was dried over Na$_2$SO$_4$, filtered and evaporated to yield a yellow solid. Column chromatography (hexane:ethyl acetate, 70:30 v/v), gave a yellow solid, 3.57 g (60%). ^{1}H NMR confirmed the identity of the product.[4] ^{1}H NMR: δ 2.73 (t, 4H), 1.58 (q, 4H), 1.36-1.26 (m, 8H), 0.89 (t, 6H) (Figure A4).

2.3.3 Synthesis of 2,2,2-trimethoxy-4,5-dipentyl-1,3,2-dioxaphospholene (13)

Trimethyl phosphite (2.06 g, 16.64 mmol) was cooled to 0 °C (ice/water). Dodecane-6,7-dione (3.0 g, 15 mmol) dissolved in dry DCM (20 mL) was added dropwise from an addition

flask and the reaction mixture allowed to warm to room temperature under nitrogen; stirring was continued for 24 h. Completion of the reaction was indicated by the disappearance of the yellow color. The crude product was isolated as an oil by evaporation of solvent; its ^{1}H NMR spectrum (δ 3.59 (d, 9H, OCH_3), 2.17 (t, 4H), 1.51 (q, 4H), 1.34-1.26 (m, 8H), 0.89 (t, 6H)) (Figure A5) indicated that it was sufficiently pure for use in the next step.

2.3.4 Synthesis of *m*-pbhxH$_2$ (5)

Isophthalaldehyde (0.60 g, 4.47 mmol) was dissolved in dry DCM (20 mL), followed by addition of 2,2,2-trimethoxy-4,5-dipentyl-1,3,2-dioxaphospholene (2.88 g, 8.94 mmol). The mixture was stirred at room temperature under nitrogen and monitored by ^{1}H NMR. Reaction was judged to be complete when the isophthalaldehyde CHO peak (~10 ppm) had disappeared (ca. 12 h). Then methanol (30 mL) was added and the mixture refluxed for 3 h; solvent was removed to yield a light-brown oily product. Column chromatography (hexane-ethyl acetate, 70:30 v/v) yielded **5** as a colorless oil, 1.00 g (45%). ^{1}H NMR: δ 16.81 (s, 2H), 7.42 (t, 1H), 7.14 (dd, 2H, J = 7.59, 1.41 Hz), 7.00 (s, 1H), 2.10 (t, 8H), 1.52 (q, 8H), 1.25-1.12 (m, 16H), 0.82 (t, 12H) (Figure A3).

2.3.5 Synthesis of Copper Molecular Square, Cu$_4$(*m*-pbhx)$_4$ (14)

CuSO$_4$·5H$_2$O (0.401 g, 1.6 mmol) was dissolved in 30 mL distilled water; ammonia solution was added in drops with stirring until a royal blue solution was formed. Into this solution was added a solution of *m*-pbhxH$_2$ (**5**) (0.8 g, 1.6 mmol) in DCM (40 mL) and stirring continued for 4 h; the olive green organic phase was dried over Na$_2$SO$_4$ and the solvent removed to yield a dark green solid, 0.87 g (97%). Anal. Calcd. for C$_{128}$H$_{192}$O$_{16}$Cu$_4$ (M = 2241.07): C 68.60, H 8.64; Found: C 68.42, H 8.51. Crystals for X-ray analysis were grown by layering

methanol on a chloroform solution. Anal. Calcd. for (Cu$_4$(m-pbhx)$_4$·2CH$_3$OH, M = 2305.15): C 67.73, H 8.75; Found: C 68.00, H 8.64.

2.3.6 Synthesis of Adducts

a) **14**-bpe (**15**): Square **14** (0.020 mg, 0.008 mmol) was dissolved in chloroform (2 mL); this was layered with 1,2-bis(4-pyridyl)ethylene (0.006 g, 0.03 mmol) in methanol (3 mL). The solution was left for 10 days at −20 °C, and blue block-shaped crystals had formed. Anal.Calcd. for (Cu$_4$(m-pbhx)$_4$(μ-bpe)·2CH$_3$OH, M = 2606.75): C 65.89, H 8.16, N 1.07; Found: C 66.16, H 8.20, N 0.80. (b) **14**-bpa (**17**): This adduct was prepared in the same procedure as in (a) above, except that 1,2-bis(4-pyridyl)ethane (bpa) was used in place of (bpe). After seven days, blue crystals formed. (c) Cu$_4$(m-pbhx)$_4$·C$_{60}$ (**18**): square **14** (0.015 g, 0.006 mmol) and C$_{60}$ (0.005 g, 0.006 mmol) were dissolved in 1,2-dichlorobenzene (2 mL). This was carefully layered with acetonitrile (3 mL) and left at −20 °C. After 4 days dark brown crystals had formed. (d) Cu$_4$(m-pbhx)$_4$·C$_{70}$ (**19**): The same procedure in (c) above was followed except that C$_{70}$ was used in place of C$_{60}$. After 7 days, dark brown crystals had formed.

2.4 References

(1)   Pariya, C.; Sparrow, C. R.; Back, C. K.; Sandi, G.; Fronczek, F. R.; Maverick, A. W. *Angew. Chem. Int. Ed.* **2007**, *46*, 6305.

(2)   Ramirez, F.; Patwardhan, A. V.; Ramanathan, N.; Desai, N. B.; Greco, C. V.; Heller, S. R. *J. Am. Chem. Soc.* **1965**, *87*, 543.

(3)   Ramirez, F.; Bhatia, S. B.; Patwardhan, A. V.; Smith, C. P. *J. Org. Chem.* **1967**, *32*, 3547.

(4)   Jiangning, J.; Kee-in, L. *J. Korean. Chem. Soc.* **2005**, *49*, 150.

(5)   Zibuck, R.; Seebach, D. *Helv. Chim. Acta.* **1988**, *71*, 237.

(6)   Ma, C. T. L.; MacLachlan, M. J. *Angew. Chem. Int. Ed.* **2005**, *44*, 4178.

(7)   Gothard, C. M.; Nowick, J. S. *J. Org. Chem.* **2010**, *75*, 1822.

(8)   Wiester, M. J.; Mirkin, C. A. *Inorg. Chem.* **2009**, *48*, 8054.

(9)   Uehara, K.; Kasai, K.; Mizuno, N. *Inorg. Chem.,* **2007**, *46*, 2563.

(10)   Moulton, B.; Lu, J. J.; Mondal, A.; Zaworotko, M. J. *Chem. Comm.* **2001**, 863.

(11)   Rakita, P. E.; Kopperl, S. J.; Fackler, J. P. *J. Inorg. Nucl. Chem.* **1968**, *30*, 2139.

Chapter 3: Synthesis of Internally Substituted *m*-Phenylenebis(β-Diketone) Ligands and Their Molecular Squares

3.1 Introduction

This chapter is part of the project that was begun by Jace Sandifer.[1] In chapter 2, I showed that using longer alkyl chains in the β-diketone moieties of *m*-pbhxH$_2$ (Figure 3.1) greatly improves the solubility of the resulting molecular square. We were further interested in functional substituents on the aromatic ring of *m*-pbaH$_2$.
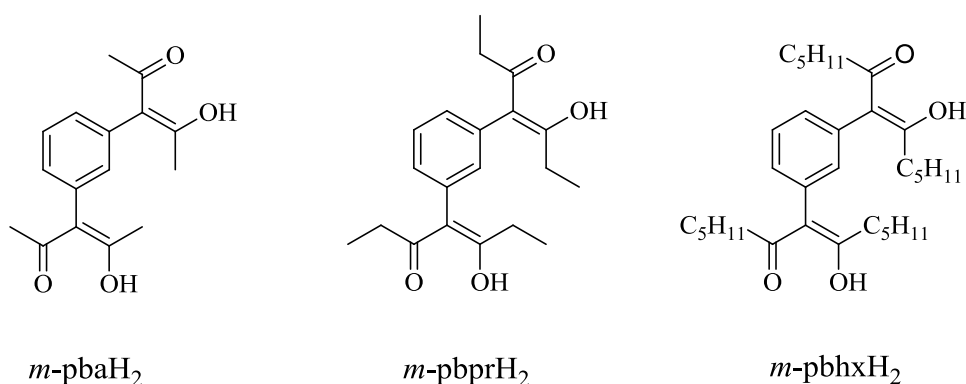
Figure 3.1 Bis(β-diketone) ligands for making molecular squares.

Sandifer prepared 5-MeO-*m*-pbaH$_2$ (**20**) and 5-BuO-*m*-pbaH$_2$ (**21**) (see Figure 3.2) and their resulting molecular squares (see Figure 3.3) were found to be soluble in various solvents.[1] He also did some preliminary studies on 2-MeO-*m*-pbaH$_2$ (**22a**) (Figure 3.2); I took up the project on **22a** where I improved on the yields and purity of the precursors leading to **22a**. In addition I prepared 2-MeO-*m*-pbprH$_2$ (**22b**) (Figure 3.2). Although molecular hexagons were expected from all of these ligands due to the 120° angle between their β-diketone moieties, only molecular squares have been isolated. We believe this is because distortions at the β-diketone moieties enable them to bend away from coplanarity with the metal centers. The squares may be kinetic products and not the thermodynamic ones.
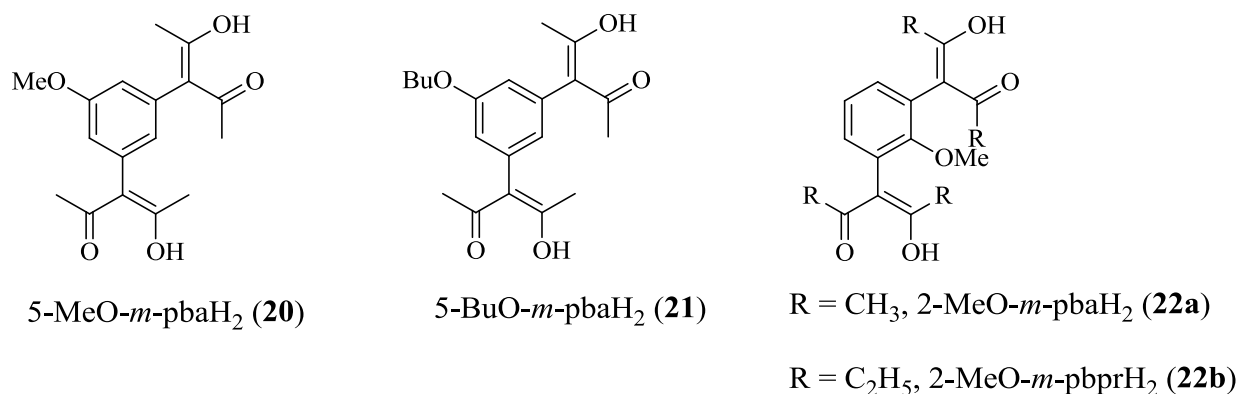
Figure 3.2 Bis(β-diketone) ligands **20**, **21**, and **22** for molecular squares

R = CH$_3$, [Cu$_4$(5-MeO-*m*-pba)$_4$] (**23**)
R = n-Bu, [Cu$_4$(5-BuO-*m*-pba)$_4$] (**24**)
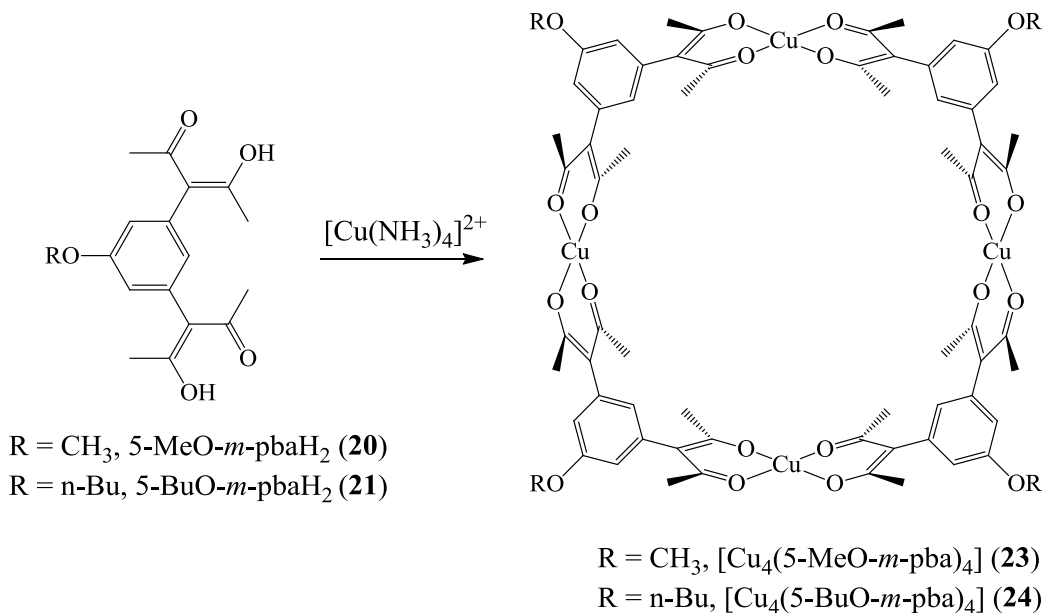
Figure 3.3 Treatment of bis(β-diketones) **20** and **21** with Cu^{2+} yields molecular squares **23** and **24**.

Adding functional groups to the 2-position of the aromatic ring of the *m*-pbaH$_2$ ligand as in **22a**, **b** is attractive because if the substituents are large enough, they may cause steric interactions which may lead to formation of a larger macrocycle such as a molecular pentagon or a molecular hexagon. Also we wanted to study the effects of changing the chemical environment inside the squares. The Fujita group has reported a coordination cage (nanoball) whose interior is

decorated with polyethylene glycol (PEG) substituents.[2] Here the optimized synthesis of **22a**, and synthesis of **22b** and their copper molecular polygons are reported.

3.2 Results and Discussion

3.2.1 Syntheses of the Ligands

These were prepared from 2-methoxyisophthalaldehyde, a compound which was prepared by Sandifer through microwave assisted synthesis. He reported a yield of 77% and its color as a yellow solid. He mentioned that the compound was not clean because there were extra peaks in its ^{1}H NMR spectrum which were not expected. I prepared the 2-methoxyisophthalaldehyde using the procedure developed by Bennani et al.[3] and obtained a yield of 97%. Sandifer avoided preparing this compound using the Bennani procedure because of the toxicity of PCC, but I think that the procedure is better than the microwave one because the yield and purity of the product is high, although PCC should be handled with care.

2-MeO-*m*-pbaH$_2$ (**22a**) was also prepared by Sandifer, who reported it as a yellow liquid in 10% yield, but he mentioned that the compound could have been impure as indicated by the presence of ethyl acetate peaks and extra aromatic peaks in its ^{1}H NMR spectrum. I isolated **22a** as a white solid after column chromatography in 45% yield. Elemental analysis agrees with the calculated values. ^{1}H NMR of this compound showed well resolved peaks with the right integrations, except the aromatic region where the peaks are not individually resolved. 2-MeO-*m*-pbprH$_2$ (**22b**) was obtained by an analogous procedure as a colorless oil. The ^{1}H NMR spectrum of 2-MeO-*m*-pbprH$_2$ (**22b**) showed the same behavior in the aromatic region as that of 2-MeO-*m*-pbaH$_2$ (**22a**).

3.2.2 Preparation of Copper Complexes

When **22a** was treated with Cu^{2+}, complex **25a** precipitated out immediately as a dark-green insoluble product. This product may have the molecular square structure shown in Figure 3.4, but I was unable to study it further due to its lack of solubility. However, when **22b** was treated with Cu^{2+}, a dark-green CH_2Cl_2 solution was formed and molecular square **25b** (Figure 3.4) was isolated as a dark green powder on evaporation of the solvent, yield (70%). The solubility of **25b** was determined (see table 3.1).

R = CH₃, 2-MeO-*m*-pbaH₂ (**22a**)
R = C₂H₅, 2-MeO-*m*-pbprH₂ (**22b**)

R = CH₃, [Cu₄(2-Meo-*m*-pbpr)₄] (**25a**)
R = C₂H₅, [Cu₄(2-MeO-*m*-pbpr)₄] (**25b**)
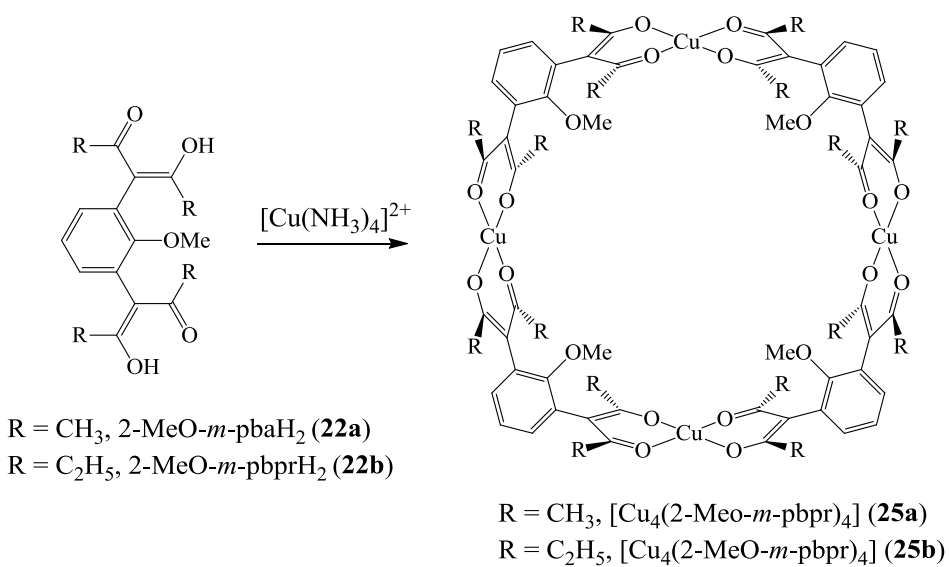
Figure 3.4 Reaction of bis(β-diketones) **22a, b** with Cu^{2+} yields molecular squares **25a, b**.

3.2.3 Solubility of Squares

Table 3.1 below shows the solubility of molecular squares **23**, **24**, and **25b** made from ligands **20**, **21**, and **22b** respectively. The effects of alkoxy substituents on different positions of the aromatic ring of *m*-pbaH₂ on solubility of the molecular squares are clearly seen. Squares **23** and **24** have alkoxy substituents on the outside since the alkoxy groups are on the 5-positions of

41

the aromatic rings of m-pbaH$_2$, while square **25b** is decorated on the inside as the methoxy groups are on the 2-position of the aromatic rings of the ligand.

The table shows that square **24**, with the longer butoxy group, is soluble in a wider range of solvents than the methoxy analog (**23**). The methoxy square **23** is soluble in about the same *number* of solvents as the unsubstituted square Cu$_4$(m-pba)$_4$ **3**. However, the 5-methoxy groups do change the solubility of the square, making it soluble in polar solvents such as methanol. In contrast, the solubility of the molecular square does not change much when the methoxy group is on the 2-position of the aromatic ring (square **25b**). The molecular square **25b** was analyzed by single crystal X-ray and the structure is shown in Figure 3.5.

The Cu---Cu distance in the square **25b** is 14.39 Å. The structure lies on an S$_4$ axis in the crystal and the OCH$_3$ groups alternate up and down. The space filling model of the square as shown in Figure 3.6 reveals the cavity to be too crowded to accommodate guest molecules.

Table 3.1 Solubility of molecular squares **3**, **23**, **24**, and **25b**

Solvent	Solubility			
	Square **3**	Square **23**	Square **24**	Square **25b**
Chloroform	**Soluble**	Insoluble	**Soluble**	**Soluble**
Dichloromethane	**Soluble**	**Soluble**	**Soluble**	**Soluble**
o-Dichlorobenzene	Insoluble	Insoluble	**Soluble**	Insoluble
Toluene	Insoluble	Insoluble	**Soluble**	**Soluble (hot)**
Chlorobenzene	Insoluble	Insoluble	**Soluble**	Insoluble
Tetrahydrofuran	Insoluble	**Soluble**	**Soluble**	Insoluble
Bromobenzene	Insoluble	Insoluble	**Soluble**	Insoluble
Benzene	Insoluble	Insoluble	**Soluble**	Insoluble
Methanol	Insoluble	**Soluble**	Insoluble	Insoluble
DMF	Insoluble	Insoluble	Insoluble	Insoluble
Acetonitrile	Insoluble	Insoluble	Insoluble	Insoluble

Figure 3.5 Crystal structure of Cu_4(2-MeO-*m*-pbpr)$_4$ (**25b**). Hydrogen atoms have been omitted for clarity.

Figure 3.6 Space filling model of the square **25b** showing the crowding of the cavity by the internal OCH_3 groups.

Table 3.2 X-ray crystallographic and structure refinement data for **25b**.solvate.

compound	**25b**.solvate
empirical formula	$C_{84}H_{104}Cu_4O_{20} \cdot 6.75\ C_2H_3N$
formula weight	1964.95
crystal system	Tetragonal
space gp	P4/nnc
a, Å	25.5002(6)
b, Å	25.5002(6)
c, Å	17.3192(6)
α, deg	90
β, deg	90
γ, deg	90
V, Å^3	11262.0(5)
Z	4
T, K	90
D_{calcd}, g cm^{-3}	1.159
cryst dimen, mm	0.35x0.29x0.18
θ limits, deg	4.64<θ<68.28
Rflns, meas/unique/obs	87833/5236/4704
Data/param	5236/269
μ, mm^{-1}	1.349
R ($I > 2\sigma(I)$)	0.0435
R_w (all data)	0.1392
GOF	1.069

3.2.4 Attempted Reaction of Square 25b with Guest Molecules

When square **25b** was treated with guest molecules such as 4,4'-bipyridine, 1,2-bis(4-pyridyl)ethane (bpa), and 1,2-bis(4-pyridyl)ethylene (bpe), green precipitates formed. Normally, when these guests bind to our Cu molecular squares, the color of the solution or solid changes from green to blue; thus, we believe these reactions did not yield adducts. This is most likely because of interference from the internal methoxy groups in **25b**.

3.3 Experimental

3.3.1 General Considerations

2-methoxyisophthalic acid, pyridinium chlorochromate (PCC), and lithium aluminum hydride were purchased from Sigma-Aldrich. Elemental analysis was performed by M-H-W Labs, Phoenix, Arizona. ^{1}H NMR spectra were recorded on Bruker (250 or 400 MHz) spectrometers, with $CDCl_3$ as the solvent. The phospholenes 2,2,2-trimethoxy-4,5-dimethyl-1,3,2-dioxaphospholene[4,5] and 2,2,2-trimethoxy-4,5-diethyl-1,3,2-dioxaphospholene[6] were prepared following literature methods.

Syntheses of the precursors leading to 2-MeO-*m*-pbaH$_2$ are described elsewhere.[1] However I optimized the yields of the following compounds:

3.3.2 2-methoxy-1,3-benzenedimethanol

This compound was prepared following the reported procedure.[1,7] Lithium aluminum hydride (0.54 g, 14.1 mmol) was suspended in dry THF (40 mL). Into this suspension was added in drops a solution of dimethyl 2-methoxyisophthalate[1] (1.0 g, 4.5 mmol) in THF (20 mL) from an addition flask. Then the reaction was stirred at room temperature under N_2 for 24 h. The mixture was cooled to 0 °C and an aq. solution of H_2SO_4 (16 mL, 1 M) was added slowly,

followed by ethyl acetate (100 mL). The organic phase was separated and washed with brine (100 mL), and dried with Na_2SO_4. On evaporation, a white solid was obtained (0.65 g, 86%).

3.3.3 2-methoxyisophthalaldehyde

This compound was prepared according to the procedure developed by Bennani et al. to convert 5-*tert*-butyl-1,3-benzenedimethanol to 5-*tert*-butylisophthalaldehyde.[3] 2-methoxy-1,3-benzenedimethanol (0.5 g, 2.9 mmol) was dissolved in dichloromethane (30 mL) and added to a mixture of pyridinium chlorochromate (PCC) (1.92 g, 8.9 mmol) and celite (8 g) in dichloromethane (40 mL). The mixture was stirred vigorously at room temperature for 4 h, and then filtered through a short pad of silica gel. The pad was rinsed with a 1:1 mixture of dichloromethane and ethyl acetate. Solvent was removed to yield a white solid, 0.46 g (97%). ^{1}H NMR: δ 10.4 (s, 2H, CHO), 8.1 (d, 2H), 7.4 (t, 1H), 4.1 (s, 3H, OCH$_3$). Anal. Calcd. for $C_9H_8O_3$ (M = 164.16): C 65.85, H 4.91; Found: C 65.64, H 5.19.

3.3.4 2-methoxy-*m*-phenylenebis(acetylacetone), 2-MeO-*m*-pbaH$_2$ (22a)

2-methoxy-isophthalaldehyde (0.20 g, 1.2 mmol) and 2,2,2-trimethoxy-4,5-dimethyl-1,3,2-dioxaphospholene (0.51 g, 2.4 mmol) were dissolved in dichloromethane (5 mL) and the solution stirred at room temperature under nitrogen. The reaction mixture was monitored by ^{1}H NMR until the reaction was complete as indicated by the disappearance of the 2-methoxyisophthalaldehyde –CHO peak. Then methanol (30 mL) was added and the mixture refluxed for 3 h, allowed to cool to room temperature and the solvent removed. Column chromatography of the crude product (ethyl acetate-hexane, 1:4 v/v) yielded a white solid, 0.16 g (45%). The ^{1}H NMR of **22a** is the same as what Sandifer observed.[1] Anal. Calcd. for $C_{17}H_{20}O_5$ (M = 304.34): C 67.09, H 6.62; Found: C 67.31, H 6.75.

3.3.5 4,4'-(2-methoxy-*m*-phenylenebis(3,5-heptanedione)), 2-MeO-*m*-pbprH$_2$ (22b)

This compound was prepared using the same procedure as **22a** above, except that 2,2,2-trimethoxy-4,5-diethyl-1,3,2-dioxapholene was used instead. 2-methoxyisophthalaldehyde (0.20 g, 1.2 mmol) and 2,2,2-trimethoxy-4,5-diethyl-1,3,2-dioxapholene (0.58 g, 2.4 mmol) were dissolved in dichloromethane (5 mL) and allowed to react. Column chromatography of the crude product using ethyl acetate-hexane (1:4 v/v) yielded a colorless oil, 0.13 g (30%). ^{1}H NMR δ: 16.9 (s, 2H), 7.10-7.18 (m, 3H, aromatic), 3.5 (s, 3H, OCH$_3$), 2.2 (q, 8H), 1.1 (t, 12H) (Figure A6).

3.3.6 Synthesis of Copper Molecular Squares

25a - CuSO$_4$·5H$_2$O (0.41 g, 1.6 mmol) was dissolved in distilled water (50 mL) and ammonia solution added dropwise until a royal blue solution formed. Into this solution was added 2-MeO-*m*-pbaH$_2$ (**22a**) (0.5 g, 1.6 mmol) in dichloromethane (40 mL). Immediately a dark green insoluble solid precipitated out.

25b - CuSO$_4$·5H$_2$O (0.277 g, 1.1 mmol) was dissolved in water (40 mL), and ammonia solution added dropwise until a royal blue solution was formed. Into this solution was added 2-MeO-*m*-pbprH$_2$ (**22b**) (0.4 g, 1.1 mmol) in DCM (40 mL) and the mixture stirred at room temperature for 4 h. The organic phase (olive green) was dried over Na$_2$SO$_4$ and the solvent removed under reduced pressure. The residue was washed with methanol and air dried to yield a dark green solid, 0.66 g (70%). Calcd. Anal. for C$_{84}$H$_{104}$Cu$_4$O$_{20}$: C 59.77, H 6.21: Found, C 59.64, H 6.24. Crystals suitable for X-ray analysis were grown by dissolving the complex in hot toluene and layering it with acetonitrile.

3.4 References

(1)   Sandifer, J. *MS Thesis, Louisiana State University,* **2009**.

(2)   Tominaga, M.; Suzuki, K.; Murase, T.; Fujita, M. *J. Am. Chem. Soc.* **2005**, *127*, 11950.

(3)   Bennani, Y. L.; Marron, K. S.; Mais, D. E.; Flatten, K.; Nadzan, A. M.; Boehm, M. F. *J. Org. Chem.* **1998**, *63*, 543.

(4)   Ramirez, F.; Patwardhan, A. V.; N.;, R.; Desai, N. B.; Greco, C. V.; Heller, S. R. *J. Am. Chem. Soc.* **1965**, *87*, 543.

(5)   Ramirez, F.; Bhatia, S. B.; Patwardhan, A. V.; Smith, C. P. *J. Org. Chem.* **1967**, *32*, 3547.

(6)   Pariya, C.; Sparrow, C. R.; Back, C. K.; Sandi, G.; Fronczek, F. R.; Maverick, A. W. *Angew. Chem. Int. Ed.* **2007**, *46*, 6305.

(7)   Hayama, T.; Baldridge, K. K.; Wu, Y. T.; Linden, A.; Siegel, J. S. *J. Am. Chem. Soc.* **2008**, *130*, 1583.

Chapter 4: Synthesis of Bis(β-Ketoenamine) Ligands and Their Molecular Squares

4.1 Introduction

In this chapter, two bis(β-ketoenamine) ligands and their metal molecular squares are discussed. Bis(β-ketoenamines) have the potential to generate porous metal-organic materials because they are chelating ligands like β-diketones, although they have been employed much less frequently.[1] The ligands (**1**) and (**2**) (Figure 4.1), and their copper molecular squares are reported elsewhere.[2] We were interested to study the squares by NMR and also by electrochemistry. Since copper molecular squares cannot be studied by NMR due to the paramagnetic nature of Cu(II), we wished to prepare molecular squares from metals such as nickel and palladium: Square-planar Ni(II) and Pd(II) complexes are nearly always diamagnetic. However, Ni(II) β-diketonates are usually octahedral and paramagnetic, and Pd(II) β-diketonates, though square-planar and diamagnetic, are often easily reduced to Pd metal. For supramolecular chemistry with Ni(II), we decided to convert our bis(β-diketones) into bis(β-ketoenamines): Both Ni(II) and Pd(II) are d^8 systems and are known to react with β-ketoenamines to yield square planar diamagnetic complexes which can be studied by NMR.[1,3,4] Therefore, we converted the bis(β-diketones), *m*-pbaH$_2$ (**1**) and *m*-pbprH$_2$ (**2**) to bis(β-ketoenamines), *m*-pbiH$_2$ (**26**) and *m*-pbpriH$_2$ (**27**) (see Figure 4.1), through microwave assisted synthesis (scheme 4.1). When treated with Cu^{2+}, ligands **26** and **27** yield copper molecular squares; while **27** affords a nickel square on reaction with Ni^{2+}. The copper and nickel molecular squares have been studied by UV-visible spectroscopy and electrochemistry; the nickel square has been studied by ^{1}H NMR. The squares have been characterized by single crystal X-ray analysis.

R = Me, *m*-pbaH$_2$ (**1**)   R = Me, *m*-pbiH$_2$ (**26**)

R = Et, *m*-pbprH$_2$ (**2**)   R = Et, *m*-pbpriH$_2$ (**27**)
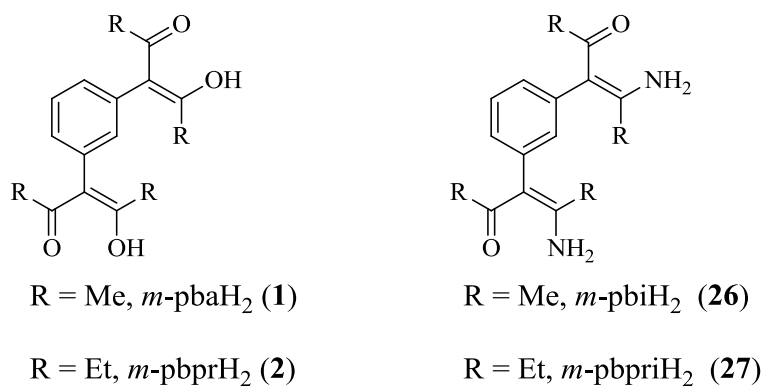
Figure 4.1 Bis(β-diketones) **1** and **2**, and their bis(β-ketoenamine) analogs **26** and **27**.

4.2 Results and Discussion

4.2.1 Synthesis of the Ligands

The work by the Braibante group, which used a domestic microwave oven to convert β-dicarbonyl compounds to ketoenamines,[5] motivated us to try microwave reactions. Treatment of *m*-pbaH$_2$ (**1**) and *m*-pbprH$_2$ (**2**) with ammonium acetate in toluene in microwave yielded *m*-pbiH$_2$ (**26**) and *m*-pbpriH$_2$ (**27**) in 86 and 80% respectively after column chromatography (Scheme 4.1). These reactions took 40 m to complete. Attempts to prepare a bis(β-ketoenamine) from the ligand *m*-pbhxH$_2$ (**5**) (see Figure 2.2 in chapter 2) did not succeed. The molecular squares from this ligand were expected to be soluble in a wider range of solvents. The nickel square in particular could enable us to study its reactions with a variety of guest molecules. Both bis(β-ketoenamine) ligands **26** and **27** were analyzed by ^{1}H NMR and their spectra (see Appendix, Figures A7 and A9) were compared with those of their bis(β-diketone) analogs **1** and **2** (Appendix, Figures A1 and A2). The enol peak (16.64 ppm) in bis(β-diketone) **1** (Figure 1A) is replaced by two broad singlets at 10.53 ppm and 5.07 ppm, which are assigned to NH protons in ketoenamine **26** (Figure A7). . The peak at 10.53 ppm is assigned to the NH proton (a1) which is

hydrogen-bonded to the oxygen atom, while the peak at 5.07 ppm is the free NH proton (a2). Methyl protons in **1** appear as one singlet at 1.91 ppm, while **26** shows two CH_3 singlets. Aromatic proton peaks around 7 ppm in ketoenamine **26** are shifted slightly upfield compared to the diketone **1**. Similarly, the ^{1}H NMR spectrum of bis(β-ketoenamine) **27** (Figure A9) shows amine peaks at 10.64 ppm and 5.05 ppm. Crystal structures of **26** and **27** are shown in Figure 4.2.

R = Me, *m*-pbaH$_2$, (**1**)   R = Me, *m*-pbiH$_2$, (**26**)

R = Et, *m*-pbprH$_2$, (**2**)   R = Et, *m*-pbpriH$_2$, (**27**)

Scheme 4.1 Conversion of bis(β-diketones) (**1** and **2**) to bis(β-ketoenamines) (**26** and **27**).

26   27

Figure 4.2 Crystal structures of bis(β-ketoenamines) *m*-pbiH$_2$ (**26**) and *m*-pbpriH$_2$ (**27**).

51

4.2.2 Synthesis of the Metal Squares

The two ligands were treated with $Cu(NO_3)_2 \cdot 3H_2O$ and $Ni(NO_3)_2 \cdot 3H_2O$ in DMF solution, in the presence of triethylamine as base. Reaction of the *m*-pbiH$_2$ ligand with $Ni(NO_3)_2 \cdot 3H_2O$ led to immediate precipitation of a brown insoluble product. This material may be the molecular square Ni$_4$(*m*-pbi)$_4$; however, its low solubility made further study difficult, and I decided not to pursue it further. In contrast, no precipitates were observed when the two ligands were treated with $Cu(NO_3)_2 \cdot 3H_2O$, and also when *m*-pbpriH$_2$ was treated with $Ni(NO_3)_2 \cdot 3H_2O$.

(a) Cu$_4$(*m*-pbi)$_4$ (28) and Cu$_4$(*m*-pbpri)$_4$ (29)

Both *m*-pbiH$_2$ and *m*-pbpriH$_2$ react with Cu^{2+} in DMF in the presence of Et$_3$N to yield dark green solutions which deposit dark green crystals after several days. Square **28** is insoluble, which limited further study, while **29** is soluble in both chloroform and dichloromethane.

(b) Ni$_4$(*m*-pbpri)$_4$ (30)

Ligand **27** reacts with Ni^{2+} in DMF in the presence of Et$_3$N to yield a red solution. The solid microcrystalline product, **30**, precipitates out when acetonitrile vapor is allowed to diffuse into the red solution. Other solvents which precipitate the product are acetone and ethyl acetate, although the yields are lower than in the case of acetonitrile. Nickel square **30** is soluble in chloroform and dichloromethane solvents. The ^{1}H NMR spectrum of the Ni$_4$(*m*-pbpri)$_4$ (**30**) is depicted in Figure A11. This spectrum shows that the NH peak of the ligand **27** at 10.64 ppm (Figure A9) has disappeared, as expected if nickel binds to the ligand by displacing proton a1. The free NH peak (a2) of the *m*-pbpriH$_2$ ligand **27** at 5.05 has shifted to 5.41 ppm in the nickel molecular square **30**. The spectrum of the molecular square displays a single ligand environment suggesting the formation of a symmetric species such as a metallacycle. [6-8]

4.2.3 UV-Vis Analysis

The UV-Vis spectra of molecular squares **29** and **30** were compared with that of the β-diketone molecular square, $Cu_4(m\text{-pba})_4$ (**3**) (see Figure 4.3). The spectrum of the β-diketone molecular square, $Cu_4(m\text{-pba})_4$ in chloroform, Figure 4.3 A shows two d-d absorption bands with maxima at 546 (ϵ = 177) and 670 nm (ϵ = 182 M^{-1} cm^{-1}). These bands are comparable (on a per metal atom basis) to those for $Cu(acac)_2$ (λ = 532 (ϵ = 26) and 658 nm (ϵ = 34 M^{-1} cm^{-1})).[9] Spectrum B is that of $Cu_4(m\text{-pbpri})_4$ in chloroform, showing one broad band with a maximum at 593 nm (ϵ = 304 M^{-1} cm^{-1}). Figure 4.3 C is the spectrum of $Ni_4(m\text{-pbpri})_4$ in chloroform, also showing one broad band with a maximum at 569 nm (ϵ = 323 M^{-1} cm^{-1}). We were especially interested in the UV-Vis spectrum of $Cu_4(m\text{-pbpri})_4$. This is because both $Cu_4(m\text{-pba})_4$ and $Cu_4(m\text{-pbpri})_4$ are green, both in solution and in the solid state. Since the colors of the two compounds are very similar, the details of the electronic spectra can help to distinguish them from each other.
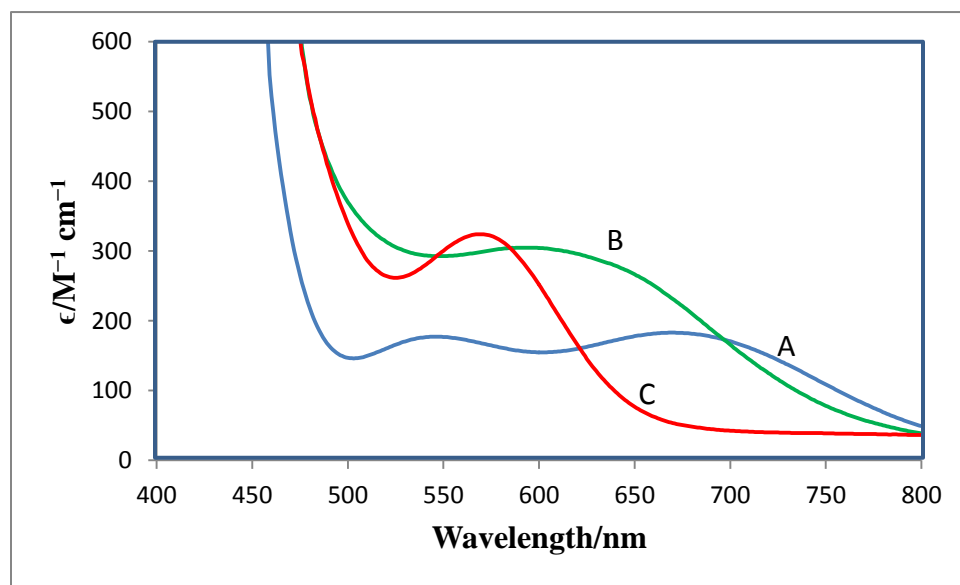

Figure 4.3 Room-temperature electronic absorption spectra: (A) $Cu_4(m\text{-pba})_4$ (**3**), (B) $Cu_4(m\text{-pbpri})_4$ (**29**), and (C) $Ni_4(m\text{-pbpri})_4$ (**30**). All the squares were dissolved in chloroform.

4.2.4 Electrochemistry

The squares **29** and **30** were studied by electrochemistry and their cyclic voltammograms are shown in Figures 4.4 and 4.5. Cyclic voltammograms for $Ni_4(m\text{-pbpri})_4$ show a partially reversible wave with $E_{1/2}$ = 0.70 V (Figure 4.4). $Cu_4(m\text{-pbpri})_4$ showed several waves (Figure 4.5); the best-defined one is an irreversible oxidation wave at 0.74 V. The ferrocene (Fc/Fc^+) reference redox couple appears at ca. 0.27 V under these conditions. These values are more anodic than those reported for the binuclear β-ketoenamine complexes $Ni_2(BBI)_2$ (0.26 V vs. Fc/Fc^+) and $Cu_2(BBI)_2$ (0.36 V vs. Fc/Fc^+).[1] The voltammograms are also less reversible than those for $M_2(BBI)_2$ (for example, i_{pc}/i_{pa} = 0.62 and ΔE_p = 0.22 V for $Ni_4(m\text{-pbpri})_4$, vs. 0.81 and 0.063 V for $Ni_2(BBI)_2$ under similar conditions).

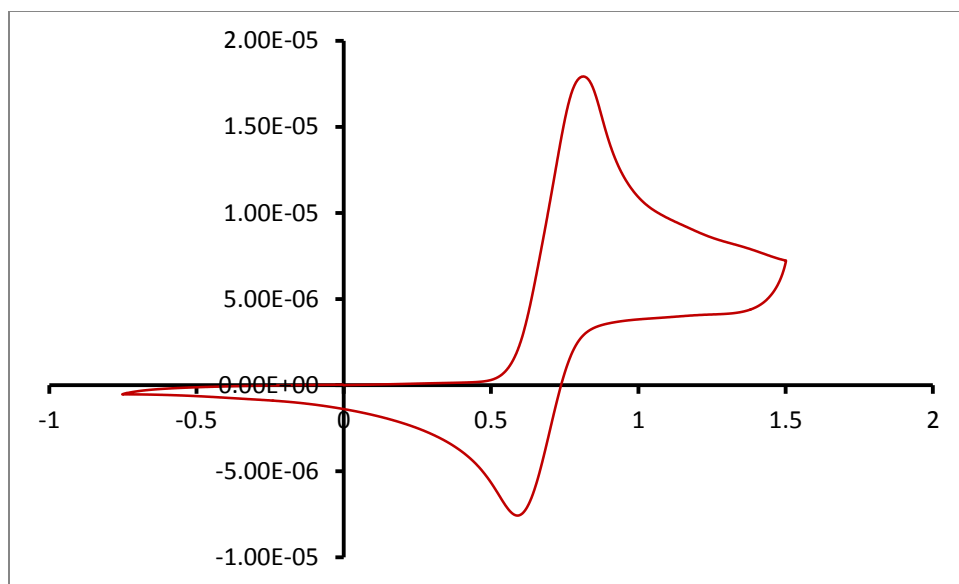**Figure 4.4** Cyclic voltammogram for $Ni_4(m\text{-pbpri})_4$: 1.0 x 10^{-3} M in CH_2Cl_2, with 0.1 M $(Bu_4N)PF_6$ as the supporting electrolyte; Pt working electrode; Ag/Ag^+ reference electrode.

Figure 4.5 Cyclic voltammogram for $Cu_4(m\text{-pbpri})_4$: 1.0 x 10^{-3} M in CH_2Cl_2, with 0.1 M $(Bu_4N)PF_6$ as the supporting electrolyte; Pt working electrode; Ag/Ag^+ reference electrode.

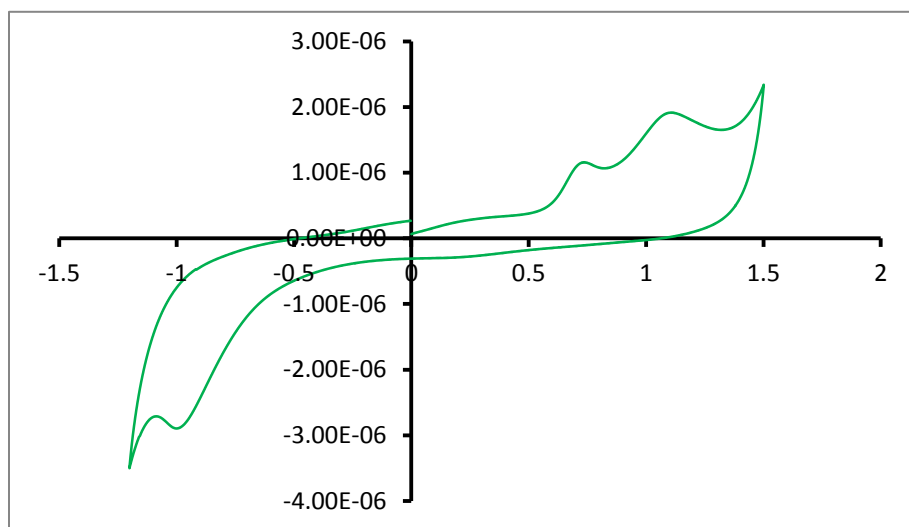### 4.2.5 Structural Characterization

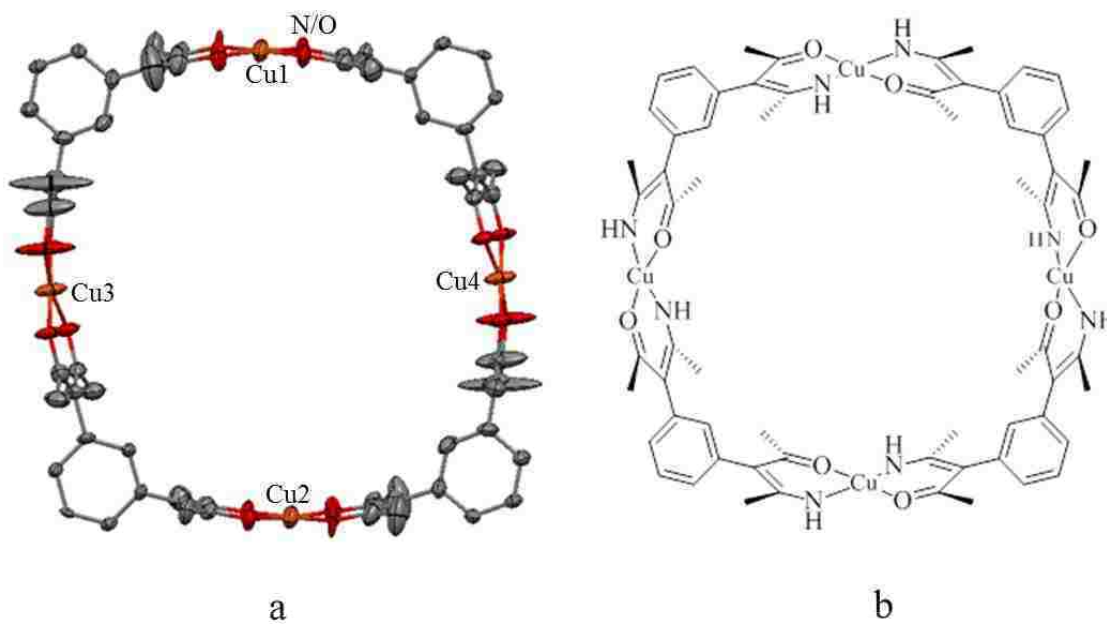Crystal structures of **28**, **29**, and **30** are shown in Figures 4.6- 4.8.

Figure 4.6 Crystal structure of (a) $Cu_4(m\text{-pbi})_4$ (**28**), and (b) Chemdraw picture of the square.
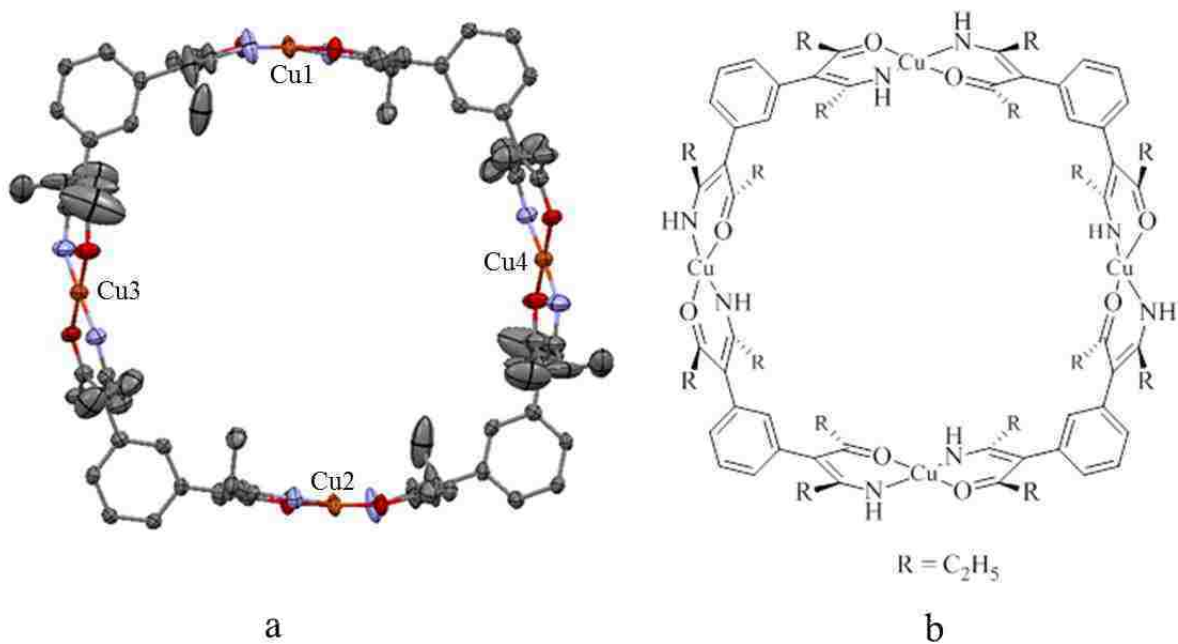
Figure 4.7 (a) Crystal structure of $Cu_4(m\text{-pbpri})_4$ (**29**), (b) Chemdraw picture of the square.
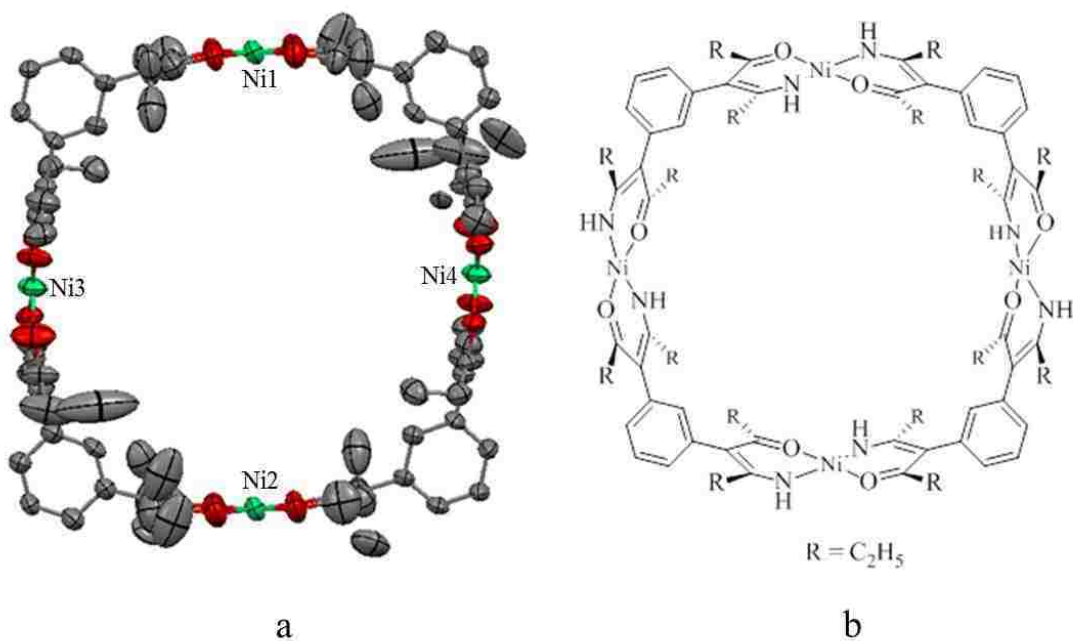

Figure 4.8 (a) Crystal structure of $Ni_4(m\text{-pbpri})_4$ (**30**), (b) Chemdraw picture of the square.

The M---M (M = Cu, Ni) distances in the metal squares of **28**, **29**, and **30** from β-ketoenamine ligands **26** and **27** are similar to the Cu$\cdots$Cu distances in the squares, Cu$_4$(m-pba)$_4$ (**3**) and Cu$_4$(m-pbpr)$_4$ (**4**),[2] from their β-diketone analogs **1** and **2** respectively. The distances are shown in table 4.1.

Table 4.1 M---M distances in metal squares from β-diketones **1**, **2** and β-ketoenamines **26**, **27**.

Metal square	M1---M2 (Å) (M = Cu, Ni)	M3---M4 (Å) (M = Cu Ni)
Cu$_4$(m-pba)$_4$ (**3**) [2]	14.32	14.65
Cu$_4$(m-pbpr)$_4$ (**4**) [2]	14.01	14.66
Cu$_4$(m-pbi)$_4$ (**28**)	14.22	14.74
Cu$_4$(m-pbpri)$_4$ (**29**)	14.59	14.50
Ni$_4$(m-pbpri)$_4$ (**30**)	13.89	14.58

4.2.6 Attempted Host-Guest Chemistry

Squares **29** and **30** were treated with guest molecules such as 4,4-bipyridine, 1,2-bis(4-pyridyl)ethylene (bpe), 1,2-bis(4-pyridyl)ethane (bpa), C$_{60}$ and C$_{70}$. The pyridine derivatives largely yielded precipitates with colors that were very similar to those of the respective "empty" β-ketoenamine squares (green for **29** and brown for **30**). C$_{60}$ and C$_{70}$ with the squares afforded crystalline products, but these did not diffract well, so we were unable to determine their structures.

Table 4.2 X-ray crystallographic and structure refinement data for **28**.solvate and **29**.solvate.

compound	**28**.solvate	**29**.solvate
empirical formula	$C_{64}H_{72}Cu_4N_8O_8$ $\cdot 5.2C_3H_7NO$	$C_{180}H_{104}Cu_4N_8O_8\cdot$ 4.29 $CHCl_3$
formula weight	1715.56	2071.96
crystal system	Triclinic	Triclinic
space group	$P\bar{1}$	$P\bar{1}$
a, Å	7.6956(3)	9.0577(4)
b, Å	16.5759(7)	16.3334(6)
c, Å	17.3629(7)	17.4694(7)
α, deg	109.132(3)	70.830(2)
β, deg	93.435(3)	85.460(3)
γ, deg	91.714(3)	87.947(3)
V, Å^3	2085.86(15)	2433.37(17)
Z	1	1
T, K	90	90
D_{calcd}, g cm^{-3}	1.366	1.414
cryst dimen, mm	0.13x0.06x0.02	0.23x0.14x0.07
θ limits, deg	3.2<θ<44.7	2.6<θ<58.7
Rflns, meas/unique/obs	13090/4368/2642	25401/6800/5642
Data/param	4368/387	6800/472
μ, mm^{-1}	1.697	4.671
R ($I > 2\sigma(I)$)	0.058	0.0483
R_w (all data)	0.151	0.1395
GOF	0.950	1.070

4.3 Experimental

NMR spectra were recorded on Bruker (250 or 400 MHz) spectrometers, with $CDCl_3$ as solvent. Elemental analysis was performed by M-H-W Laboratories, Phoenix, Arizona. Microwave reactions were performed in a CEM microwave oven. UV-Vis spectra were recorded by Bang,[10] in $CHCl_3$ solution, using an Aviv Model 14DS spectrophotometer. Cyclic voltammograms were recorded by Dr. Hwang and Brian Imsick, using an electrochemical apparatus in the Nesterov group.

4.3.1 Microwave Assisted Synthesis of *m*-pbiH₂ (26) and *m*-pbpriH₂ (27)

m-pbiH₂ (26): *m*-pbaH₂ (0.50 g, 1.82 mmol) was placed in an 80 mL microwave reaction vessel with toluene (30 mL). Into this solution was added ammonium acetate (0.56 g, 7.28 mmol), and the mixture placed in the microwave oven (200 °C, 400 W, 30 m). After the reaction was complete, the solvent was removed completely by rotary evaporation to obtain a white solid which was easily purified by column chromatography (ethyl acetate-hexane, 90:10 v/v), yield 430 mg (86%) of *m*-pbiH₂. Crystals of *m*-pbiH₂ suitable for single-crystal X-ray analysis were grown from $CHCl_3$ by layering with hexane. ^{1}H NMR: δ 10.53, 5.07 (br, 4H, NH_2), 7.34 (t, 1H), 7.10 (d, 2H), 7.01 (s, 1H), 1.86 (s, 6H), 1.72 (s, 6H) (Figure A7). ^{13}C NMR: δ 196.5, 159.5, 140.7, 135.4, 130.2, 128.8, 109.9, 29.2, 22.2 (Figure A8). Anal. Calcd for $C_{16}H_{20}N_2O_2$ (M = 272.34): C, 70.56; H, 7.40; N, 10.29. Found: C, 70.76; H, 7.64; N, 10.47.

m-pbpriH₂ (27): Reaction of *m*-pbprH₂ (0.50 g, 1.5 mmol) and ammonium acetate (0.47 g, 6.0 mmol) under the same microwave conditions as reported for (26) above yielded 400 mg (80%) of *m*-pbpriH₂ after column chromatography (ethyl acetate/hexane, 70/30). Crystals suitable for single-crystal X-ray analysis were deposited from $CHCl_3$ solution by layering with

hexane over a period of 4 days. ^{1}H NMR: δ 10.64, 5.05 (br, 4H, NH$_2$), 7.34 (t, 1H), 7.11 (dd, 2H,

j = 7.56, 1.60 Hz), 7.03 (s, 1H), 2.10-1.98 (m, 8H), 1.01 (t, 6H), 0.96 (t, 6H) (Figure A9). ^{13}C

NMR: δ 200.0, 163.9, 139.9, 136.1, 130.5, 128.7, 108.8, 33.9, 27.8, 12.0, 9.2 (Figure A10). Anal.

Calcd for C$_{20}$H$_{28}$N$_2$O$_2$ (M = 328.45): C, 73.14; H, 8.59; N, 8.53; Found: C, 72.91; H, 8.44; N,

8.44.

4.3.2 Synthesis of Copper and Nickel Squares

Cu$_4$(*m*-pbi)$_4$ (28): *m*-pbiH$_2$ (0.05 g, 0.18 mmol) and Et$_3$N (0.036 g, 0.36 mmol) were

dissolved in DMF (30 mL) and stirred for 2 h. Into this solution was added Cu(NO$_3$)$_2$·3H$_2$O

(0.044 g, 0.18 mmol) in DMF (30 mL). The resultant dark green solution was left standing for 4

days during which time dark green crystalline material precipitated. This was collected, washed

with DMF and CH$_3$CN, and dried in air for 12 h to yield a dark green solid, 0.033 g (54%).

Square **28** is insoluble in common solvents and so could not be recrystallized; hence, single

crystal X-ray analysis was carried out on the as-synthesized crystals.

Cu$_4$(*m*-pbpri)$_4$ (29): *m*-pbpriH$_2$ (0.10g, 0.30 mmol) and Et$_3$N (0.06 g, 0.60 mmol) were

dissolved in DMF (50 mL) and stirred for 2 h. A solution of Cu(NO$_3$)$_2$·3H$_2$O (0.074 g, 0.30

mmol) in DMF (50 mL) was added, and the solution turned dark green. It was left standing for 5

days where dark green crystalline product precipitated. This was collected, washed with DMF

and CH$_3$CN and air dried for 12 h to yield a dark green solid, 0.073 g (61%). Anal. Calcd. for

C$_{80}$H$_{104}$N$_8$O$_8$Cu$_4$ (M = 1559.91): C, 61.60; H, 6.72; N, 7.18; Found: C, 61.22; H, 6.57; N, 6.98.

Single crystals for X-ray analysis were prepared from CHCl$_3$ solution by layering with 2-

propanol.

Ni$_4$(*m*-pbpri)$_4$ (30): A solution of *m*-pbpriH$_2$ (0.20 g, 0.61 mmol) and Et$_3$N (0.12 g, 1.2 mmol) in DMF (10 mL) was stirred for 2 h and treated with a solution of Ni(NO$_3$)$_2$·6H$_2$O (0.177 g, 0.61 mmol) in DMF (10 mL). A pale yellow solution was formed which turned red within a few seconds. Solvent vapor diffusion of CH$_3$CN into this DMF solution led to precipitation of a red microcrystalline product after seven days. The solid was collected, washed with DMF and CH$_3$CN, and air dried for 12 h to yield a red-brown solid, 0.11 g (47%). ^{1}H NMR: δ 7.27 (t, 1H), 7.04 (dd, 2H, *J* = 7.44, 1.0 Hz), 6.88 (br s, 1H), 5.41 (s, 2H, NH), 1.90-1.71 (m, 8H), 0.9 (q, 6H), 0.82 (q, 6H) (Figure A11). Anal. Calcd. for C$_{80}$H$_{104}$N$_8$O$_8$Ni$_4$ (M = 1540.50): C 62.37; H 6.80; N 7.27: Found: C 62.15; H 6.79; N 7.23. Crystals for X-ray analysis were grown from CHCl$_3$ solution by layering with 2-propanol.

4.4 References

(1)   Bradbury, J. R.; Hampton, J. L.; Martone, D. P.; Maverick, A. W. *Inorg. Chem.* **1989**, *28*, 2392.

(2)   Pariya, C.; Sparrow, C. R.; Back, C. K.; Sandi, G.; Fronczek, F. R.; Maverick, A. W. *Angew. Chem. Int. Ed.* **2007**, *46*, 6305.

(3)   Bennett, A. M. A.; Foulds, G. A.; Thornton, D. A. *Polyhedron* **1989**, *8*, 2305.

(4)   Maverick, A. W.; Fronczek, F. R.; Martone, D. P.; Bradbury, J. R. *J. Coord. Chem.* **1989**, *20*, 149.

(5)   Braibante, H. T. S.; Braibante, M. E. F.; Rosso, G. B.; Oriques, D. A. *J. Braz. Chem. Soc.* **2003**, *14*, 994.

(6)   Tominaga, M.; Suzuki, K.; Kawano, M.; Kusukawa, T.; Ozeki, T.; Sakamoto, S.; Yamaguchi, K.; Fujita, M. *Angew. Chem. Int. Ed.* **2004**, *43*, 5621.

(7)   Hall, J. R.; Loeb, S. J.; Shimizu, G. K. H.; Yap, G. P. A. *Angew. Chem. Int. Ed.* **1998**, *37*, 121.

(8)   Fujita, M.; Yazaki, J.; Ogura, K. *J. Am. Chem. Soc.* **1990**, *112*, 5645.

(9)   Maverick, A. W.; Klavetter, F. L. *Inorg. Chem.* **1984**, *23*, 4129.

(10)   Bang, S. *Unpublished Results.*

Chapter 5: Triphenylamine Based Bis(β-Diketone) Ligands and Their Copper(II) Complexes

5.1 Introduction

The previous chapters report on molecular squares from m-pbaH$_2$ derivatives. Because of the 120° angle between its β-diketone moieties, m-pbaH$_2$ was expected to generate a molecular hexagon on reaction with square planar metal ions, and yet all of the MOPs isolated so far have been molecular squares. As part of our efforts to make larger molecular polygons, we prepared the new triphenylamine-based bis(β-diketone) ligands tpbaH$_2$ (**31**) and tpbprH$_2$ (**32**) (Figure 5.1). Also these ligands will have more room inside to accommodate internal functional groups.

Triphenylamine   tpbaH$_2$ (**31**)   tpbprH$_2$ (**32**)
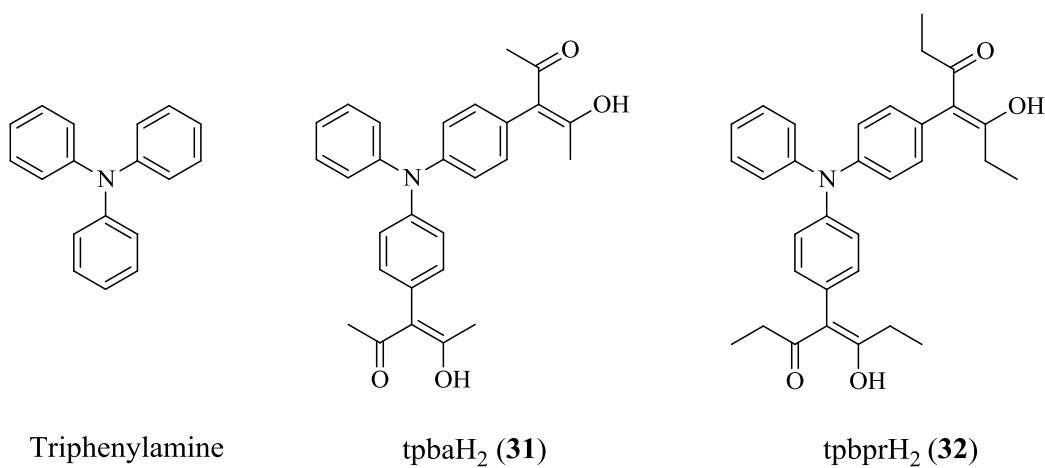
Figure 5.1 Structures of triphenylamine and the bis(β-diketone) ligands tpbaH$_2$ (**31**) and tpbprH$_2$ (**32**).

As with m-pbaH$_2$, the 120° angle between the β-diketone moieties in these ligands should permit the formation of molecular hexagons on treatment with Cu^{2+}. (In contrast to aliphatic amines, triarylamines generally exhibit trigonal planar geometry at N.) However, it is possible that ligands **31** and **32** might yield molecular squares if the experience our group had with m-pbaH$_2$[1] is something to go by. The new ligands should yield larger pores than m-pbaH$_2$ and its analogs, which means that the squares may be able to accommodate larger guest molecules. Here

we report syntheses of the ligands and the copper complex of **32** and its characterization by ESI-MS and microanalysis.

## 5.2 Results and Discussion

5.2.1 Ligands

The two compounds (**31** and **32**) are isolated as white solids after stirring 4,4'-diformyltriphenylamine[2] (**33**) with 2,2,2-trimethoxy-4,5-dimethyl-1,3,2-dioxaphospholene[3] and 2,2,2-trimethoxy-4,5-diethyl-1,3,2-dioxaphospholene[1] respectively (scheme 5.1) for 12 days at room temperature under N_2. These reactions are quite slow and the product yields are low (17 and 14% for **31** and **32** respectively).

R = CH$_3$, tbpaH$_2$ (**31**)
R = C$_2$H$_5$, tpbprH$_2$ (**32**)
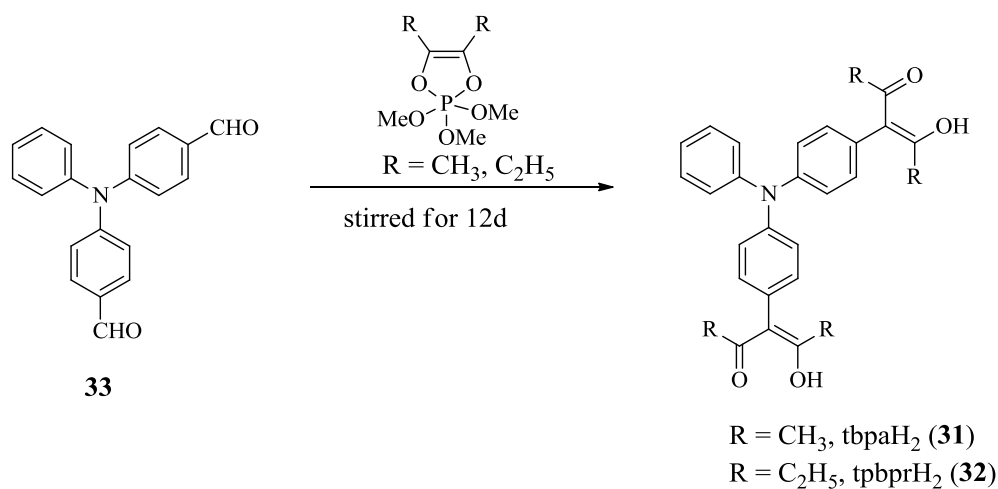
Scheme 5.1 Reaction of 4,4'-diformyltriphenylamine (**33**) with phospholenes affords bis(β-diketones) tpbaH$_2$ (**31)** and tpbprH$_2$ (**32**).

The formation of our previously mentioned β-diketones take shorter reaction times to complete, i.e in less than 24 h and it involves stirring the aldehydes with phospholenes at room temperature overnight, followed by refluxing the intermediate in methanol. In this particular case, the reaction does not require refluxing in methanol, but it requires more time. Prior to this

study, the thiophene-based bis(β-diketone) ligands (see scheme 5.2) had been prepared in a similar procedure in our group.[4] This reaction took about ten days of stirring the 2,5-thiophenedicarboxaldehyde with pholenes at room temperature and did not require refluxing in methanol, but it requires more time. The yields were also low (~20%).
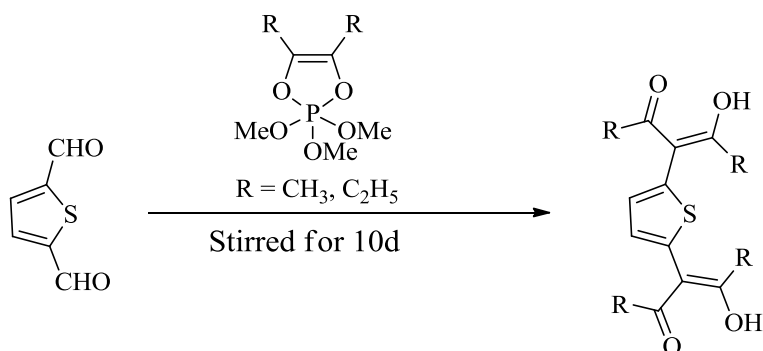
Scheme 5.2 Reaction of 2,5-thiophenedicarboxaldehyde with pholenes yields thiophene-based bis(β-diketones).

The crystal structures of tpbaH$_2$ (**31**) and tpbprH$_2$ (**32**) are shown in Figure 5.2. In the solid state, **31** and **32** are in the enol form, which is in agreement with solution NMR data.
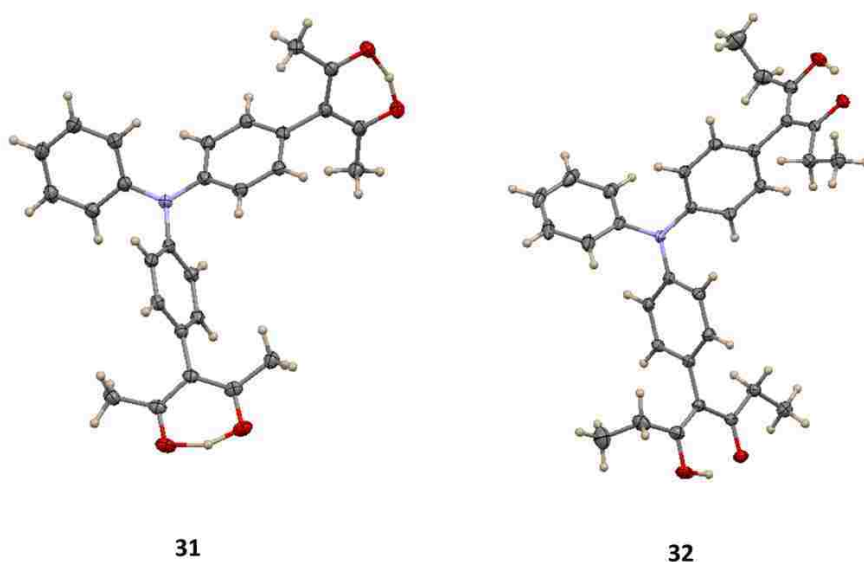
Figure 5.2 Crystal structures of bis(β-diketone) ligands **31** and **32**.

5.2.2 Copper Complexes

Reaction of **31** with Cu^{2+} resulted in an insoluble product, while **32** afforded a dark green material (**34**) that is soluble in chloroform and dichloromethane. We were unable to obtain 34 in crystalline form for direct structural characterization. However, its microanalysis (C, H, N) agrees with calculated values for $Cu_n(tpbpr)_n$. Also we were able to analyze it by ESI-MS. Our spectrometer has a maximum m/z limit of 3000, and if complex **34** is a molecular hexagon, then its molecular weight is 3354.9; this means that the parent ions $Cu_n(tpbpr)_n^+$, (n≥6) cannot be observed. However, smaller complexes (i.e $Cu_n(tpbpr)_n^+$, n < 6) would have parent ions below m/z = 3000 and should be observed. We saw no signal for the pentamer (m/z ~ 2796). In the tetramer region, signals were observed at 2234.7-2241.7 whose isotope distribution pattern matches with the theoretical distribution. This pattern is assigned to the tetramer, $[M+H]^+$, m/z = 2237.7 (see Figure 5.3). Additional signals are assigned to $Cu_3(tpbpr)_3^+$ (1675.5-1680.5) and $Cu_2(tpbpr)_2^+$ (1116.4 -1121.3).

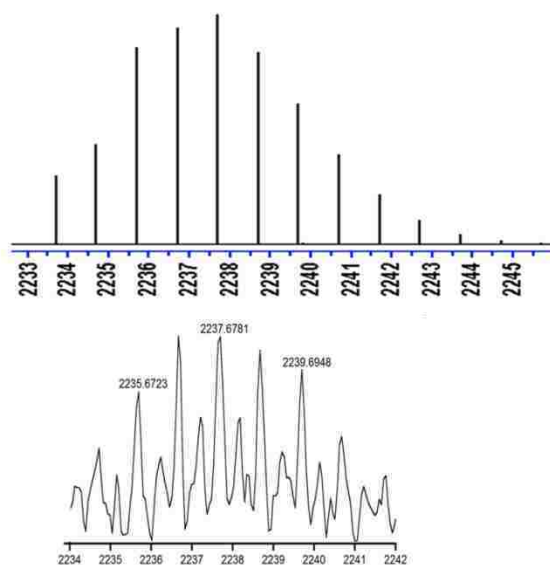**Figure 5.3** Calculated (top) and experimental (bottom) ESI-MS spectra of parent ion ($[M+H]^+$, $Cu_4(tpbpr)_4H^+$) of **34**.

Elemental analysis (C, H, N) for complex **34** agrees with calculated values for $Cu_n(tpbpr)_n$, (n = 4). One possible geometry for $(Cu_4(tpbpr)_4)$, generated by molecular modeling (HyperChem), is shown in Figure 5.4.

The predicted Cu---Cu distance in the model of square **34** is ~20 Å. Attempts to obtain adducts of **34** with guest molecules such as 4,4'-bipyridine, 1,2-bis(4-pyridyl)ethylene (bpe) and 1,2-bis(4-pyridyl)ethane (bpa) did not succeed. This is probably because these guests are not large enough to bridge two opposite N atoms in the cavity of **34**.
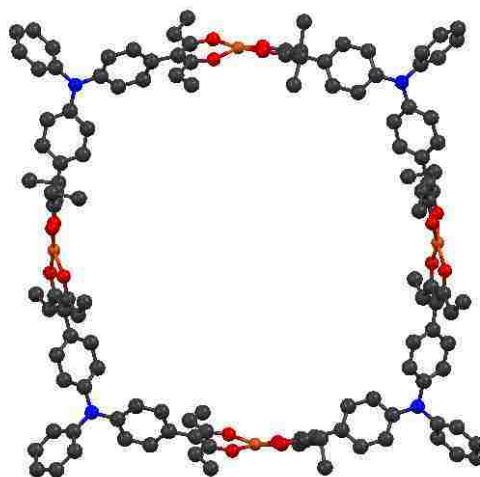
Figure 5.4 A model of molecular square **34** $(Cu_4(tpbpr)_4)$. Color coding: Carbon black, Nitrogen blue, Oxygen red and Copper orange. Hydrogen atoms omitted for clarity.

5.3 Experimental

5.3.1 Materials and Methods

DMF was purchased from Sigma-Aldrich and distilled once; phosphorus oxychloride and triphenylamine were acquired from Sigma-Aldrich and used as received. ESI-MS was performed

on an ESI-TOF instrument (Agilent-6210 TOF-LC/MS). Elemental analysis was performed by M-H-W Labs, Phoenix, Arizona. NMR spectra were recorded on a Bruker 400 MHz spectrometer with $CDCl_3$ as the solvent. 4,4'-Diformyltriphenylamine,[2] 2,2,2-trimethoxy-4,5-dimethyl-1,3,2-dioxaphospholene[3] and 2,2,2-trimethoxy-4,5-diethyl-1,3,2-dioxaphospholene[1] were prepared by literature methods.

5.3.2 Synthesis of the Ligands

a) $tpbaH_2$ (**31**): 4,4'-Diformyltriphenylamine (1.5 g, 4.9 mmol) (**33**) was dissolved in dichloromethane (10 mL). Into this solution was added 2,2,2-trimethoxy-4,5-dimethyl-1,3,2-dioxaphospholene (2.06 g, 9.8 mmol) and the mixture stirred under nitrogen for 12 days. This reaction was monitored by ^{1}H NMR where the enol peak was not observed after stirring overnight but it started appearing after 4 days and continued to get larger until no change in the peak's size was observed after 12 days.[4] The aldehyde –CHO resonance peak at 9.90 ppm gradually became smaller and finally disappeared during this period. The crude product was isolated by removal of solvent, and purified by column chromatography (ethyl acetate: hexane, 1:4 v/v) to yield a white solid, 0.390 g (17%), mp 185-190 °C. ^{1}H NMR: δ 16.67 (s, 2H, OH), 7.31 (t, 3H), 7.15 (d, 2H), 7.10, 7.04 (*AB*, 8H, aromatic CH), 1.96 (s, 12H) (Figure A13). ^{13}C NMR: δ 191.1, 146.8, 131.9, 131.0, 129.5, 125.0, 123.7, 123.6, 114.7, 24.2 (Figure A14). Anal. Calcd. for $C_{28}H_{27}NO_4$ (M = 441.52): C 76.17; H 6.16; N 3.17: Found: C 75.87; H 6.17; N 3.09. Crystals suitable for X-ray analysis were grown by slow evaporation of a solution in ethyl acetate-hexane.

b) $tpbprH_2$ (**32**): The same procedure for preparing **31** was followed except that 2,2,2-trimethoxy-4,5-diethyl-1,3,2-dioxaphospholene (1.86 g, 7.8 mmol) and 4,4'-

diformyltriphenylamine (1.2 g, 3.9 mmol) were mixed together and dissolved in dichloromethane. After the reaction was complete (as judged by the disappearance of CHO aldehyde peak), the crude product was isolated by the removal of the solvent and purified by column chromatography (ethyl acetate/hexane: 1:4) to give a white solid, 0.280 g (14%), mp 135-139 °C. ^{1}H NMR: δ 16.72 (s, 2H, OH), 7.32 (t, 3H), 7.16 (d, 2H), 7.09, 7.03 (*AB*, 8H, aromatic CH), 2.21 (q, 8H), 1.07 (t, 12H) (Figure A15). ^{13}C NMR: δ 194.3, 146.8, 132.1, 130.4, 129.5, 125.2, 123.6, 123.5, 113.4, 29.9, 9.6 (Figure A16). Anal. Calcd. for $C_{32}H_{35}NO_4$ (M = 497.62): C 77.24; H 7.09; N 2.81: Found: C 77.45; H 6.90; N 2.85. Crystals for X-ray analysis were grown by slow evaporation of a solution in ethyl acetate-hexane.

5.3.3 Synthesis of Copper Complexes

a) Complex **33**: $CuSO_4·5H_2O$ (0.24 g, 0.9 mmol) was dissolved in distilled water (50 mL) and ammonia solution was added in drops with stirring until a royal blue solution was formed. Into this solution was added the ligand **31** (0.3 g, 0.9 mmol) in dichloromethane (40 mL). Immediately a dark green insoluble powder precipitated out.

b) Complex **34**: This complex was prepared in the same procedure as for **33** above, except that the ligand **32** was used instead. Thus, $CuSO_4·5H_2O$ (0.10 g, 0.4 mmol) in distilled water (40 mL) was added ammonia solution in drops until a royal blue solution formed and the ligand **32** (0.20 g, 0.4 mmol) in dichloromethane (30 mL) was added. The mixture was stirred for 3 h. The dark-green organic layer was dried over Na_2SO_4 and evaporated to yield a dark-green solid, 0.112 g (50%). Anal. Calcd. for $C_{128}H_{132}Cu_4N_4O_{16}$ (M = 2236.62): C 68.74; H 5.95; N 2.50: Found: C 68.92; H 6.16; N 2.60

5.4 References

(1)   Pariya, C.; Sparrow, C. R.; Back, C. K.; Sandi, G.; Fronczek, F. R.; Maverick, A. W. *Angew. Chem. Int. Ed.* **2007**, *46*, 6305.

(2)   Mallegol, T.; Gmouh, S.; Meziane, M. A. A.; Blanchard-Desce, M.; Mongin, O. *Synthesis-Stuttgart* **2005**, 1771.

(3)   Ramirez, F.; Patwardhan, A. V.; Ramanathan, N.; Desai, N. B.; Greco, C. V.; Heller, S. R. *J. Am. Chem. Soc.* **1965**, *87*, 543.

(4)   Marcos, Y. *PhD Dissertation, Louisiana State University,* **2009**.

Chapter 6: Conclusions and Prospects

This dissertation focuses on synthesis of β-diketone and β-ketoenamine ligands for molecular polygons. Chapters 2-4 discuss syntheses of derivatives of m-pbaH$_2$ and their molecular squares. Chapter 5 discusses triphenylamine based bis(β-diketones) and their copper complexes.

The new m-pbhxH$_2$ ligand, with pentyl chains replacing the methyl groups in the β-diketone moieties of m-pbaH$_2$, was successfully prepared beginning with 6-dodecyne. Reaction of this ligand with copper resulted in a molecular square that is soluble in a wide range of solvents. Single crystal X-ray diffraction confirmed formation of the square with molecular formula [Cu$_4$(m-pbhx)$_4$(MeOH)$_2$]. Host-guest reactions of the square with a variety of guest molecules were studied. In most of the cases green precipitates formed; in other cases, the color of solutions changed from dark green or blue to dark blue then to brown and eventually brown precipitates were deposited; and in a few cases crystals formed. The crystalline products were analyzed by single crystal X-ray diffraction. The squares with 1,2-bis(4-pyridyl)ethylene (bpe) and 1,2-bis(4-pyridyl)ethane (bpa) were confirmed by single crystal X-ray analysis with molecular formula Cu$_4$(m-pbhx)$_4$(μ-bpe)(MeOH)$_2$ and Cu$_4$(m-pbhx)$_4$(μ-bpa)(MeOH)$_2$ respectively. Preliminary results from the crystals formed between the square and C$_{60}$ (dark brown) revealed a 1:1 adduct, while the square with anthracene formed blue-green crystals which did not diffract well.

The 2-MeO-m-pbaH$_2$ ligand, with a methoxy group in the internal 2-position of its aromatic ring, was prepared previously by Jace Sandifer, though in low yield. Its synthesis has been improved by increasing yield and purity, and the closely related 2-MeO-m-pbprH$_2$, with ethyl substituents, was synthesized as well. Treatment of 2-MeO-m-pbprH$_2$ with copper afforded

a molecular square that is soluble in chloroform and dichloromethane. Single crystal X-ray analysis revealed the square with methoxy groups on the inside. Treatment of the square with guest molecules did not yield adducts; we attribute this to interference from the methoxy groups.

The two ligands m-pbaH$_2$ and m-pbprH$_2$ were converted to their ketoenamine analogs m-pbiH$_2$ and m-pbprH$_2$ through microwave assisted synthesis. Both bis(β-ketoenamines) afforded molecular squares when treated with Cu^{2+}. The longer-chain m-pbpriH$_2$ also yielded a molecular square when treated with Ni^{2+}. Single crystal X-ray analysis confirmed the formation of the squares. The two M$_4$(m-pbpri)$_4$ squares were studied by UV-VIS and by electrochemistry. The nickel square is diamagnetic and was studied by NMR.

Two new bis(β-diketone) ligands based on triphenylamine were prepared for the first time. The ligands are formed when 4,4'-diformyltriphenylamine and phospholenes are stirred together for a long time (12 days). When treated with copper, the methyl version of the ligand yielded an insoluble product while the ethyl version yielded a copper complex that is soluble in chloroform and dichloromethane. Attempts to crystallize the complex yield yellow-green precipitates which may suggest that the complex is unstable in solution and it degrades. The soluble complex was analyzed by ESI-MS and microanalysis and the data agree with the calculated values for a molecular square and thus a molecular square is proposed for this complex.

I have explored the effects of changing alkyl substituents, coordinating atoms, and aromatic-ring substituents on the chemistry of m-pbaH$_2$ and its molecular squares. Further studies could be done on these molecules. For example, since 2-MeO-m-pbprH$_2$ afforded a molecular square; it indicates that the methoxy group does not prevent formation of the macrocycle. This

study could be extended further by introducing larger functional substituents on the 2-position of m-pbaH$_2$ to test the possibility of formation of larger macrocycles.
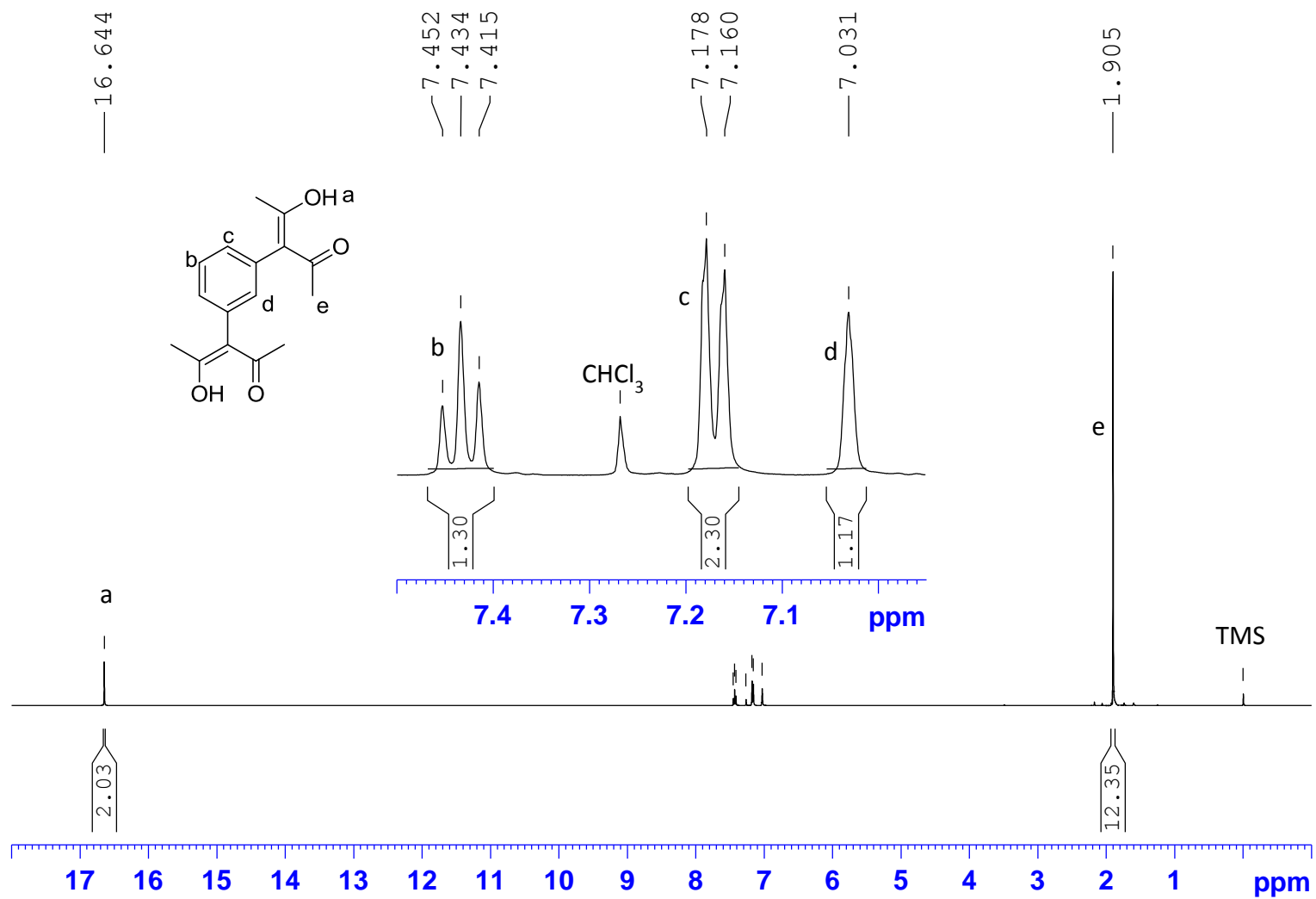
Appendix: Spectra

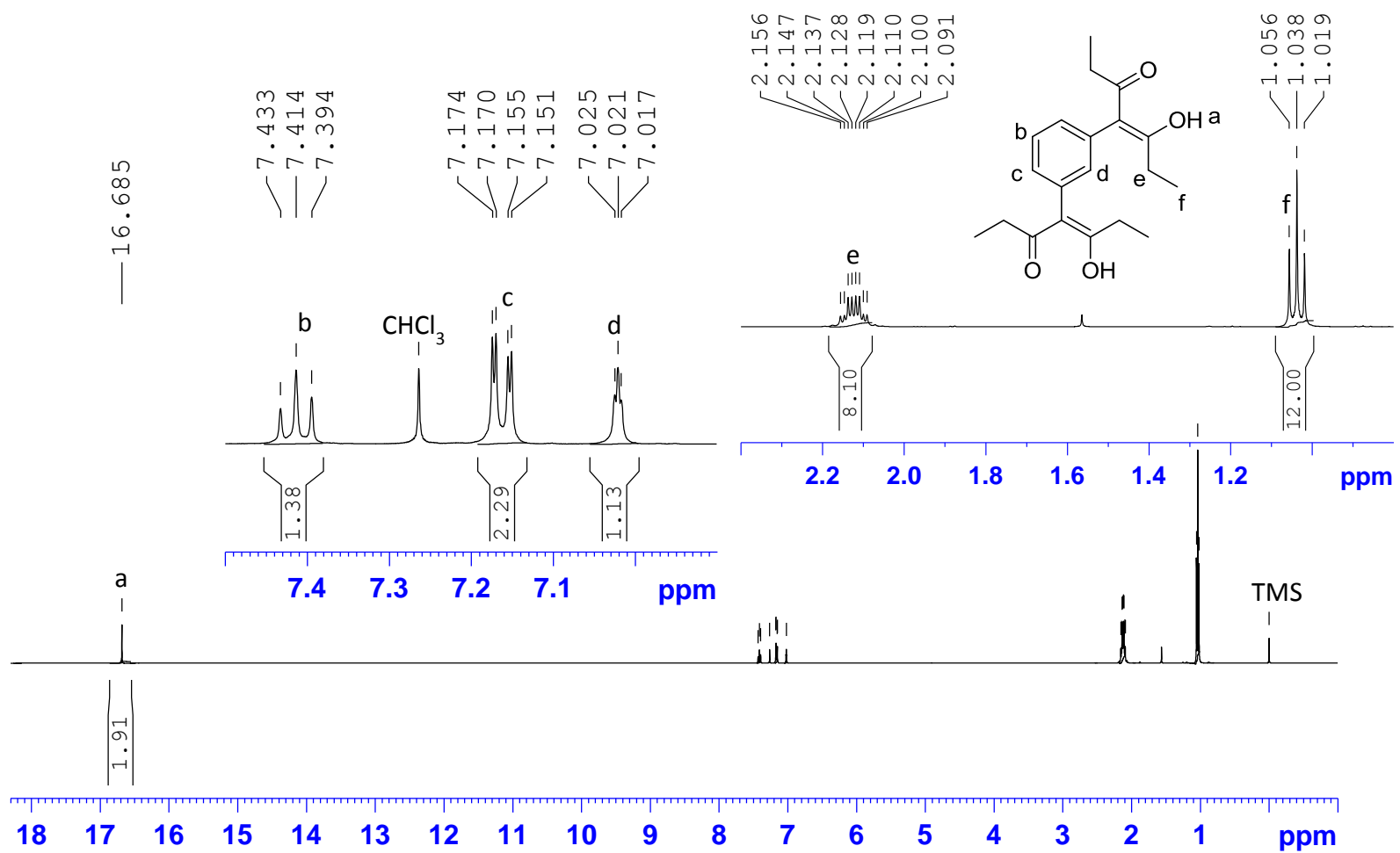**Figure A1** ^{1}H NMR spectrum of *m*-pbaH$_2$ (**1**).

Figure A2 ^{1}H NMR spectrum of *m*-pbprH$_2$ (**2**).
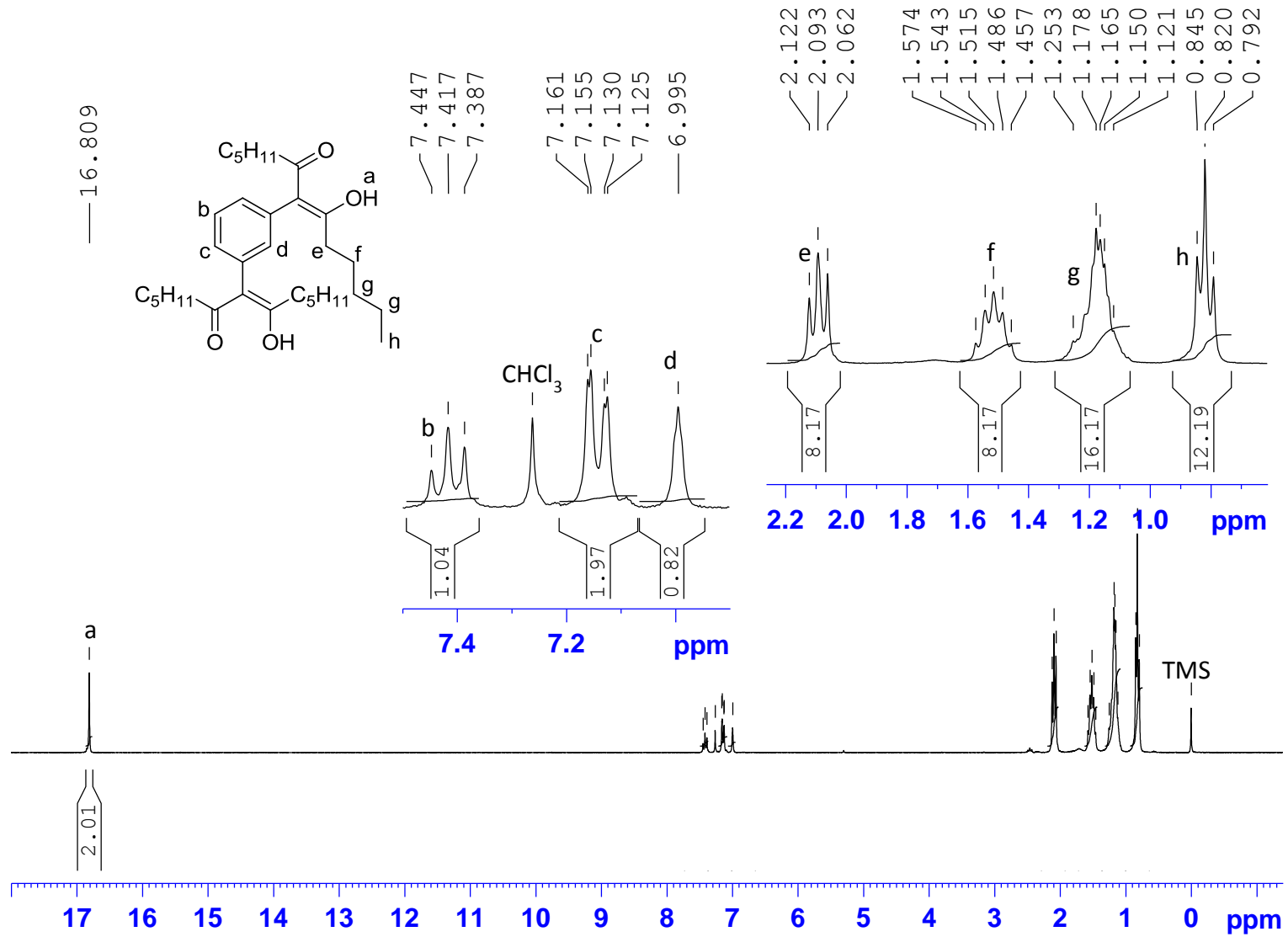
Figure A3 ^{1}H NMR spectrum of *m*-pbhxH$_2$ (**5**)
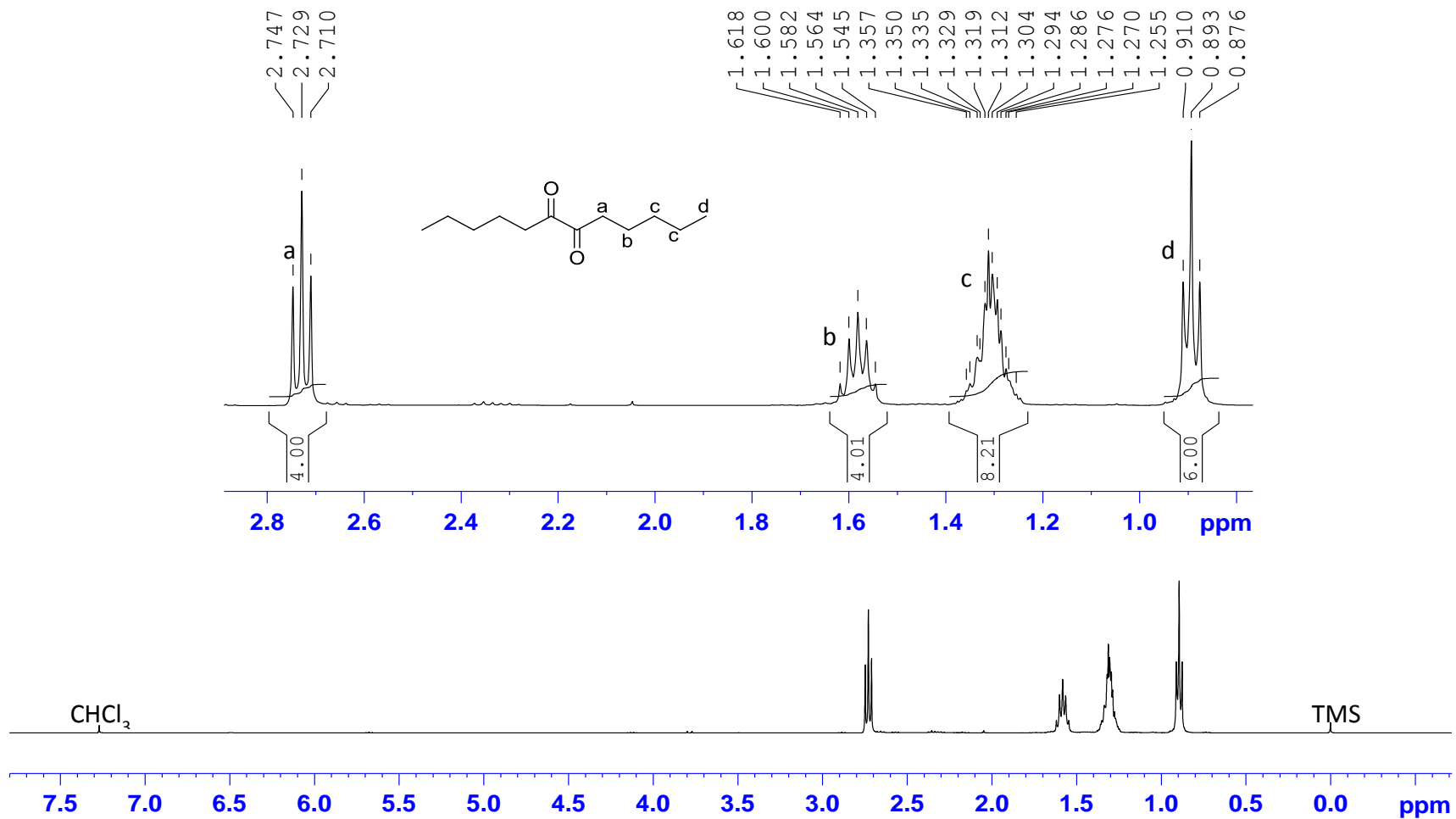
Figure A4 ^{1}H NMR spectrum of dodecane-6,7-dione (**12**).
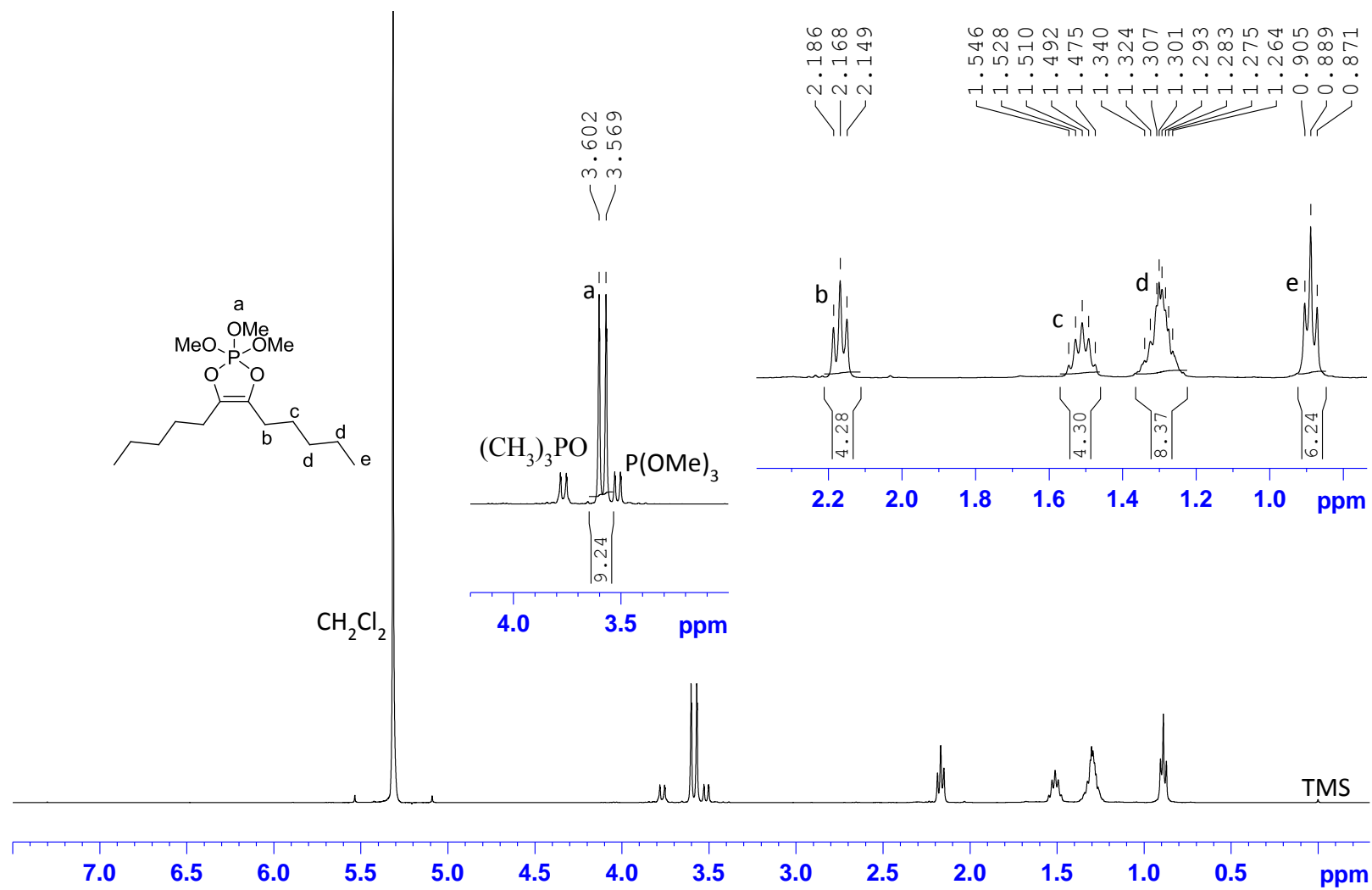
Figure A5 ^{1}H NMR spectrum of crude pholene **13**.
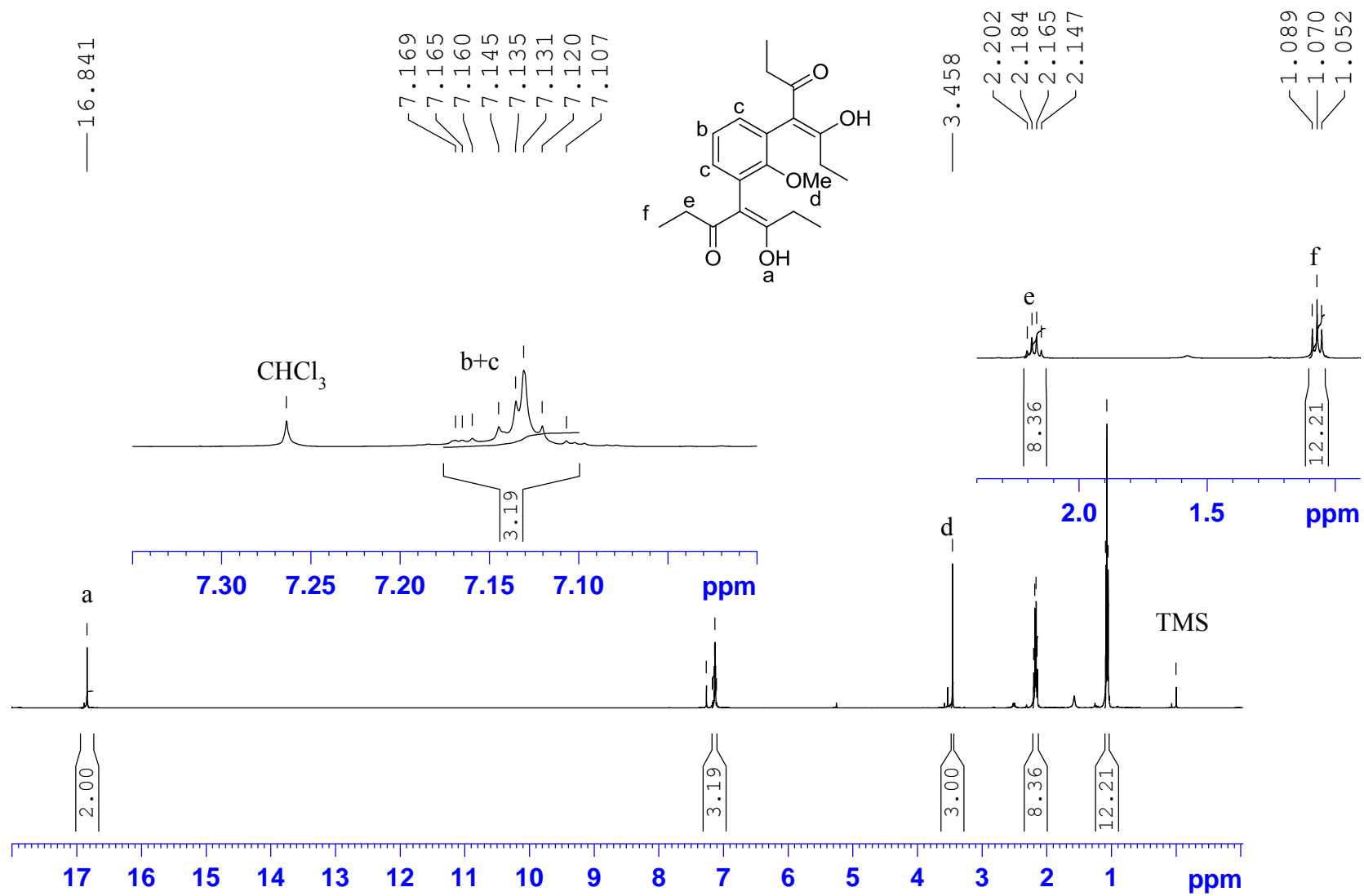
Figure A6 ^{1}H NMR spectrum of 2-MeO-*m*-pbprH$_2$ (**22b**).
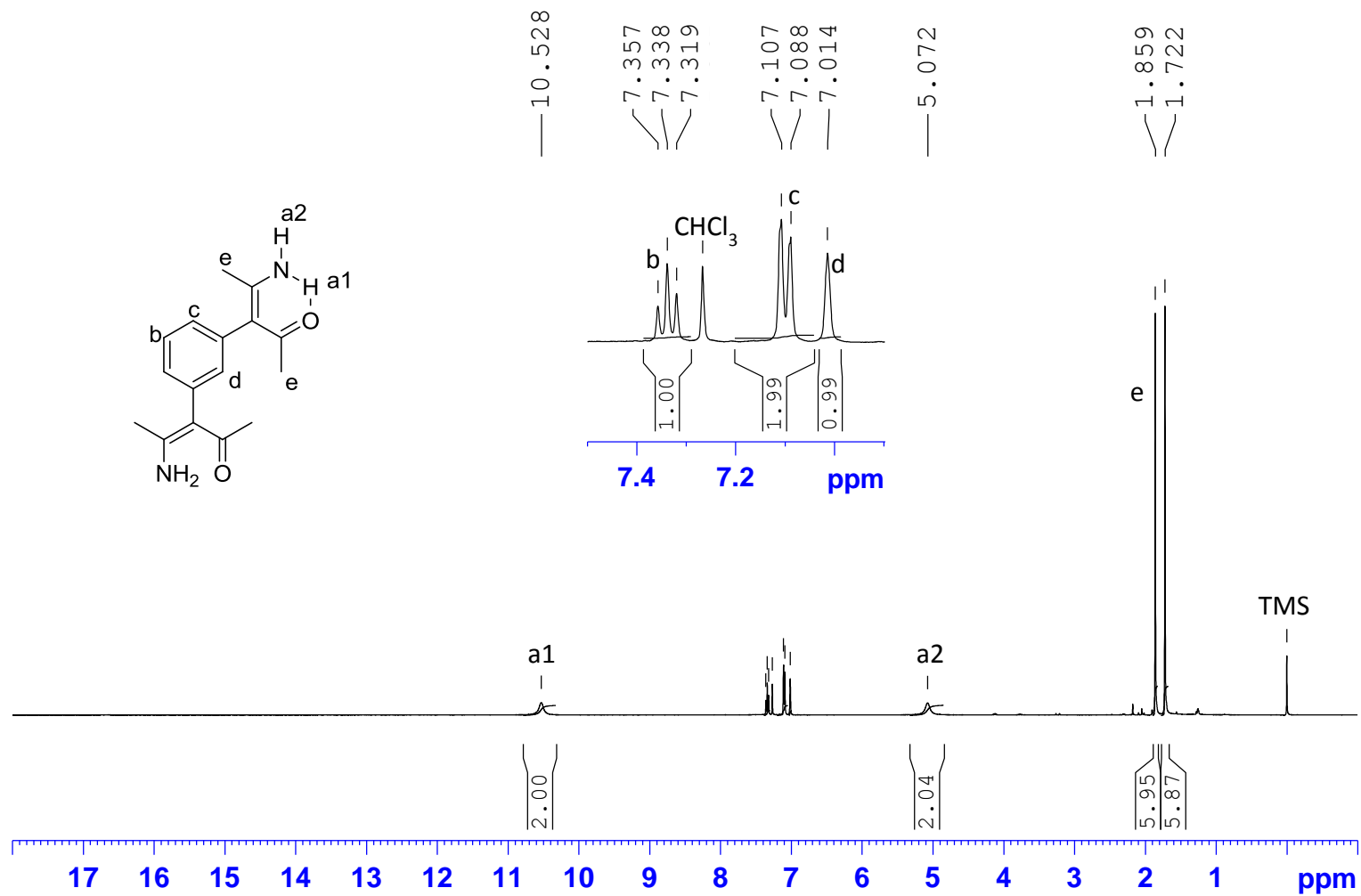
Figure A7 ^{1}H NMR spectrum of *m*-pbiH$_2$ (**26**)
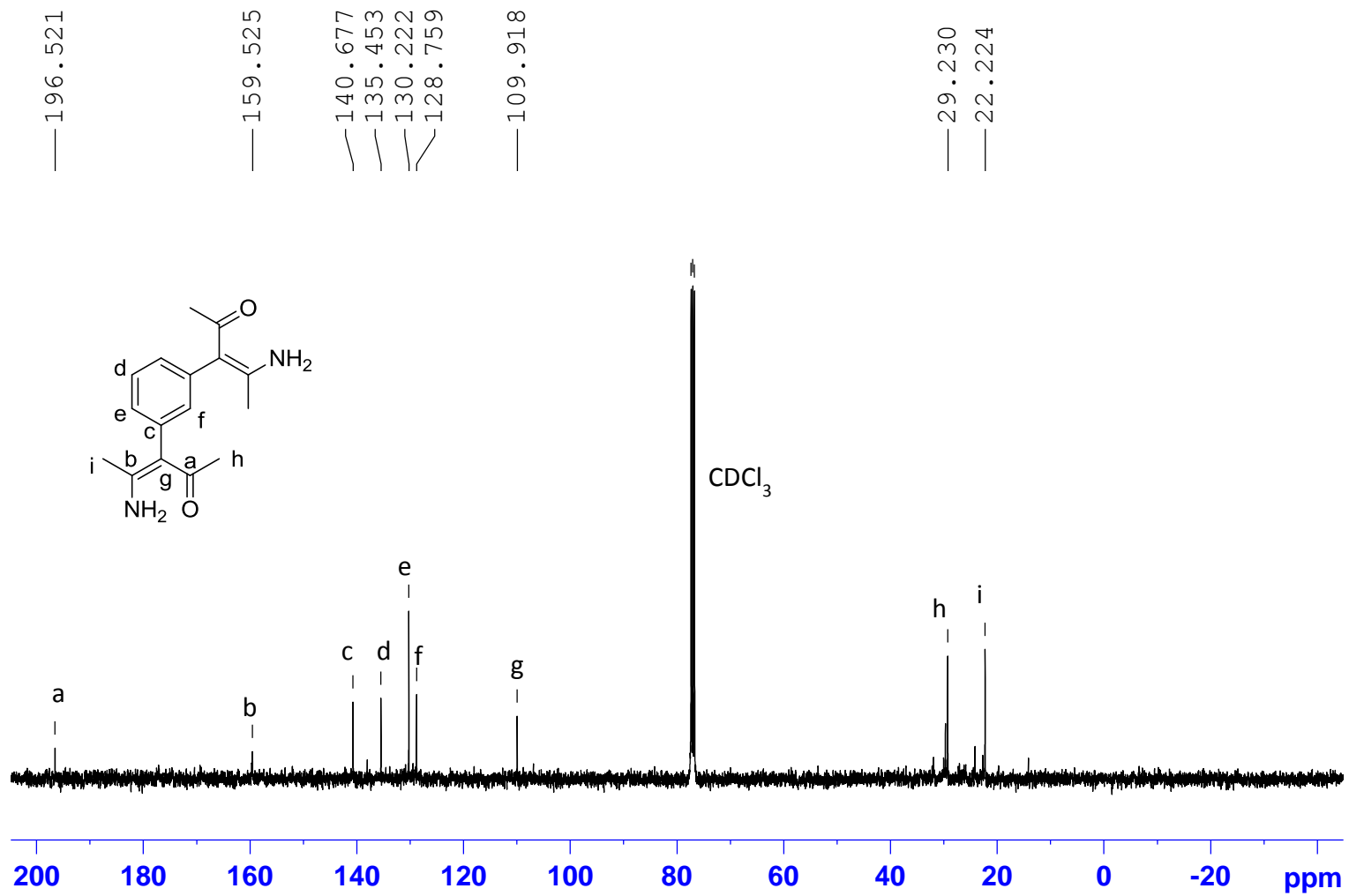
Figure A8 ^{13}C NMR spectrum of *m*-pbiH$_2$ (**26**).
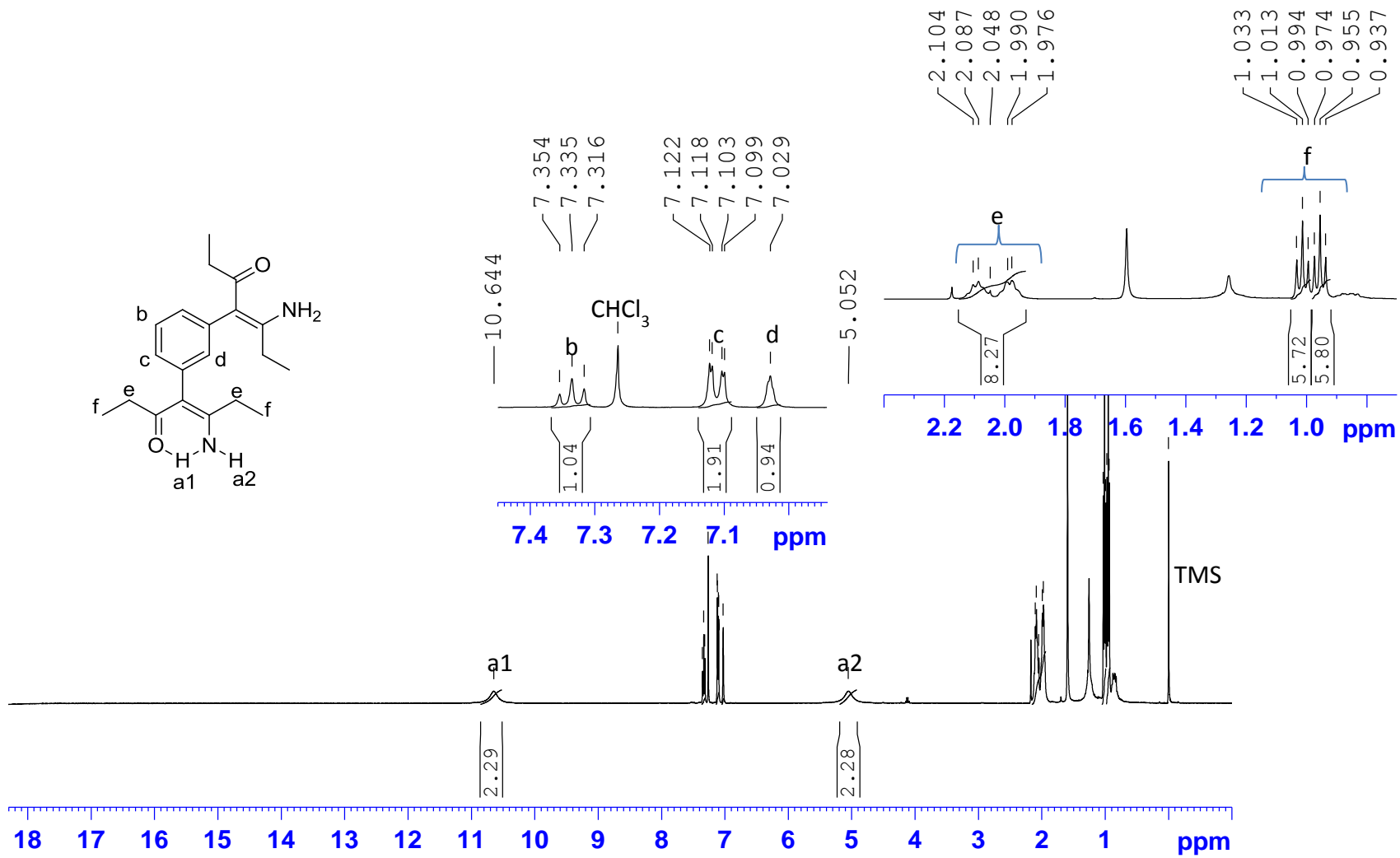
Figure A9 ^{1}H NMR spectrum of *m*-pbpriH$_2$ (**27**).
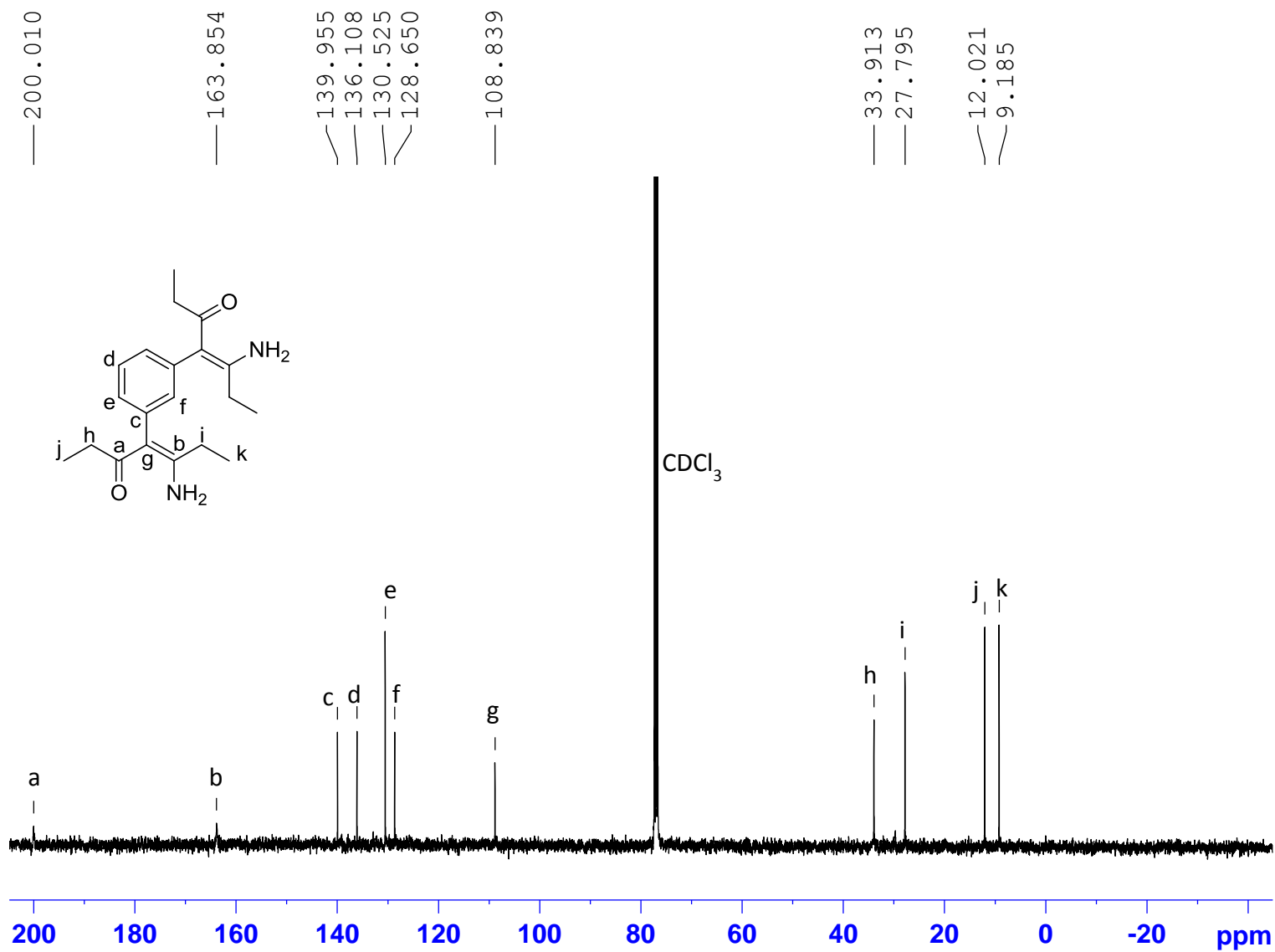
Figure A10 ^{13}C spectrum of *m*-pbpriH$_2$ (**27**).
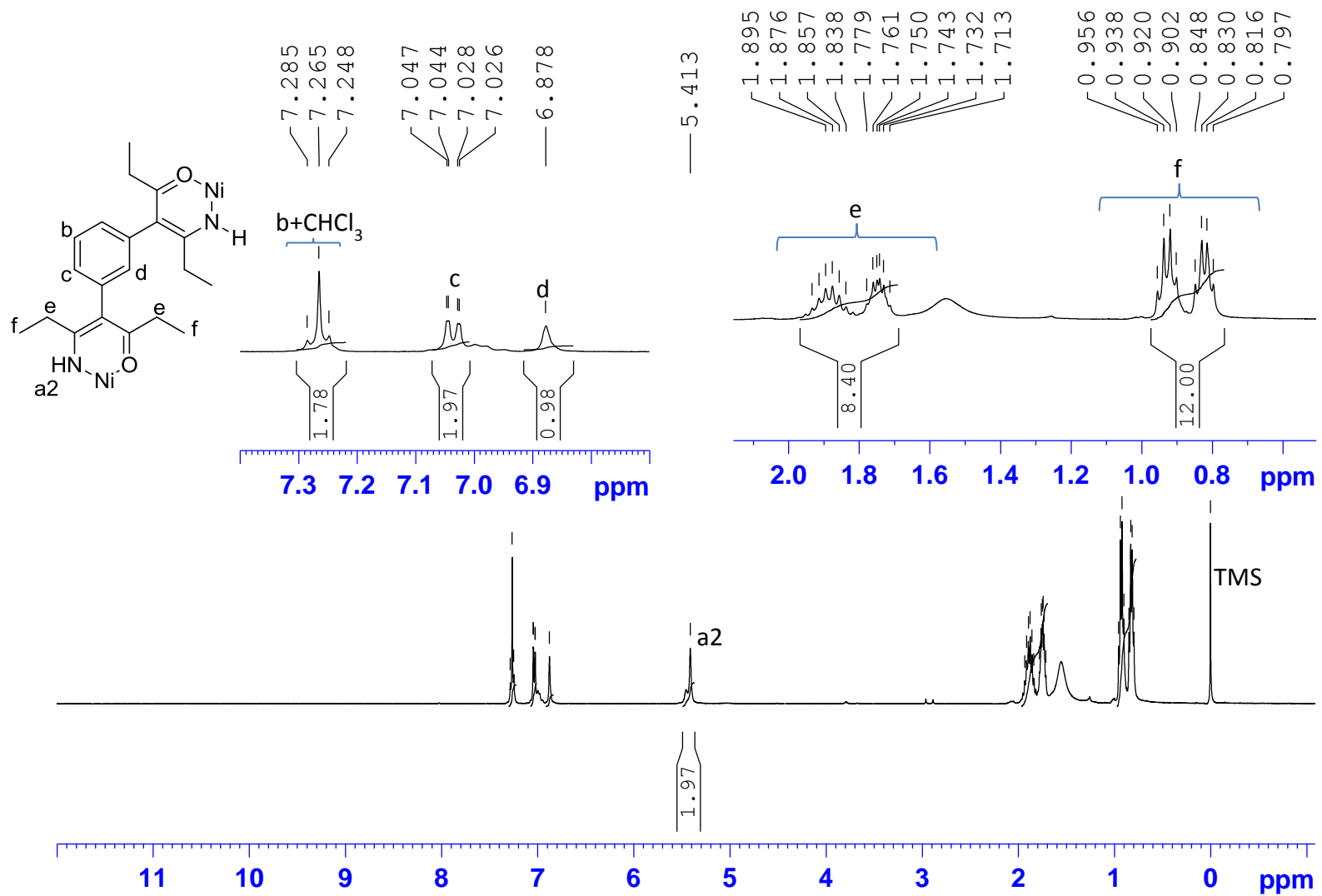
Figure A11 ¹H NMR spectrum of Ni₄(*m*-pbpri)₄ molecular square (**30**).
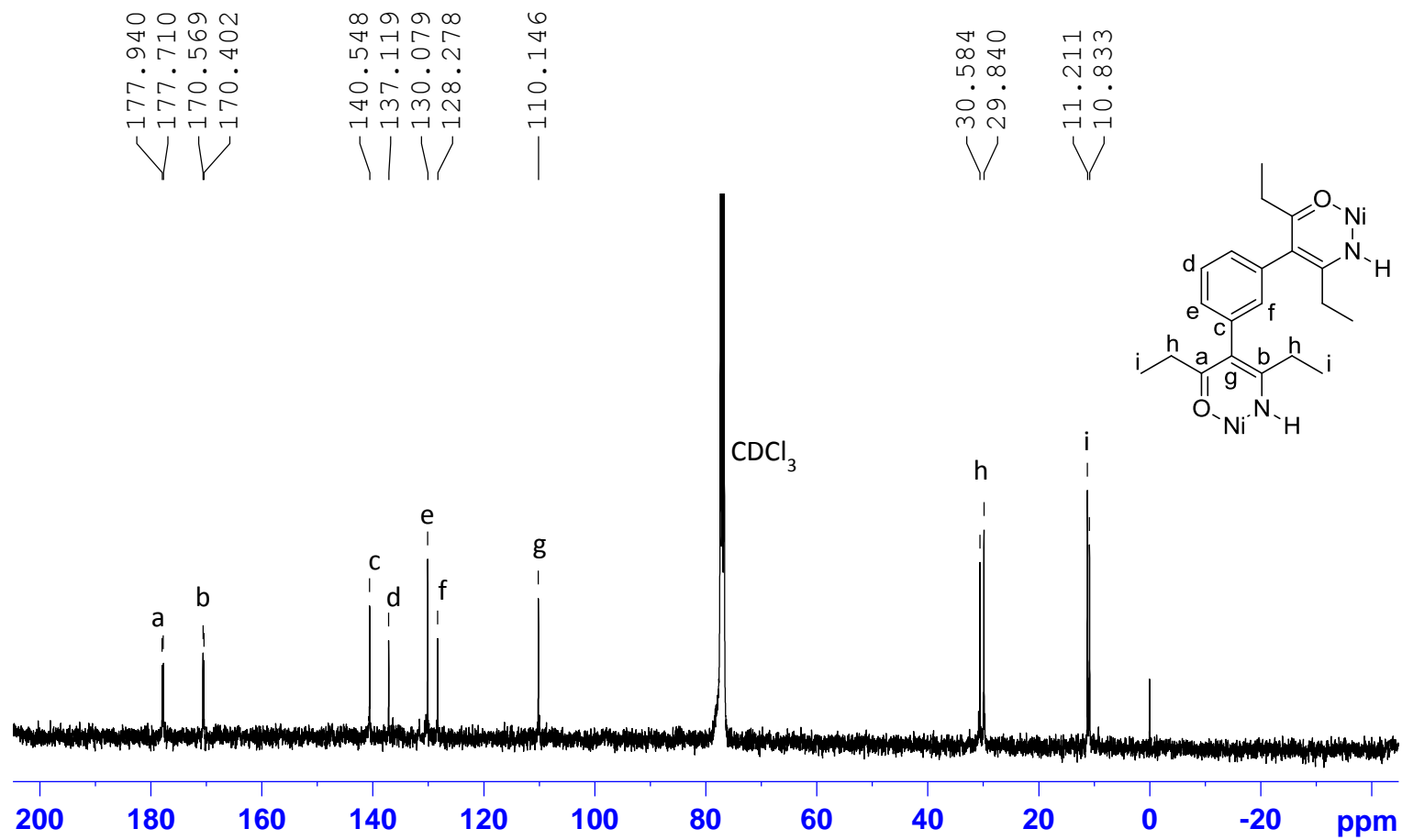
Figure A12 ^{13}C NMR spectrum of $Ni_4(m\text{-pbpri})_4$ molecular square (**30**).
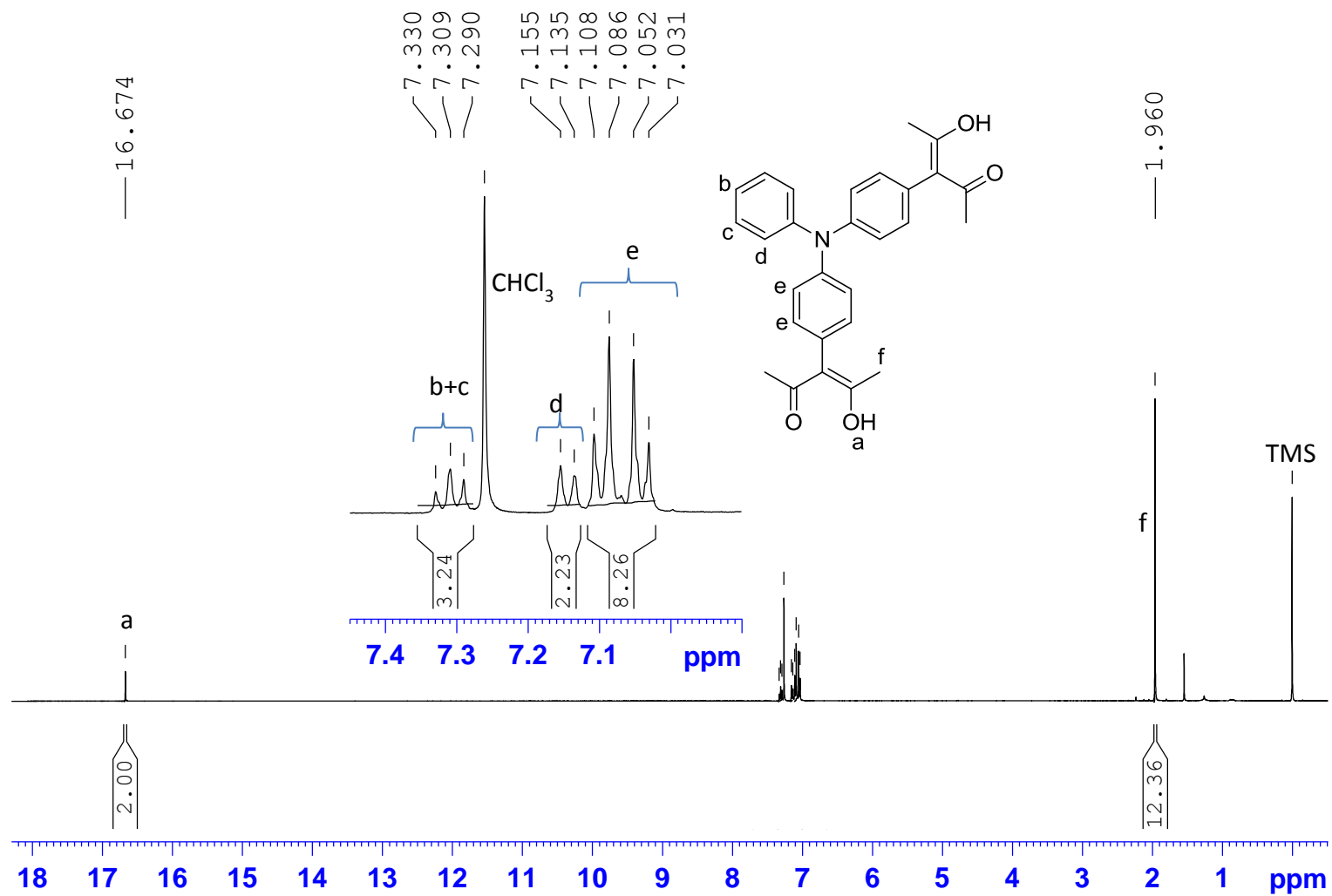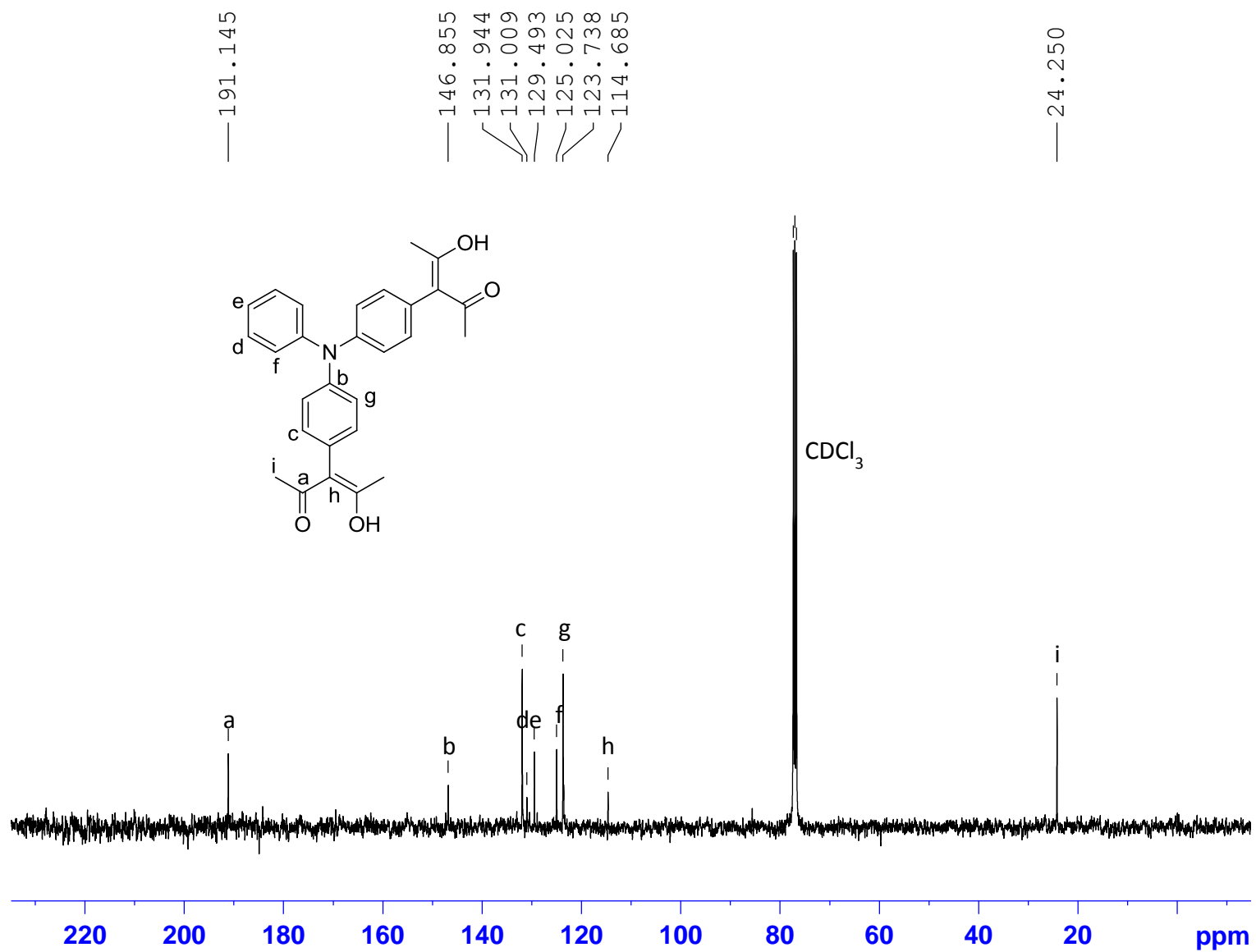
Figure A13 ^{1}H NMR spectrum of tpbaH$_2$ (**31**).

Figure A14 ^{13}C NMR spectrum of tpbaH$_2$ (**31**).
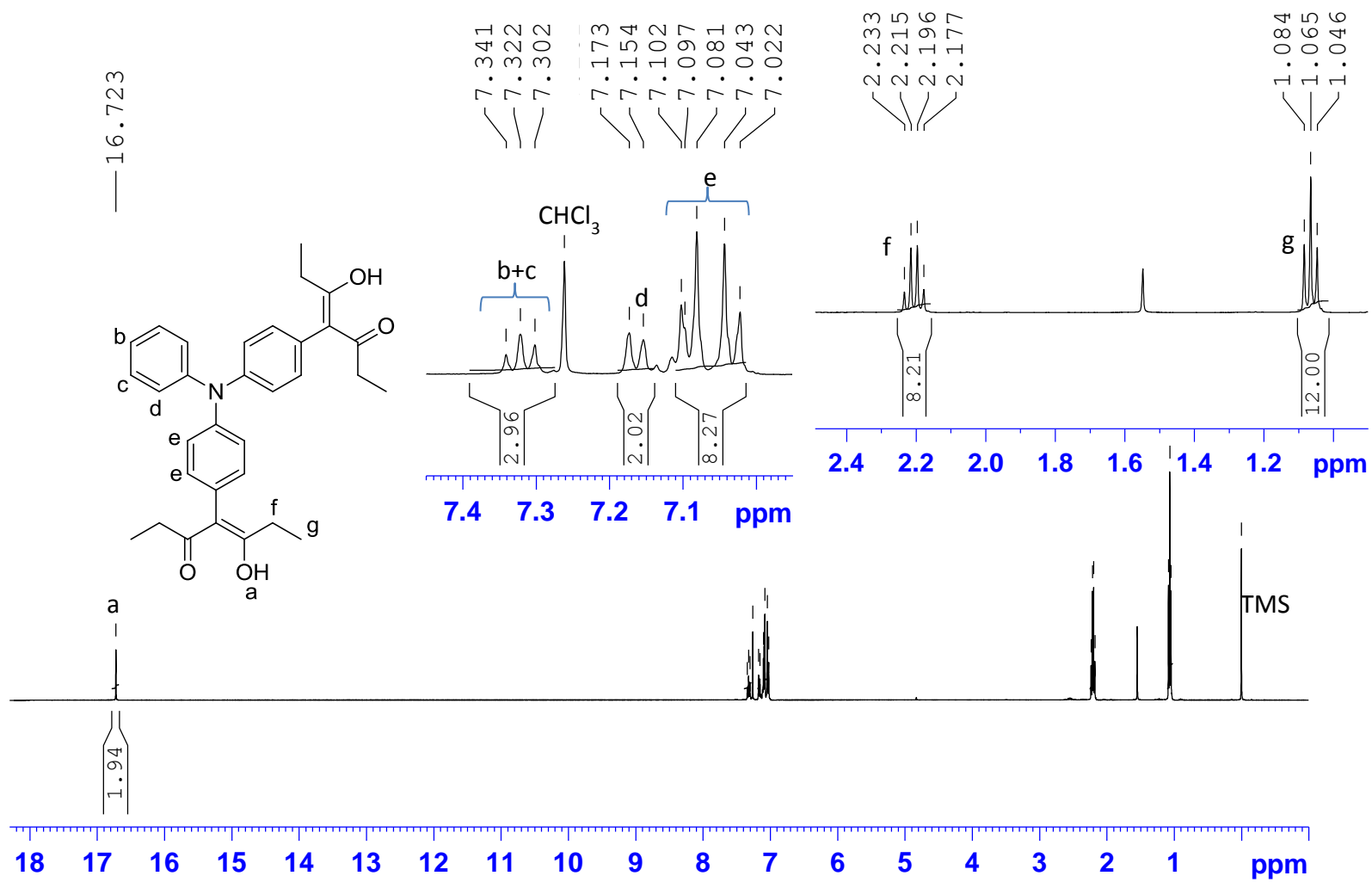
Figure A15 ^{1}H NMR spectrum of tpbprH$_2$ (**32**).
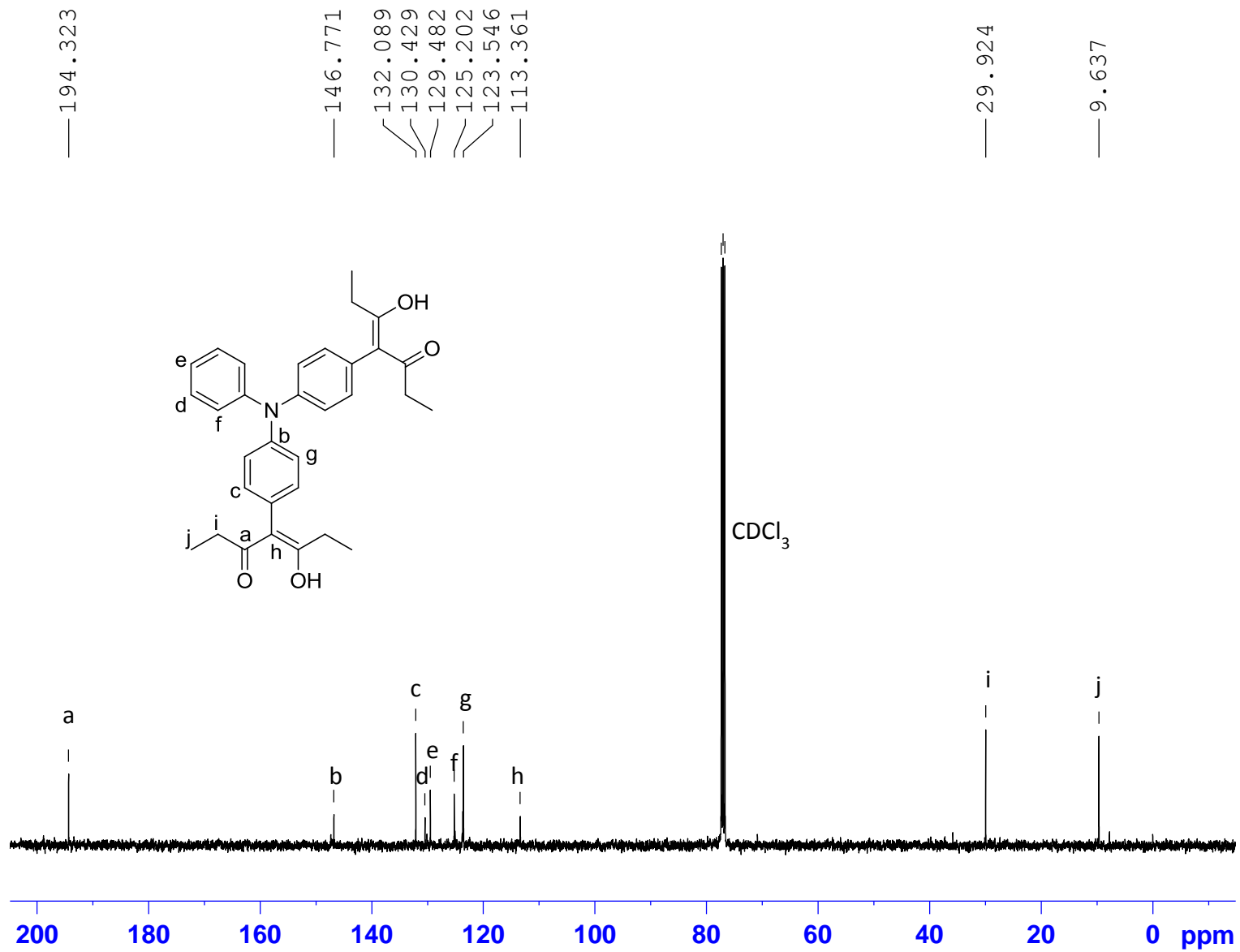
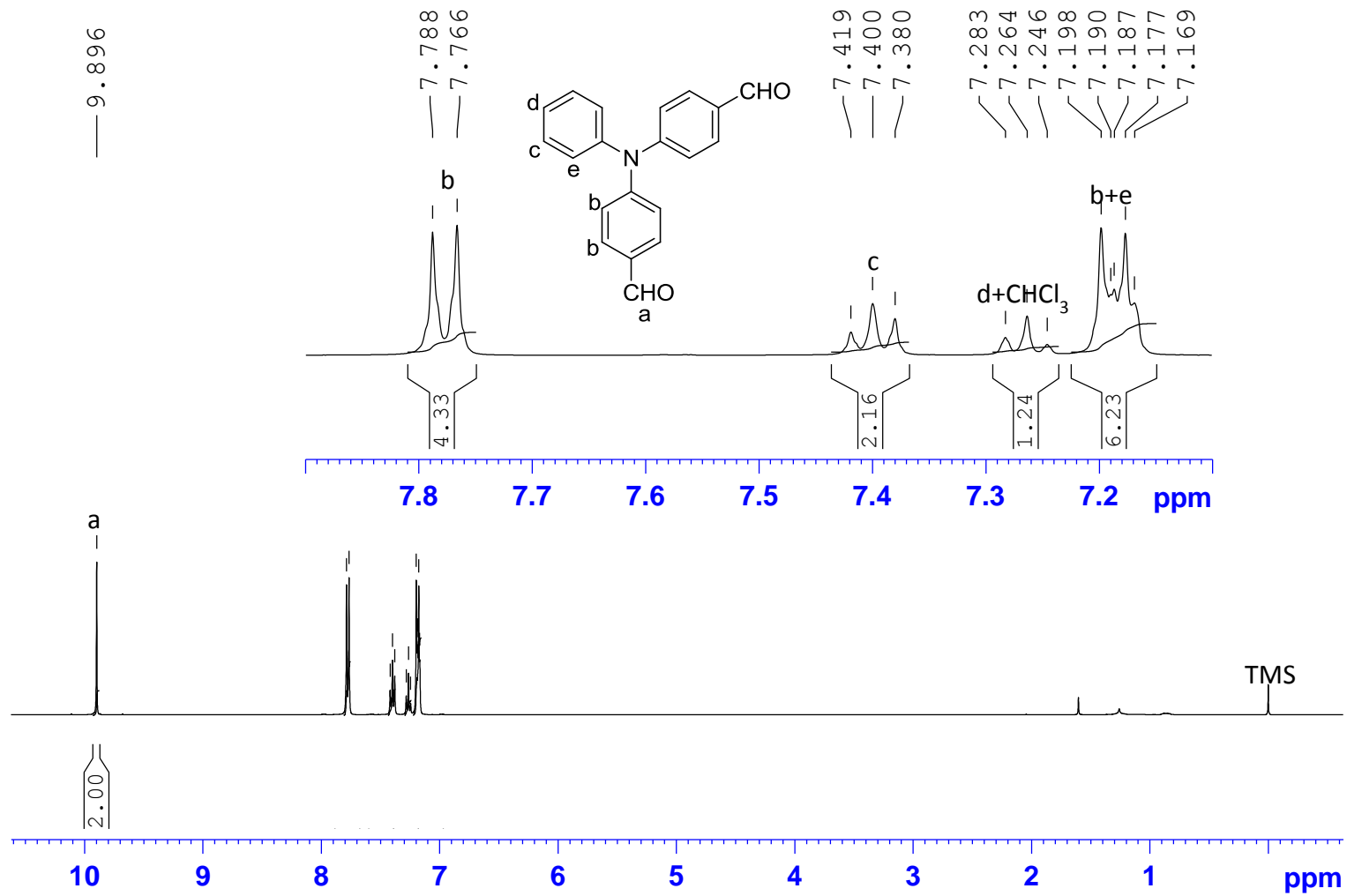**Figure A16** ^{13}C spectrum of tpbprH$_2$ (**32**).

Figure A17 ^{1}H NMR spectrum of 4,4'-diformyltriphenylamine (**33**).

Vita

Jackson K. Cherutoi was born on December 31, in Baringo District, Rift Valley Province, Kenya. He received his Bachelor of Education Science degree (Chemistry/Maths) from Moi University in 1996. He received his Master of Science degree (Chemistry) from Moi University in 2002. He is currently a candidate for the Doctor of Philosophy degree in the Department of Chemistry at Louisiana State University and Agricultural and Mechanical College with Dr. Andrew W. Maverick as his advisor.